# REMOVAL OF GASEOUS MERCURY IN NATURAL GAS BY SILVER–DOPED SUPPORT MATERIALS

Miss Juthathip Sinthao

A Thesis Submitted in Partial Fulfillment of the Requirements
for the Degree of Master of Science Program in Environmental Management
(Interdisciplinary Program)
Graduate School
Chulalongkorn University
Academic Year 2012

# การกำจัดไอปรอทในแก๊สธรรมชาติด้วยวัสดุที่ปรับสภาพด้วยโลหะเงิน

นางสาวจุฑาทิพย์ สินเธาว์

วิทยานิพนธ์นี้เป็นส่วนหนึ่งของการศึกษาตามหลักสูตรปริญญาวิทยาศาสตรมหาบัณฑิต
สาขาวิชาการจัดการสิ่งแวดล้อม (สหสาขาวิชา)
บัณฑิตวิทยาลัยจุฬาลงกรณ์มหาวิทยาลัย
ปีการศึกษา 2555

| | |
|---|---|
| Thesis Title | REMOVAL OF GASEOUS MERCURY IN NATURAL GAS BY SILVER–DOPED SUPPORT MATERIALS |
| By | Miss Juthathip Sinthao |
| Field of Study | Environmental Management |
| Thesis Advisor | Assistant Professor Siriluk Chiarakorn, Ph.D. |

Accepted by the Graduate School, Chulalongkorn University in Partial Fulfillment of the Requirements for the Master's Degree

……..Dean of the Graduate School
(Associate Professor Amorn Petsom, Ph.D.)

THESIS COMMITTEE

……..Chairman
(Assistant Professor Chantra Tongcumpou, Ph.D.)

……..Thesis Advisor
(Assistant Professor Siriluk Chiarakorn, Ph.D.)

……..Examiner
(Pichet Chaiwiwatworakul, Ph.D.)

……..Examiner
(Assistant Professor Khemarath Osathaphan, Ph.D.)

……..External Examiner
(Pongtanawat Khemthong, Ph.D.)

จุฑาทิพย์ สินเธาว์: การกำจัดไอปรอทในแก๊สธรรมชาติด้วยวัสดุที่ปรับสภาพด้วยโลหะเงิน. (REMOVAL OF GASEOUS MERCURY IN NATURAL GAS BY SILVER–DOPED SUPPORT MATERIALS) อ.ที่ปรึกษาวิทยานิพนธ์หลัก: ผศ.ดร.สิริลักษณ์ เจียรากร, 116 หน้า.

ปรอทเป็นโลหะหนักที่สามารถพบได้ทั่วไปในแก๊สธรรมชาติปรอทที่อยู่ในสถานะไอมีความเป็นอันตรายสูง งานวิจัยนี้จะศึกษาประสิทธิภาพการดูดซับของไอปรอททั้งในระบบการดูดซับแบบกะและแบบต่อเนื่อง ด้วยตัวดูดซับโลหะเงินที่กระจายตัวบนวัสดุรองรับ 2 ชนิด คือ ถ่านกัมมันต์และไททาเนียมไดออกไซด์ ด้วยเทคนิคการชุบเอิบ และทดสอบการดูดซับทั้งสองแบบ คือ แบบกะและต่อเนื่องเพื่อเปรียบเทียบกับตัวดูดซับทางการค้าซึ่งพบว่าโลหะเงินสามารถกระจายตัวได้ดีบนไททาเนียมไดออกไซด์และสามารถดูดซับได้มากที่สุด และความสามารถในการดูดซับไอปรอทขึ้นกับปริมาณของโลหะเงิน ตัวดูดซับที่มีโลหะของเงินจะทำการจับไอปรอทในรูปของอะมัลกัม ด้วยปฏิกิริยาอันดับที่ 1 โดยมีค่าพลังงานกระตุ้นเท่ากับ -185.680 กิโลจูลต่อโมล โดยตัวดูดซับที่เตรียมนี้มีความสามารถมากกว่าตัวดูดซับทางการค้าประมาณ 2.1 เท่า เมื่อพิจารณาที่อุณหภูมิ 60 องศาเซลเซียส

สาขาวิชา การจัดการสิ่งแวดล้อม ลายมือชื่อนิสิต .....

ปีการศึกษา 2555 ลายมือชื่อ อ.ที่ปรึกษาวิทยานิพนธ์หลัก .....

## 5387508620: MAJOR ENVIRONMENTAL MANAGEMENT
KEYWORDS: ADSORPTION/ MERCURY / SILVER/ NATURAL GAS /IMPREGNATION METHOD

JUTHATHIP SINTHAO: REMOVAL OF GASEOUS MERCURY IN NATURAL GAS BY SILVER–DOPED SUPPORT MATERIALS. ADVISOR: ASST.PROF.SIRILUK CHIARAKORN, Ph.D., 116 pp.

Mercury is one of the heavy metals found in natural gas. It is extremely hazardous in vapor phase. This aim of this research is to study the adsorption of Hg vapor which carried out in both static and continuous flow systems. Activated carbon and titanium dioxide were used as supports and these supports are loaded through impregnation by silver metal. The adsorption tests using the prepared adsorbents were tested against a commercial one. It was found that silver-doped adsorbents showed more uniform Hg removal, and provided higher removal rates compared to commercial adsorbent. Results also show that the increase in the amount of silver loading will also increase the amount of adsorbed mercury. The reaction between silver and mercury obeyed the first order of reaction with activation energy of -185.680 kJ/mol. Silver-supported adsorbents showed approximately 2.1 times better performance compared to the commercial adsorbent.

Field of Study: Environmental Management Student's Signature .....

Academic Year: 2012 Advisor's Signature .....

# ACKNOWLEDGEMENTS

I would like to express my gratitude to Asst. Prof. Dr. Sililuk Chailakorn, my advisor, for giving me great support, guidance, and independence. Her knowledgeable advices, scientific suggestions, and generous encouragements significantly contribute to my research. I also would like to express my deepest and sincerest appreciation to Assoc. Prof. Dr. Nurak Grisdanurak, for the opportunity to be his student. I feel really lucky to work on my thesis in his laboratory at Thammasat University under his supervision. I would like to thank the PTT research institute, for the opportunity to be one of their assistant researchers. The budget they spend on supporting my research gave me opportunity to carry out my thesis. They also gave me useful knowledge and promoted systematic thinking about environmental applications and management.

The stimulating questions and valuable suggestions on my work from the committee members, Assist. Prof. Dr. Chantra Tongcumpou, Assist. Prof. Dr. Khemarath Osathaphan, Dr. Pichet Chairatworakul, and Dr. Pongtanawat Khemthong are also acknowledged. I am also grateful to the Center of Excellence on Hazardous Substance Management (EHSM) for the International Postgraduate Programs in Environmental Management (Hazardous Waste Management) and Chulalongkorn University graduate school, for the scholarship and the financial support. My gratitude also goes to the School of Energy, Environment and Materials, King Mongkut's University of Technology Thonburi; Department of Chemical Engineering, Faculty of Engineering, Thammasat University; PTT research institute, Thailand(financial support), and National Nanotechnology Center (NANOTEC) for their laboratory facility.

The one page acknowledgement limits who I would like to thank on what they have done to support my research in times of happiness as well as troubles in each single day during those challenging research years. This is for all my teachers and friends. I will never forget all the friendship and support you provided to me during my Master's degree study.

Most of all, I am very thankful to my father, mother, and family forum limited love, intensive understanding, and freedom in living my own life.

# CONTENTS

**Page**

**Page**

**Page**

# LIST OF TABLES

# LIST OF FIGURES

**Page**

**Page**

# CHAPTER I

# INTRODUCTION

## 1.1 Motivations

There are significant contaminants that may be encountered in the drilling process of natural gas production. Generally, these major contaminants consist of heavy metals (like Hg, Cr, Cd, etc.) and water. Among these, one of the primary concerns is mercury. Mercury exists in three possible oxidation states in nature (Hg(II), Hg(I), and Hg(0)). It is predominantly found as Hg(0) in gas phase (USEPA, 2001).

Mercury is known to be a toxic element. There are several adverse effects of mercury exposure not only to human health but also to the environment. Some of these include paralysis, serious intestinal and urinary complications, and dysfunction of the central nervous system (Wụ et al., 2010). In addition, mercury is highly volatile, thus it vaporizes rapidly which makes it more difficult to control. The Environmental Protection Agency (EPA) has disclosed that the amount of Hg level in human blood that will produce possible health effects is 5.8 $\mu g/m^3$ (USEPA, 2012).

Natural gas in the Southeast Asian region is found to have high concentrations (up to 200 $mg/m^3$) of elemental Hg. Mercury can be present in different forms. It can be as the element $Hg^o$ or organic compounds such as mercuric chloride ($HgCl_2$), methyl mercuric chloride ($CH_3HgCl$), dimethyl mercury ($CH_3HgCH_3$), and diethyl mercury ($C_2H_5HgC_2H_5$) (Wilhelm and Bloom, 2000).The USEPA sets a standard Hg level in air to be less than 100 $\mu g/m^3$(Virakom, 2010). On the other hand, industries set a level of Hg in natural gas processing plant to around 10 $\mu g/m^3$ (Mokhatab and Poe, 2012).

Treatment of mercury in the liquid phase have been extensively investigated (Ghassabzadeh et al., 2010, Hutchison et al., 2008, Ma et al., 2009, and Idris et al., 2011). The removal of Hg from aqueous phase is performed using outokumpu

process, bolkem process, selenium filter process, boliden–norzink process, and sulphide precipitation (Louie, 2008). Most of them are commercial processes and these were carried by mixing elemental mercury ($Hg^o$) with an acid ($H_2SO_4$ and $H_2SeO_3$) which is very volatile in nature thus more difficult to control (Thadani, 2010). It needs to change mercury vapor to mercury liquid before doing some removal reactions. On the other hand, the treatment of mercury in vapor phase has not widely studied.

The removal of mercury from vapor phase in mainly performed by adsorption technique. Based on mercury property, physical adsorption may not be attractive. The chemical adsorption has an advantage for the removal of heavy metals. The adsorption process was investigated using various adsorbents; including calcium–based (Ghorishi et al., 1998), coal (Somoano et al., 2007), and zeolites (Morency, J. 2002) all of which are done in the vapor phase. However, the efficiencies of those adsorbents were extremely low and cost ineffective.

Different chemicals can readily form amalgam with mercury at ambient conditions such as gold, zinc, aluminum, copper and silver. These can be used as raw materials for preparing metal–doped adsorbents. Nevertheless, the disadvantages of metal-doped adsorbents have been reported by previous articles (Okabe and Mitchell, 1996). The activity of aluminum and copper in metal mercury is relatively low. Moreover, zinc has a high solubility and gold is very expensive. In this study, Ag is selected as raw material because it is known to have a strong amalgam formation compared to other commercially available metals. Silver–doped activated carbon presents a potential advantage compared to using carbon adsorbent alone, due to the chemical adsorption by the mercury on the doped metal. The supports that will be used in this study are titanium dioxide ($TiO_2$, moderate surface area) and granular activated carbon (GAC, high surface area).

This work aims to synthesize adsorbents that will achieve a high Hg adsorption capacity. The result of the adsorption on static batch and continuous flow will be compared against the performance of an existing commercial adsorbent.

## 1.2 Objective of the study

To investigate the mercury adsorption performance of silver-loaded $TiO_2$ and GAC on mercury vapor contaminated natural gas.

## 1.3 Hypotheses

1. Ag embedded on supports ($TiO_2$ and GAC) could enhance the capture of mercury vapor.
2. Surface area could play an important role in mercury vapor adsorption.

## 1.4 Scopes of the research

1. Adsorbate: Only Hg in vapor form is considered in this study.
2. Adsorbent: Titanium dioxide ($TiO_2$) and granular activated carbon (GAC) are used as adsorbent supports. They will be modified by loading with Ag. Silver precursor in this study is silver nitrate ($AgNO_3$).
3. Preparation: Wet impregnation method is used to synthesize the adsorbents. Ag loadings considered are 5% and 15% by weight.
4. Removal testing: Both static batch and flow systems are performed.

## 1.5 Expected outcomes

1. Mercury vapor adsorption capacities by the synthesized adsorbents are higher than commercial adsorbents.
2. The adsorbents can be prepared in a simple process, providing cost effectiveness compared to existing commercial adsorbents.

# CHAPTER II

# BACKGROUND AND LITERATURE REVIEW

## 2.1 Natural gas

Natural gas is a combustible mixture of hydrocarbon gases composed primarily of methane ($CH_4$). Natural gas processing produces very valuable by–products such as natural gas liquids (NGLs), including ethane($C_2H_6$), propane ($C_3H_8$), butane ($C_4H_{10}$), iso–butane ($C_4H_{10}$), pentane ($C_5H_{12}$), naphtha and natural gasoline. It also contains acid gases ($CO_2$, $H_2S$, $CH_3SH$, and $C_2H_5SH$), other gases ($N_2$ and He), water vapor ($H_2O$), and mercury (Hg) (Speight, 2007). Figure 2.1 shows the components of natural gas and NGLs.

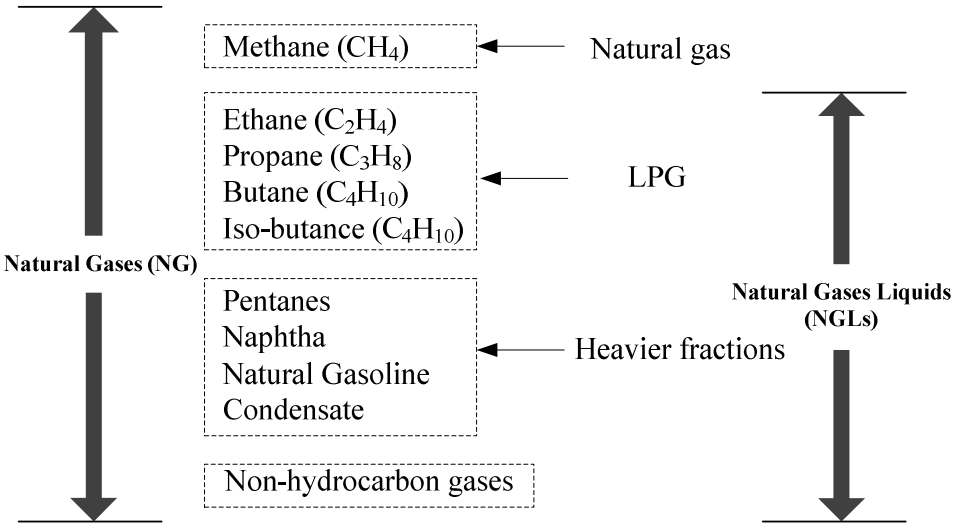


**Figure 2.1** The compositions of natural gas.

### 2.1.1 Natural gas processing plants

Industrial gas plants varies considerably in shape and size–from a simple gas receiving and letdown terminal to a full gas processing facility with NGL extraction and sulfur recovery (Megren, 2012). In order to define the type of gas processing plant and its different treating units, the products to be obtained and its specifications

should be fixed, where the quantity and type of feed impurities determine the necessary treatment steps.

Figure 2.2 shows a typical scheme for most gas processing plants designed to produce pipeline gas from sour gas. Each process operation module consists of a single piece or a group of equipment performing a specific function (Manning and Thompson, 1991). All the modules will not necessarily be present in every gas plant. However, the actual processes used depend on the feed–gas composition and the sales specifications for both the gas and liquid products (Mokhatab et al., 2006). The choice of process modules to be used and their arrangement are determined during the design stage of each gas–field development project.

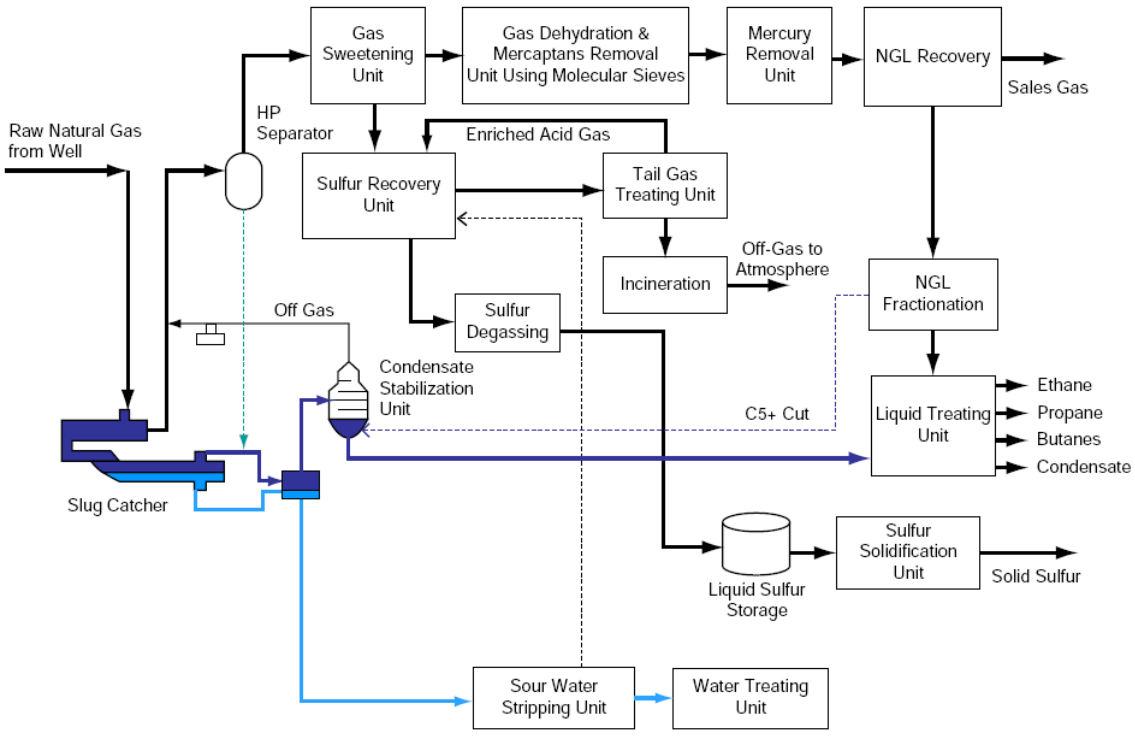


**Figure 2.2** Typical schemes for natural gas and NGL processing.
(Mokhatab and Poe, 2012)

In general, there are several pollutants in a natural gas processing plant. The EARTHWORKS (2006) presents a list of these pollutants both in vapor and liquid phases as shown in Table 2.1.

**Table 2.1** Pollutant and their sources in natural gas processing.

| Pollutant | Hazards | Source |
|---|---|---|
| BTEX (Benzene, Toluene, Ethylbenzene and Xylenes) | Benzene is a known carcinogen. Toluene may affect the reproductive and central nervous systems. Ethylbenzene and xylenes may have respiratory and neurological effects. | - Venting of natural gas<br>- Pits<br>- Produced water<br>- Dehydration |
| $CH_4$ (Methane) | Methane has an explosive nature. | - Venting of natural gas<br>- Dehydration |
| Diesel fuel (A complex mixture of hydrocarbons) | Both fuel and exhaust contains carcinogenic substances like benzene and Polycyclic Aromatic Hydrocarbons (PAHs). | - Stimulation fluids<br>- Oil-based drilling muds<br>- Engines/heavy equipment |
| $H_2S$ (Hydrogen sulfide) | Aggravates respiratory conditions, and affects neurological system, cardiovascular system and can cause problems in the central nervous system. | - Venting and flaring of natural gas (if present in the oil and gas formations)<br>- Migration from soils |
| Metals (Arsenic, Barium, Cadmium, Chromium, Lead, **Mercury**, Selenium, Zinc and others) | Each metal poses different health hazard. Possible toxic effects include skin problems, hair loss, kidney damage, high blood pressure, increased cancer and neurological damage risk, and others. | - Drilling muds<br>- Stimulation fluids<br>- Pits<br>- Produced water<br>- Venting and flaring<br>- Diesel exhaust |
| $NO_x$ (Nitrogen oxides) | Reacts with Volatile Organic Compounds (VOCs) to form ground-level ozone and smog, which can trigger respiratory problems. Reacts with other | - Compressor engines<br>- Flaring<br>- Diesel and natural gas engine exhaust |

| Pollutant | Hazards | Source |
|---|---|---|
| | chemicals to form particulate pollution, which can damage lungs and cause respiratory illness, heart conditions and premature death. Reacts with common organic chemicals to form toxics that may cause biological mutations. | |
| PAHs (Polycyclic Aromatic Hydrocarbons) | Several agencies have classified some PAHs as probable or possible carcinogens. Animal studies show reproductive effects. | - Diesel exhaust<br>- Flaring<br>- Pits |
| Partic–ulate matter Small particles suspended in air. | Can be inhaled and cause health effects like respiratory ailments, aggravation of asthma and allergies, painful breathing, shortness of breath, chronic bronchitis and premature death. May combine with other air pollutants to aggravate health problems. Some particulates, such as diesel exhaust are carcinogenic. | - Diesel exhaust<br>- Pits (dust from)<br>- Venting and flaring |
| $SO_2$ (Sulfur dioxide) | Reacts with other chemicals to form particulate pollution, which can damage lungs and cause respiratory illness, heart conditions and premature death. | - Diesel and natural gas engine exhaust<br>- Flaring |
| VOCs, include BTEX formaldehyde and others. | React with $NO_x$ to form ground-level ozone and smog, which can trigger respiratory problems. Can cause health problems such as cancer. | - Venting and flaring of natural gas<br>- Pits<br>- Oily wastes<br>- Diesel and natural gas engine exhaust<br>- Compressors |

### 2.1.2 Natural gas pretreatment systems

In the conventional NGL recovery plants, feed gas must be pretreated to remove acid gases, water, and mercury to produce a purified gas suitable for liquid recovery.

The typical specification to be met is $H_2S$ removal to less than 4 ppmv, $CO_2$ to less than 1%–2%, water to less than 10 ppmv, and mercury to levels of 0.01 mg/$Nm^3$ (Mokhatab and Poe, 2012) Natural gas processing plants, pollutant substances which must carry out reduction using special technique would like to use natural gas as mainly a feedstock for reformers. Typically natural gas pretreatment consists of mercury removal, acid gas sweetening and natural gas drying in molecular sieve adsorbents (Petersen et al., 2011) as shown in Figure 2.3. Depending on the downstream processing steps and the concentration of the sour gas components, it may be necessary to remove $H_2S$ and $CO_2$ from the natural gas. They can be removed along with water through adsorption. Mercury removal on the other hand usually involves utilization of mercury guard beds to protect people and equipment.

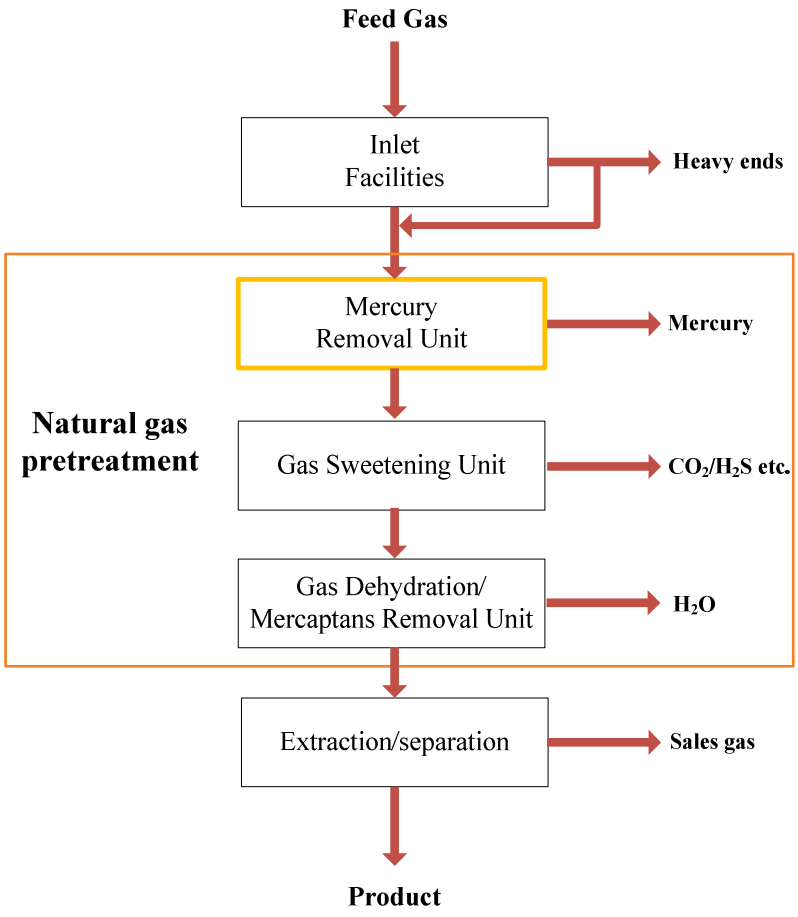


**Figure 2.3** Pretreatment of natural gas (LINDE, 2012).

The derivatives of Hg are the major contaminants in natural gas. Mercury removal unit (MRU) in the natural gas processing plant has gained importance due to environmental concerns which propelled many countries to put a limit on Hg emission. Pretreatment of natural gas involves a single MRU while another processing pretreatment has multiple units such as acid and mercaptans.

## 2.2 Mercury (Hg)

Mercury is a chemical element classified as a heavy metal with the symbol Hg. It is the only metal that is known to exist in liquid form at room temperature and hydrophobic by nature. It is found in different valent to, such as +2 (mercuric), +1 (or mercurous), and 0 (elemental) (ATSDR, 1999). It is toxic and volatile. The properties of Hg are shown in Table 2.2.

**Table 2.2** Physical properties of elemental Hg (USEPA, 2001)

| Property | Element facts |
|---|---|
| Atomic Number | 80 |
| Atomic weight | 200.59 amu |
| Atomic protons/electrons | 80 |
| Atomic neutrons | 121 |
| Boiling point | 356.58˚C |
| Crystal structure | Rhombohedral |
| Density | 13.456 g/cm$^3$ at 20˚C |
| Saturation vapor pressure | 0.16 N/m$^3$ (pas cal) at 20˚C |

Hg has high boiling point and relatively high vapor pressure. The vapor pressure data of mercury is important in determining its feasible concentrations from triple point to critical point.

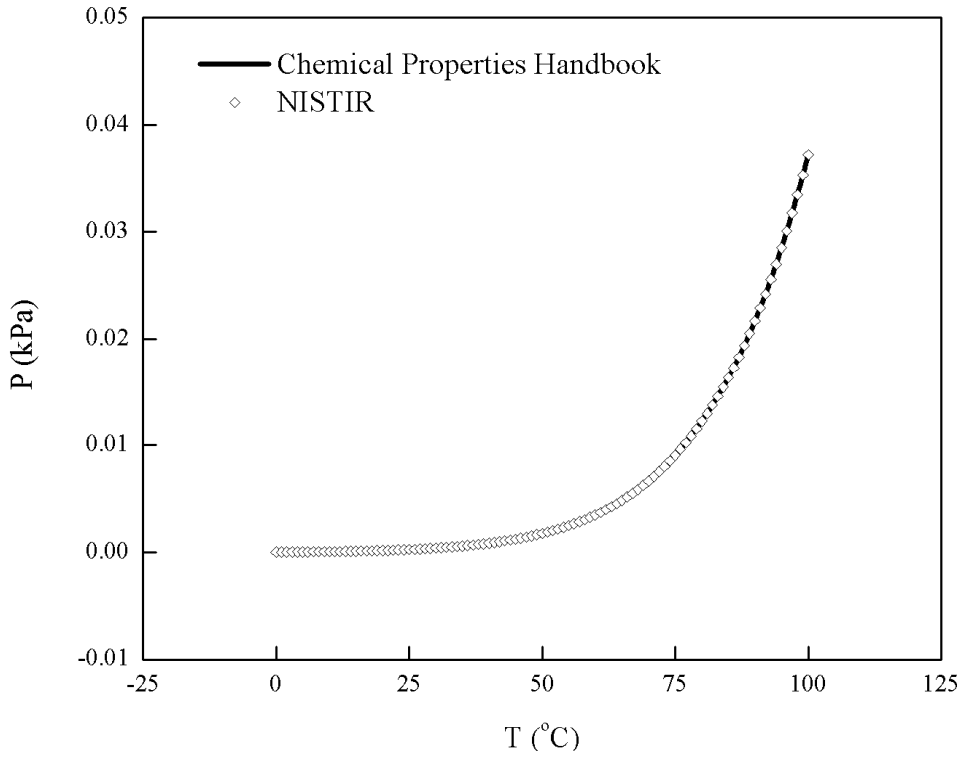


**Figure 2.4** Temperature dependence of the vapor pressure of saturated liquid Hg. (Yaws, 2003 and Huber et al., 2006)

The equation is Wagner–type form (Huber et al., 2006), where the terms of the equation are selected using a simulated annealing optimization algorithm as shown in Figure 2.4. To improve the reliability of the equation at low temperatures, heat-capacity data were used in addition to vapor–pressure data.

### 2.2.1 Sources of Hg

The main source of human exposure to mercury is coal smoke. Useful mercury-based materials (thermometers, street lamps, cosmetics, electrical batteries and dental silver amalgam fillings) also emit residual mercury when discarded (Reilly et al., 2010).

#### 2.2.1.1 Mercury in water

Phase of liquids, Hg in air finally passes into rivers, lakes and oceans after travelling long distances together with wind as show in Figure 2.5. Mercury

contaminating rain ground and seawater poses both health and environmental hazards. Normally, Hg has valance states of +2, +1, and 0 in natural waters. In anaerobic sediments, the solubility product of HgS is a variety of redox state and chemical transformations are of environmental significance so low that Hg(II) (aqueous phase) is below detection limits. On the other hand, in aerobic waters Hg is toxic to aquatic biota as well as humans. In humans, it binds sulfur groups in recycling amino acids and enzymes, rendering them inactive (Schnoor, 1996). Bioconcentration in fish, shellfish, and humans is a major problem evidenced by the Minimata Bay disaster in Japan where more than 900 people died and 2 million suffered health problems such as permanent neurological damage when they ate mercury contaminated fish (McCurry, 2006).

In the marine environment, submicron clay particles are distributed throughout the oceans because of slow setting. Pelagic organisms agglomerate and excrete the mercury–bearing clay particles, thus promoting sedimentation as one sink of Hg from the mid–oceanic food chain. Another source of Hg to biota is uptake of dissolved Hg by phytoplankton and algae.

#### 2.2.1.2 Mercury in air

Hg is released into air by outgassing of soil, transpiration and decay of vegetation, and man-made emissions. Most Hg is adsorbed onto atmospheric particulate matter or in elemental gaseous state.

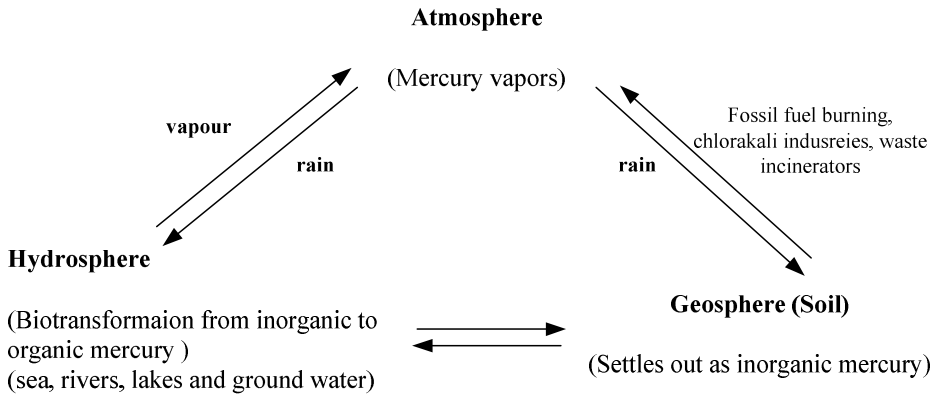


**Figure 2.5** Mercury and environment (Zahir et al., 2005).

Figure 2.5 shows how mercury is transported and transformed in the environment. Hg vapor is the primary source of the contamination in the environment. Both natural and man–made mercury emissions are in its inorganic form which is metallic mercury vapor. Mercury vapor is carried off to great distances by wind and eventually falls in water bodies. In the aquatic environment, inorganic mercury is microbiologically transformed into lipophilic organic compound, methyl mercury (Eisler, 1987). This transformation makes mercury more prone to biomagnifications in food chains.

### 2.2.2 Toxicity of mercury

There have been animal and plant studies dedicated of mercury toxicity. The effects of exposure to any hazardous substance depend on the dose, the duration, kind of exposure, personal traits and habits, and whether other chemicals are present.

#### 2.2.2.1 Toxicity in human

Mercury is a volatile element. When it is saturated in air, it diffuses into the blood and accumulates in liver, kidneys, brain, spleen and bone (Wụ et al., 2010) causing many health problems. There are several ways in which humans can be exposed to mercury: breathing contaminated air, ingesting contaminated water or food, and having skin contact with mercury. However, not all forms of mercury can easily enter the human body, so for safety reasons, it is important to know which form of mercury a person has been exposed to as well as the route of exposure (air, food, or skin).

***Effect to organisms*** (ATSDR, 1999)

Short–term exposure (hours) to high levels of metallic mercury vapor in the air can damage the lining of the mouth and irritate the lungs and airways, causing tightness of the chest, a burning sensation in the lungs, and coughing. Other effects from exposure to mercury vapor include nausea, vomiting, diarrhea, increases in blood pressure or heart rate, skin rashes, and eye irritation.

The nervous system is very sensitive to mercury. Different forms of mercury have different effects on the nervous system, because they do not all move

through the body in the same way. When metallic mercury vapors are inhaled, they readily enter the bloodstream and are carried throughout the body and can move into the brain. Breathing in or swallowing large amounts of methyl mercury also results in some of the mercury moving into the brain and affecting the nervous system. Inorganic mercury salts, such as mercuric chloride, do not enter the brain as readily as methyl mercury or metallic mercury vapor. There are reported incidents in other countries where people who ate fish contaminated with large amounts of methyl mercury or seed grains treated with methyl mercury or other organic mercury compounds developed permanent damage to the brain. Permanent damage to the brain has also been shown to occur from exposure to sufficiently high levels of metallic mercury. Whether exposure to inorganic mercury results in brain or nerve damage is not as certain, since it does not easily pass from the blood into the brain. Metallic mercury vapors or organic mercury may affect many different areas of the brain and their associated functions, resulting in a variety of symptoms. These include personality changes (irritability, shyness, and nervousness), tremors, changes in vision (constriction or narrowing of the visual field), deafness, muscle in coordination, loss of sensation, and difficulties with memory.

The kidneys are also sensitive to the effects of mercury. Mercury accumulates in the kidneys which entail higher exposure and thus causing more damage. All forms of mercury can cause kidney damage if large amounts enter the body. If the kidneys are exposed to small amounts of mercury only, it is likely to recover once the body clears itself of the contamination.

Levels of metallic mercury in workplace air are much greater than the levels normally encountered by the general population. Current levels of mercury in workplace air are low due to increased awareness of mercury's toxic effects. Because of the reduction in the allowable amount of mercury in workplace environment, fewer workers are expected to have symptoms of mercury toxicity. Most studies on humans who breathed metallic mercury vapor for a long time indicate that mercury from this type of exposure does not affect the ability to have children. Studies in workers exposed to metallic mercury vapors have also not shown any mercury–related increase in cancer.

#### 2.2.2.2 Toxicity in gas plants

In gas plants, Hg is present in a few parts per billion. Mercury compounds can be found in both organic and inorganic forms. These compounds pose health and safety hazards in gas plants. For instance, mercuric chloride ($HgCl_2$), methyl mercuric chloride ($CH_3HgCl$), dimethyl mercury ($CH_3HgCH_3$), diethyl mercury ($C_2H_5HgC_2H_5$) can cause damage to process equipment (aluminum heat exchangers commonly used in LNG plants, cryogenic hydrocarbon recovery plants, and petrochemical plants) (Marsch, 1990). It can also potentially compromise the health and safety of plant operators. In petrochemical plants, mercury can deactivate downstream catalyst. In case, if Hg is allowed to reside in a natural gas plants uncheck which Hg has caused an ammonia production gas plant explosion (Eckersley, 2010). Petrochemicals Processing Plant of Thailand (PTT) has assigned Hg (vapor) a threshold limit value (TLV) of 0.0001 mg/$Nm^3$ of air as a time–weight average (TWA) for a normal 8–hour per workday and a 40–hour per workweek. Mercury removal, in this particular case, is required to be done on the raw feed gas (Figure 2.3). The main concern; therefore, is how to treat natural gas that is not necessarily bone dry.

### 2.2.3 Mercury removal methods in gas plants

There are several methods to remove Hg. The removal methods below are applicable for Hg in vapor phases only (Louie, 2008)**.**

Outokumpu process

Hg reacts with $H_2SO_4$ (aq.) at 150–180°C forming $HgSO_4$ precipitant, as shown in eq. (2.1). The reaction takes place in a scrubber. $HgSO_4$ precipitate is further separated.

$$Hg\ (g) + H_2SO_4\ (aq) + 0.5O_2\ (g) \longrightarrow HgSO_4\ (s) + H_2O\ (l) \qquad (2.1)$$

Bolkem process

Hg is taken in drying tower which reacts with $H_2SO_4$ to form $HgSO_4$. After that, $HgSO_4$ is reacted with Hg at 50°C to form $Hg_2SO_4$, as shown in eq. (2.2).

$$HgSO_4\ (s) + Hg\ (g) \longrightarrow Hg_2SO_4\ (s) \qquad (2.2)$$

Selenium filter process

Selenium filter process can remove approximately 90% of the total mercury vapor however this process is suitable for low Hg concentration only. The selenium filter, which contains porous inert material, is soaked with selenium acid. The acid is then dried; red amorphous selenium precipitate is obtained. This red amorphous selenium precipitate can react with mercury vapor to form HgSe. The mechanism of this process is shown in eq. (2.3–2.5).

$$SeO_2\ (aq) + H_2O\ (l) \longrightarrow H_2SeO_3\ (aq) \quad (2.3)$$

$$H_2SeO_3\ (aq) + H_2O\ (l) + 2SO_2\ (aq) \longrightarrow Se\ (s) + 2H_2SO_4\ (aq) \quad (2.4)$$

$$Hg\ (g) + Se\ (s) \longrightarrow HgSe\ (s) \quad (2.5)$$

Boliden−norzink process

This process involves oxidation of mercury vapor by mercuric chloride to form mercurous chloride (calomel). Mercuric chloride ($HgCl_2$) is circulated over a packed tower. When mercury contaminants in the gas passes through the packing, the mercury reacts with chloride to form mercurous chloride, as shown in eq. (2.6).

$$HgCl_2\ (aq) + Hg\ (g) \longrightarrow Hg_2Cl_2\ (s) \quad (2.6)$$

Sulphide precipitation

The operation amount of hydrogen sulphide ($H_2S$) gas is injected into the gas phase. After that, it reacts with mercury to form mercury sulphide (HgS). The mercury sulphideis separated by using drying tower, as shown in eq. (2.7–2.9).

$$2H_2S\ (g) + SO_2\ (aq) \longrightarrow 3S\ (s) + 2H_2O\ (l) \quad (2.7)$$

$$S\ (s) + Hg\ (g) \longrightarrow HgS\ (s) \quad (2.8)$$

$$H_2S\ (g) + Hg\ (g) \longrightarrow HgS\ (s) + H_2\ (g) \quad (2.9)$$

Carbon filter

The most popular method in removing mercury in gas phase is by adsorption using activated carbon. However, this method is suitable for low concentration of mercury only.

However, there methods are not cost effective. Except, carbon filter method and the adsorption of Hg over modified carbon filter material is focused in this study.

## 2.3 Adsorption

Adsorption is the process by which certain components of a fluid (liquid or gas) phase are transferred to and held at the surface of a solid. Moreover, the adsorption processes is classified into 2 types, physisorption and chemsorption (Jose, 2009). Physisorption is the most common form of adsorption. The molecules are adsorbed by Van Der Waals forces, and attached themselves to the surface of the solid. The molecules remain intact, and can be freed easily (the forces are small, and short–ranged). In chemisorption, on the other hand, the molecules undergo a chemical bonding with the molecules of the solid. This attraction is stronger than the force holding the solid together. If the molecules are removed, they are formed to different compounds.

### 2.3.1 Adsorption mechanism

The adsorption mechanism involves four steps (Horikawa and Nicholson, 2011): 1) Bulk solution transport; the adsorbate is transported from bulk solution to the boundary layer of the wastewater surrounding the adsorbent, 2) Film diffusion transport; the adsorbate is transported by molecular diffusion through the boundary layer surrounding the adsorbent particles, 3) Pore transport; after passing through the boundary layer, the adsorbate is transported through the pores of the adsorbent to the available adsorption sites, as shown in Figure 2.6 and 4) Adsorption; when the adsorbate reaches the adsorption site, a bond is formed between the adsorbate and the adsorbent.

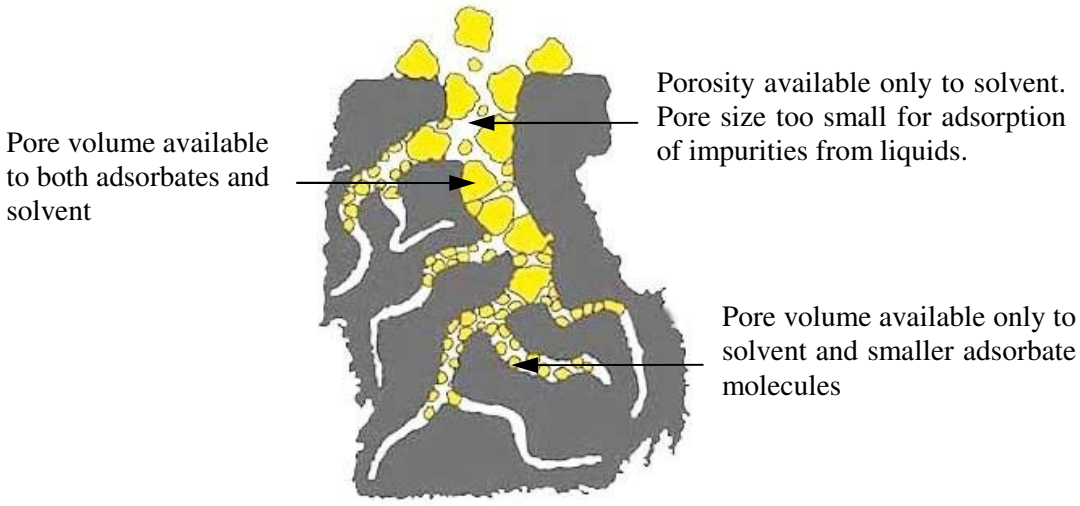


**Figure 2.6** Porous volume of adsorbate (Nisakorn Saengprachum, 2009).

Normally, the gas adsorption capacity is highly dependent on two factors: *Surface area of the adsorbent* (the adsorption capacity will be increased with the more surface area of adsorbent) and *functional group* (it is specific groups of atoms within molecules that are responsible for the characteristic chemical reaction of those molecules).

### 2.3.2 Kinetic adsorption

Chemical thermodynamics are correlation with energy and heat. These theories were able to predict the order reaction, trend of reaction and describe for how to generate of product at state of equilibrium was focused on. Chemical kinetics was study to relate between ratio of reaction from mechanism and factor such as temperature, concentration and catalyst.

Definition of chemical kinetics

1. Rate of change is transition of physical vs time such as distance pressure volume or height per time.
2. Rate of reaction is the lost of initial amount per unit time or amount of product generated per unit time.

3. Rate law is equation relations of initial concentration, rate constant and order of reaction that called differential rate law or differential rate equation.
4. Order of reaction is logarithm number in term of concentration which this number is come from the experimental (i.e. zero, fraction or minus).

The resistance to internal diffusion can be significant. However, the local rate of adsorption is assumed to be relatively fast and the resistance to external diffusion is experimentally controlled to be negligible, compared to the intraparticle diffusion (Tsai et al., 2006). For the interpretation of the kinetic batch experimental data three different kinetic models were used (Caliskan et al., 2011): (1) the pseudo–first order kinetic model (2) the pseudo–second order kinetic model (3) the intraparticle diffusion model.

#### 2.3.2.1 Pseudo–first order kinetic equation

This well–known kinetic equation was first extensively employed by Ho and McKay (1999) and may be expressed as:

$$\frac{dq_t}{dt} = k_1\left(q_e - q_t\right) \tag{2.10}$$

Where $q_e$ and $q_t$ are the amount of solute adsorbed per unit amount of adsorbent at equilibrium and any time, $t$, respectively (mg/g) and $k_1$ is the pseudo–first order rate constant (hour$^{-1}$). Integrating eq. (2.10) employing the boundary conditions that at $t$=0, $q_t$=0, and that at $t$=$t$, $q_t$=$q_t$, the linear form of the equation become:

$$\ln\left(q_e - q_t\right) = \ln q_e - k_1 t \tag{2.11}$$

The adsorption rate constant, $k_1$ (min$^{-1}$), can be obtained from the slope of the linear plot of $\ln(q_e - q_t)$ versus $t$. The reaction of first order is not dependent on initial concentration.

#### 2.3.2.2 Pseudo–second order kinetic equation

The pseudo-second order kinetic equation is:

$$\frac{dq_t}{dt} = k_1\left(q_e - q_t\right)^2 \tag{2.12}$$

Where $k_2$ is the pseudo-second-order rate constant [g/mg-hour]. On integration, employing the conditions that at $t = 0$, $q_t = 0$ and that at $t = t$, $q_t = q_t$, this equation can be re–arranged to give the linear form:

$$\frac{t}{q_t} = \frac{1}{k_2 q_e^2} + \frac{t}{q_e} \tag{2.13}$$

The plot of $t/q_t$ versus $t$ gives a linear relationship, which allows the values of $q_e$ and $k_2$ to be computed. The reaction of second order is relies on ration of initial concentration.

#### 2.3.2.3 Arrhenius equation

The activation energy value is obtained from the Arrhenius equation using the $k_1$ and $k_2$ values at different temperatures (Shafey, 2010). The following relationship can be obtained:

$$\ln k = \frac{-E_A}{R}\left(\frac{1}{T}\right) + \ln A \tag{2.14}$$

Where k is the rate constant k of chemical reaction on the absolute temperature, T is temperature (K), A is the pre–exponential factor (frequency), $E_A$ is the activation energy (kJ/mol), and R is the universal gas constant (8.314 J/mol-K).

### 2.3.3 Breakthrough and adsorption capacity

The breakthrough curve represents the evolution of the solution concentration in function of adsorption parameter such as contract time between liquid and solid

phase, solvent concentration ($C$) and temperature ($t$). The typical breakthrough curve is usually expressed by plotting the ratio of outlet to inlet adsorbate concentration ($C/C_0$) as a function of time ($t$). The breakthrough curve is expected to be S-shaped, similar with the one (Rahman et al., 1994) shown in Figure 2.7. It depicts a typical breakthrough curve where the column capacity is fully utilized. The concentration at breakthrough point is chosen arbitrarily at some low value, $C_b$. When the effluent concentration $C_x$ is approaching 90% of $C_0$ (inlet adsorbate concentration) then the adsorbent is considered to be essentially exhausted.

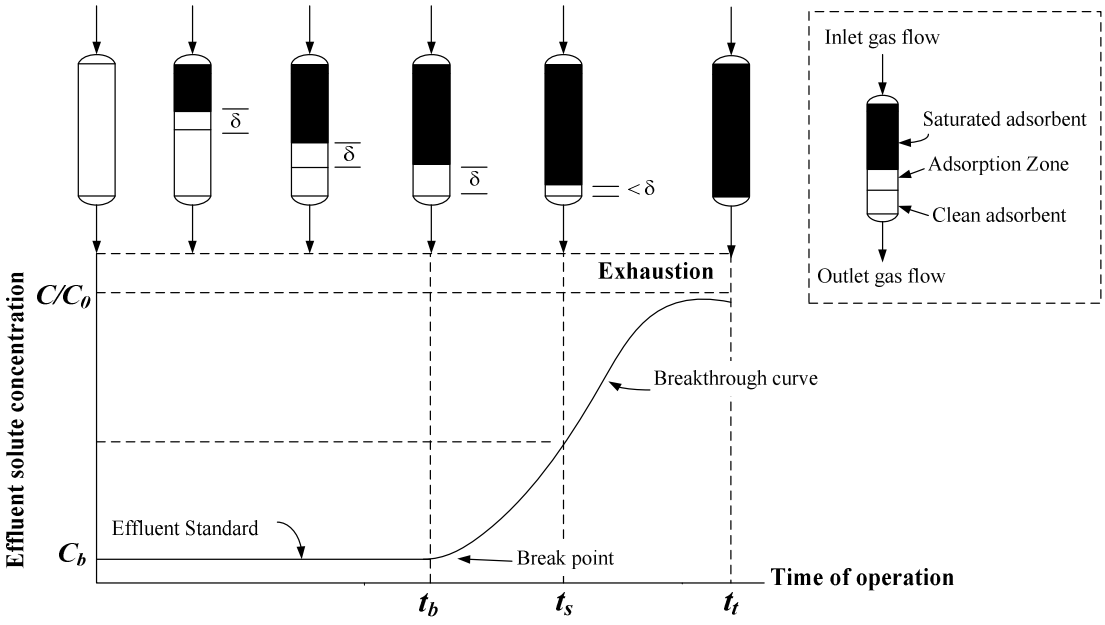


**Figure 2.7** Typical breakthrough curve and capacity (Rahman et al., 1994).

The maximum allowable outlet gas concentration ratio at break point ($t_b$) is calculated from eq. (2.15). The adsorption steps are discontinued at break point. If the adsorption were to be continued for $t > t_b$, the outlet gas concentration will rise rapidly, eventually approaching to the initial concentration as the entire bed becomes saturated ($t_t$) (eq. (2.16)). The saturated time is required to $C/C_0$.

$$t_b = \int_0^{\infty} \left(1 - \frac{C}{C_0}\right) dt \tag{2.15}$$

$$t_t = \int_0^{t_b} \left(1 - \frac{C}{C_0}\right) dt \tag{2.16}$$

The steepness of the breakthrough curve determines the extent to which the capacity of an adsorbent bed can be utilized**.** Thus, the shape of the curve is very important in determining the length of the adsorption bed. In actual practice, the steepness of the concentration profiles shown previously can increase or decrease, depending on the type of adsorption isotherm involved.

The current methods for removing Hg from natural gas use fixed beds with Hg removal materials. The gas flows through the fixed bed. Hg reacts with the reactive reagent in the Hg removal material and stays in the column, while the effluent gas is mercury–free. There are two types of Hg removal materials: non–regenerative mercury sorbents, and regenerative mercury adsorbents (amalgam).

## 2.4 Amalgam

Most dental amalgams are called silver amalgams since silver is the principal constituent that reacts with mercury. A conventional dental amalgam alloy will contain of approximately 50% mercury (Hg), 35% silver (Ag), 13% lead (tin), 1.4% Cupper (Cu) and 1% Zinc (Zn) (Henderson et al., 2001). An amalgam alloy is mixed with mercury in a process known as “Trituration”. During the process of trituration, the surface layer of the Ag–Sn alloy dissolves in the liquid mercury, and there is a reaction that leads to the formation of new phases. These new phases are solid, and their formation causes the plastic amalgam paste to solidify (Okabe, and Mitchell, 1996). A number of metallurgical phases are involved in this transformation as shown in eq. (2.17).

$$\underset{(\gamma)\ \text{powder}}{Ag_3Sn} + \underset{\text{Mercury liq.}}{Hg} \longrightarrow \underset{(\gamma)\ \text{Unreacted alloy}}{Ag_3Sn} + \underset{(\gamma_1)\ \text{amalgam}}{Ag_2Hg_3} + \underset{(\gamma_2)\ \text{matrix}}{Sn_2Hg} \qquad (2.17)$$

## 2.5 Adsorbents

Cost is an important issue in adsorbent–based processes for removing Hg from natural gas. The raw material was used several chemicals under ambient conditions such as gold, zinc, aluminum, copper and silver readily form amalgam with elemental mercury. The solubility of these metals in elemental mercury is relatively low. With zinc, it is high solubility and gold is very expensive. Aluminum copper and silver have even lower solubility than all them.

### 2.5.1 Precursors (Silver, Ag)

Ag is general inorganic chemicals but it is considered as the relatively cheap noble metal (Li et al., 2011). In order to make adsorbent holding for Hg removal more feasible, it is necessary to either reduce the amount of adsorbent needed, or decease the cost of adsorbent production. Thus, Ag loaded onto support can enhance the adsorption activity.

### 2.5.2 Support material

Titanium dioxide ($TiO_2$) and granular activated carbon (GAC) were investigated in this study because both are low cost. These supports have different surface area in order to compare the capacity adsorption of Hg effectively.

#### 2.5.2.1 Titanium dioxide ($TiO_2$)

From many recent studies, the applied use of titanium dioxide ($TiO_2$) or titania has been investigated as a support for moderate surface area. Generally, the titanium dioxide has been presented in three main structures of their crystalline forms (anatase, rutile, brookite) due to its arrangements of oxygen and titanium atom (Yasushiro and Takayuki, 2008).

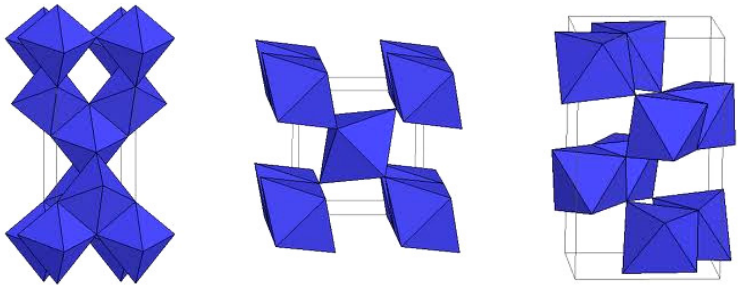

**Anatase** **Rutile** **Brookite**

**Figure 2.8** Arrangement of $TiO_2$ crystal structures (Nguyen–Phan, 2011).

#### 2.5.2.2 Granular activated carbon (GAC)

Granular activated carbon (GAC) produced from coconut shell is widely used for adsorption. This GAC are PlAO 8/30 grade and has a particle size distribution 1.86–2.34 mm. This material is used by Carbokarn Co., Ltd in Thailand. As shown in Figure 2.9, there are three main forms of activated carbon. Among these, GAC has been investigated to have the highest surface area.


**Figure 2.9** Arrangement of GAC types (Carbokarn Co., Ltd).

## 2.6 Literature review

The literature for vapor phase Hg is quite limited. The explanation in this section is then based on liquid Hg adsorption improvement. There are many techniques for adsorbent preparation such as modification, graft, and addition of metals on supports.

Expanded perlite (EP), modified adsorbent was studied in a batch experiment. It was found that the liquid Hg(II) uptake on EP was 0.35 mg/g at pH 6.5 within 180 minutes and it was corresponding Langmuir isotherm model. Expanded perlite was able to adsorp Hg(II) partially form aqueous solution less than 50% adsorption. The result was also estimated in terms of kinetic characteristics of adsorption and it was followed pseudo–second order kinetics. This reaction was identified to be exothermic at 20 to 50 degree Celsius (Ghassabzadeh, 2010). To enhance the adsorption capacity, chitosan was modified by Amino–terminated hyperbranched polyamidoamine polymers. The maximum adsorption capacity was corresponding to the optimum pH equal to 5. Using Langmuir isotherm model, maximum adsorption capacity of chitosan modified was found to be 400–500 mg/g for Hg(II) ions. The kinetics model demonstrated that the adsorption system of Hg(II) ions on chitosan observed pseudo–second–order rate model. Most of adsorption system illustrated endothermic, monolayer and chemical adsorption at higher temperature (Ma et al., 2009). Alternative adsorbent was carbonaceous generated by rice husk, cheap agricultural waste. This sorbent was prepared through $H_2SO_4$ treatment and ion exchange technique. The optimum adsorption capacities were found to be 303.03 mg/g and 384.62 mg/g (45°C and pH 6) of sulfuric acid treated rice husk dry and wet, respectively. Hg(II) ions showed a slow sorption kinetic than following pseudo–second order model. Activation energy presented approximately 54 kJ/mol for mercury ions that sorption indicating chemically controlled process (Shafey, 2010).

Graft adsorption was studied on Hg for initial concentration equal to 140 mg/L Hg(II) ions at pH 4. Clay grafted with 2–(3–(2–aminoethylthio) propylthio) ethanamine (AEPE) AEPE-montmorillonite and AEPE-hectorite were able to adsorb 46.1 and 54.7 mg/g, respectively (Phothitontimongkol et al., 2009). As seen, the adsorption is not improved much. Moreover, aromatic ligands are effective at

accelerating Hg in liquid phases and with all ligands and ratios was able to adsorp Hg at least 90% (Hutchison et al., 2008).

Pollution from coal–fired plants was controlled Hg emission. Calcium–based sorbent was applied removal of Hg and with study under conditions prevalent in coal–fired utilities. The result found Ca–based sorbent uptake of Hg(0) and $HgCl_2$ approximately 40% at 100°C and less than 10%, respectively (Ghorishi et al., 1998). The roles of wet scrubbers was removal of Hg (gas phases) from coal–fired power plants. The efficiency rise up to 75% was achieved with relationship between pH, sulfur dioxide concentration and slurry concentration (Somoano et al., 2007). Furthermore, flue gases were contaminated Hg and it was treated by zeolites sorbent and activated carbon with operating unit were 130–200 °C of temperature, concentration equal to 30–60 pm/$m^3$ and contract time around 2 second (Morency, 2002).

Studies on several compounds loaded onto supports (e.g. $Al_2O_3$**,** $TiO_2$, AC, and zeolite) were conducted. For instance, the studies included sulphur (Harada et al., 2004), metal halide and sulphate **(**Yan et al., 1990), and sulphide form of divalent transition metals (Varma et al., 2010). On the other hand, modified of adsorbents was mesoporous crystalline material–41 (MCM–41), generated from silica. This sorbents was maximum adsorption capacity 1,245 micro-mol/g for Hg(II) (Idris et al., 2011). It is important to note that adsorbents $Ag/SiO_2$ and $CuS/SiO_2/Al_2O_3$ gave higher performance in Hg removal compared with other adsorbents.

# CHEPTER III

# METHODOLOGY

The experiment is divided into two parts. First, adsorbents are prepared by wet impregnation method. These synthesized adsorbents are characterized as well. Second, adsorption of mercury vapor isotherms for each material was described. Figure 3.1 presents the scope and overview of this work.

## 3.1 Materials and apparatus

### 3.1.1 Chemicals

1. Alumina oxide, $Al_2O_3$ (Fluka–Guarantee, Switzerland)
2. Commercial adsorbent (Petroleum of Thailand)
3. Deionized (DI) water (Pure Lab Flex, Thailand)
4. Granular activated carbon, GAC (Carbokarn, Thailand)
5. Elemental mercury, $Hg^o$ (Merck, Germany)
6. Nitrogen 99.5%, $N_2$ (Praxair, Thailand)
7. Silver nitrate 99.88%, $AgNO_3$ (Carlo Erba Reagents, Italy)
8. Titanium dioxide Degussa P25, $TiO_2$ (Aeroxide®, Chaina)

### 3.1.2 Instrument and apparatus

1. General glassware and simple apparatus, including mortar, glove box, and digital balance (Ohaus Pioneer, USA)
2. Ultrasonictransonicbath (Elma, Germany)
3. Oven (WTB Binder, Germany)
4. Furnace (JSMF–30T/ JSR, Korea)
5. Water bath (JSWB–22T/ JSR, Korea)
6. X-ray diffraction, XRD (BrukerAXS:D8 Advance A25, Germany)
7. Field Emission scanning electron microscopy, FE–SEM (JEOL/JSM–6301F, UK)

8. Quantachrome instrumentsAutosorb-1(Quantachrome, USA)
9. Lumex–RA915$^{+}$mercury analyzer (Ohiolumex, USA)

## 3.2 Adsorbent preparation

Two types of materials, titanium dioxide and granular activated carbon, were used as adsorbent supports. Silver was loaded onto the materials by an impregnation technique. Two silver concentrations loading were prepared, 5% and 15% by weight. The Ag precursor used is silver nitrate ($AgNO_3$).

The details of preparation are listed in step by step below;

1. $AgNO_3$ corresponding to 5% and 15% by weight of Ag, was dissolved in DI water by vigorous stirring until the solution was homogeneous.
2. The solutions were gradually dropped onto the supports, titanium dioxide of Degussa P25 ($TiO_2$) and granular activated carbon (GAC) particles.
3. The samples were sonicated for 3 hours.
4. After the loading, the samples were dried at 80°C for 6 hours and ground with an agate mortar.
5. The obtained adsorbents in powdered form were calcined in air at 480°C for 3 hours with the heating rate of 10°C $min^{-1}$.
6. Adsorbent powders were pelletized by a mechanical method.

Figure 3.2 shows the graphical procedure of adsorbent preparation, as described above.

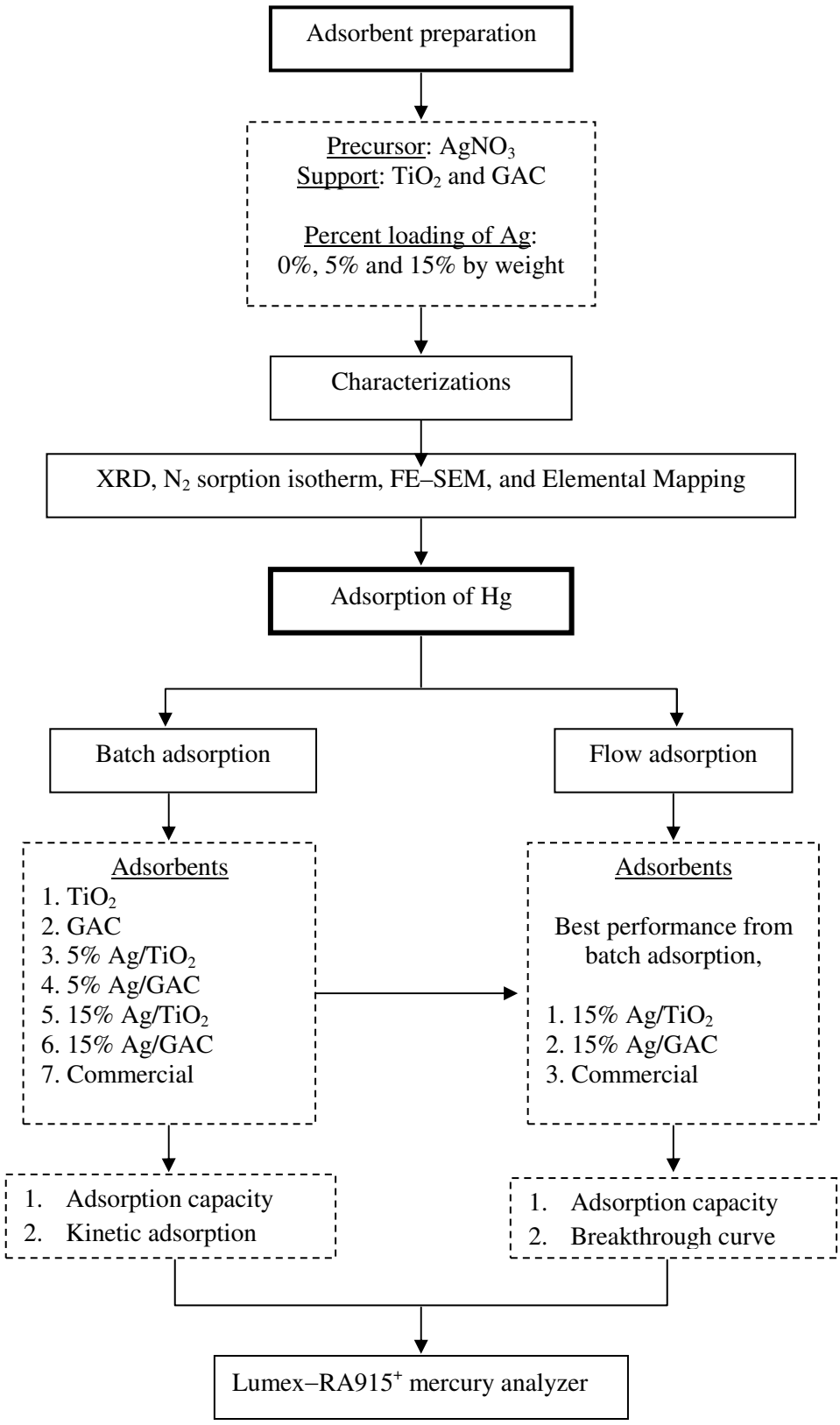


**Figure 3.1** Flow chart diagram of experiment.

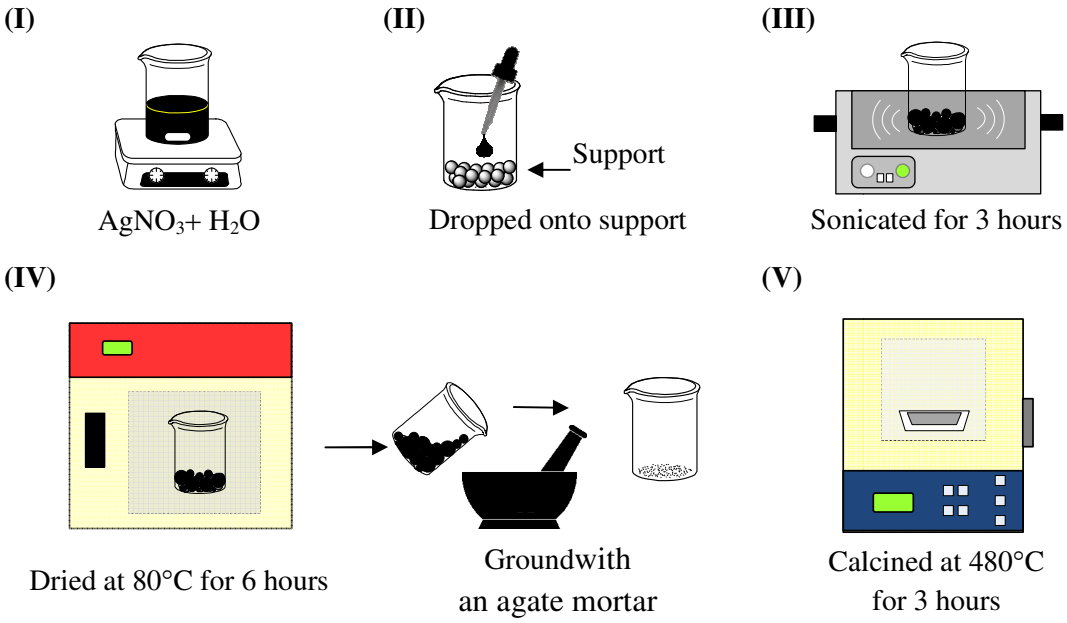


**Figure 3.2** Step–by–step procedures for Ag/supports.

## 3.3 Adsorbent Characterizations

The physical and chemical properties of synthesized adsorbents were examined by various techniques such as XRD, $N_2$ sorption isotherm, FE–SEM, and Elemental Mapping.

### 3.3.1 Structure and crystalline size by X–ray Diffraction (XRD)

The XRD patterns were obtained using radiation on Bruker AXS diffractometer. The X–ray was generated with a current CuKα of 40 mA and a potential of 40 kV. The Ag/$TiO_2$ and Ag/GAC samples were scanned from 10 to 80 degrees ($2\theta$) in steps of 0.02 degrees per second (°/sec). The average crystallite size ($D$) of catalyst was estimated using the Scherrer equation:

$$D = \frac{k\lambda}{\beta \cos\theta}$$

Where, $D$ is crystallite size (nm), $k$ is crystallite shape factor (0.90), $\lambda$ is X-ray wavelength, for CuKα (0.15418 nm), $\beta$ is the full width half maximum (FWHM) of the peak, and $\theta$ is Bragg angle.

### 3.3.2 Specific surface area by Brunauer–Emmett–Teller (BET) Equation

The surface areas of the samples were calculated by BET method at -196°C, using nitrogen as the adsorbate, for relative pressure ($P/P_0$) from 0.02–0.30 with an Autosorb-1 analyzer. Before the measurement, the sample was degassed in vacuum at 250°C for 2 hour. The BET surface area was obtained by fitting the straight part of the $1/[W(P_0/P)-1]$ versus $P/P_0$ curve from the BET equation:

$$\frac{1}{W((P_0/P)-1)} = \frac{1}{W_m C} + \frac{C-1}{W_m C}\left(\frac{P}{P_0}\right)$$

Where, $W$ is the weight of gas adsorbed at a relative pressure, $P/P_0$ is relative pressure, $W_m$ is the weight of adsorbate constituting a monolayer of surface coverage, $C$ is the BET $C$ constant, related to the energy of adsorption in the adsorbed layer and consequently its value is an indication of the magnitude of the adsorbent/adsorbate interactions.

### 3.3.3 Morphology by Field Emission Scanning Electron Microscopy (FE–SEM)

Powdered sample was scattered on an adhesive tape on a brass bar. SEM micrograph was conducted on JEOL (JSM−6301F) scanning microscope equipped with mapping. The sample was then coated with carbon and transferred into the sample chamber. The accelerating voltage was operated at 30 kV. The SEM−Mapping images were analyzed connecting the INCA 350, Oxford.

## 3.4 Mercury adsorption

### 3.4.1 Batch adsorption

Five ml of liquid $Hg^o$ was dropped in sample holders. The holder was installed with a glass–stand to hold an adsorbent, fitted over the $Hg^o$ droplet. Approximately, 0.5 gram of adsorbent was placed on glass–stand. The holder was closed tightly and wrapped with fin film. The holder was placed inside the heating bath throughout the test. Two variables of temperature and time are studied. After the experiment was carried out, adsorbed mercury was determined by a Lumex–RA915$^+$ mercury analyzer. Table 3.1 summarizes adsorption studies in all effects, while batch adsorption setup is illustrated in Figure 3.3.

**Table 3.1** Overall conditions of the batch adsorption

| Conditions | Adsorption capacity | Kinetics adsorption |
|---|---|---|
| Adsorbents | Each adsorbents | 15%Ag/$TiO_2$<br>15%Ag/GAC |
| Controlled temperature (°C) | 40 and 60 | 40 |
| Sampling time | 1, 5, 20, 40, and 60 days | 6.0–240 hours*<br>2.5–20 hours** |

Note * Sampling 15%Ag/$TiO_2$

** Sampling of 15%Ag/GAC

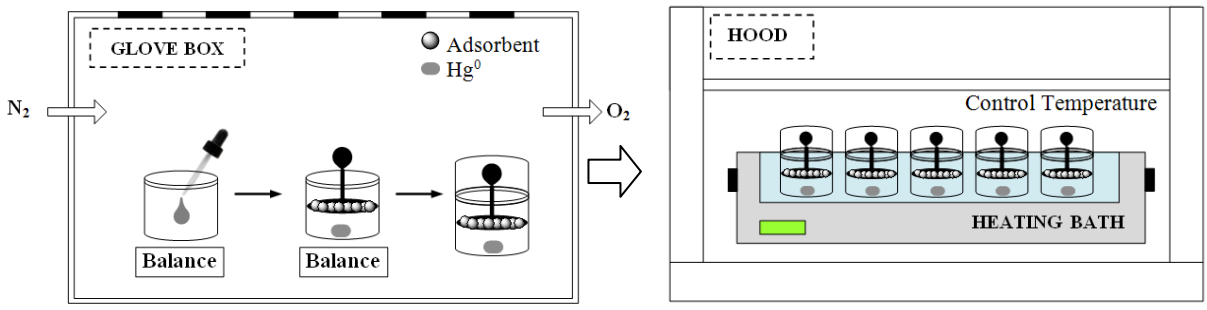


**Figure 3.3** Schematic diagram of the mercury batch adsorption.

### 3.4.2 Flow adsorption

Two adsorbents with high adsorption capacity in mercury capture were selected for further flow experiment. The adsorbents were tested against the commercial adsorbent.

A schematic diagram of flow system is shown in Figure 3.4. Nitrogen, as a carrier gas was flowed with the rate of 10 ml/min (Flow rate 1) through mercury liquid and 110 ml/min for pure nitrogen (Flow rate 2). Nitrogen carried mercury vapor at the certain concentration (Vapor mercury concentration in nitrogen carrier was controlled by the flow rate of nitrogen and temperature of the mercury liquid holder or saturator) and up–flowed to the bed of adsorbent by Teflon–line pipe. The adsorbent was packed in a glasses reactor around five grams. The effluent was monitored its mercury concentration by a Lumex–RA915$^{+}$ mercury analyzer.

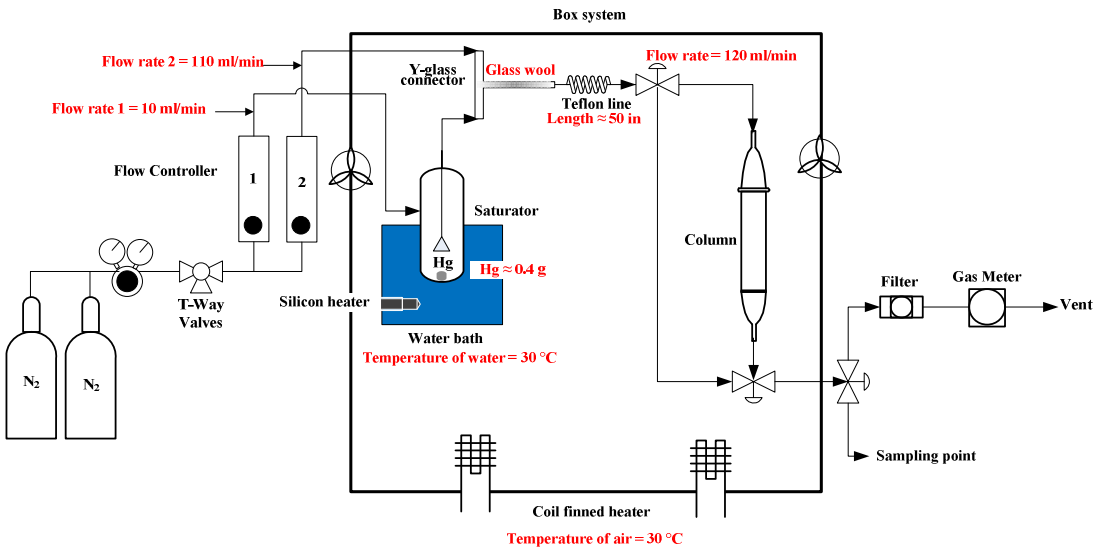


**Figure 3.4** Schematic diagram of the mercury flow adsorption.

# CHAPTER IV

# RESULTS AND DISCUSSION

The removal of Hg in vapor phase using Ag–doped supports as adsorbents was investigated in this research. The supports used were GAC and $TiO_2$. Silver is reactive as tiny particles rather than as a bulk material, thus is desired to have high dispersion of Ag onto the support. The results and discussion are divided into four parts:

- Preliminary testing of Hg adsorption with Ag–impregnated adsorbents
- Characterization of the adsorbents
- Effect of Ag loading on Hg adsorption
- Hg removal in packed column

## 4.1 Preliminary testing of Hg adsorption with Ag–impregnated adsorbents

Element Hg was dropped in sample holders. It was installed with a glass−stand to hold the adsorbent, suitable over the element Hg droplet. Half gram of adsorbent was placed on glass−stand. Afterwards, the holder was closed tightly.

The static sets were put into water bath, and the adsorption of Hg vapor was carried out at 60°C (vapor pressure = 0.0035 kPa). In this condition, mercury concentration is equal to 34.6 $\mu g/m^3$.

Preliminary experiments were conducted to predict whether Ag supported adsorbents can indeed be used for the adsorption of Hg. The two supports GAC and $TiO_2$ exhibits different surface areas, in which GAC has the higher value. 15%Ag/GAC was tested first in comparison with commercially available adsorbent for 40 days as shown in Figure 4.1. It was found out that at 60°C, 15%Ag/GAC adsorbent could adsorb Hg. The graph showed significant difference between the performances of the two adsorbents. Efficiency could further be improved when time for adsorption is extended beyond 40 days since equilibrium adsorption has not yet been reached at the 40th day.

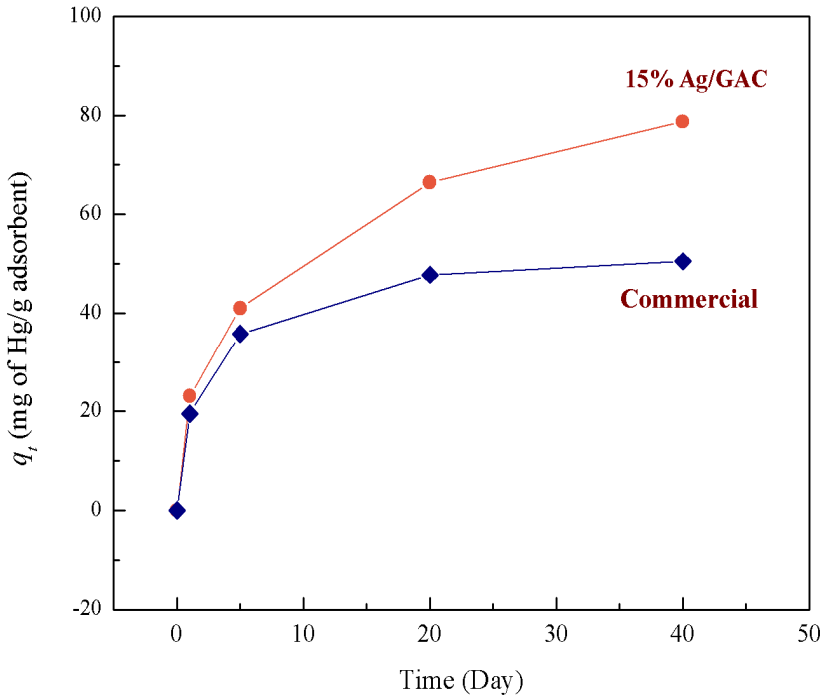


**Figure 4.1** Predicted adsorption of Hg by using 15%Ag/GAC at 60°C.

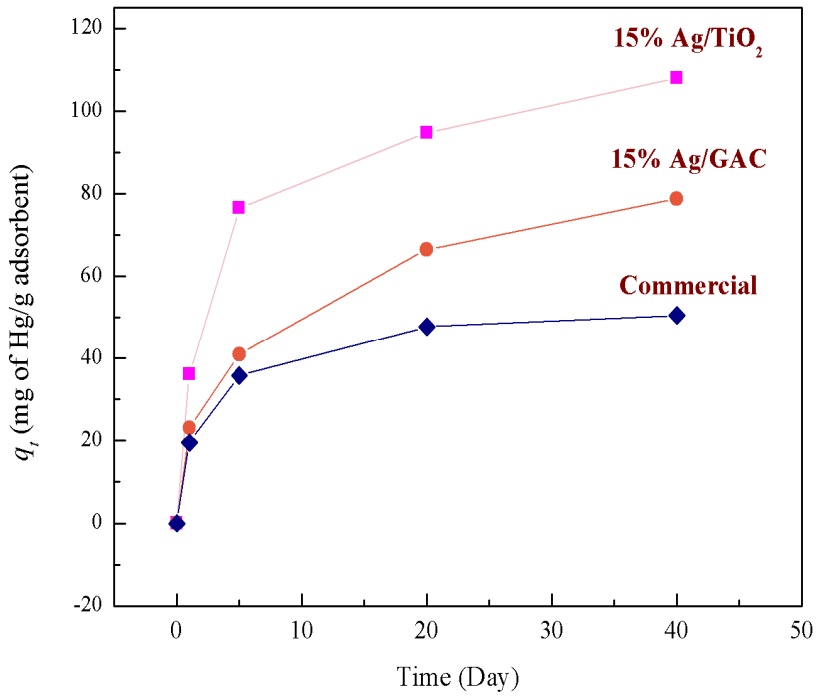


**Figure 4.2** Prediction adsorption of Hg by using 15%Ag/$TiO_2$ at 60°C.

15%Ag/$TiO_2$ was also tested for adsorption of Hg for 0–40 day at 60°C. Commercial and 15%Ag/GAC Hg adsorption was compared with the 15%Ag/$TiO_2$ adsorbent for 0–40 day at 60°C as shown in Figure 4.2. $TiO_2$ doped with Ag exhibited the highest efficiency. Furthermore, it showed high adsorption capacity even at Day 1.

The experiment was carried out at 60°C because at lower temperatures it will take longer time to wait for Hg adsorption to finish. However, at higher temperatures, the parafilm melts and water will leak into the batch set apparatus.

In conclusion, GAC and $TiO_2$ can be used as support for the Hg vapor adsorption while Ag could be reacted with Hg. Pure supports and Ag doped supports were then characterized by using XRD, $N_2$ sorption isotherm, FE–SEM and Elemental–Mapping technique to obtain more information relevant to its adsorption performance such as surface area, morphology and dispersion.

## 4.2 Characterization of adsorbents

Adsorbents used in the further study were loaded with 5 and 15% of Ag (by weight).

### 4.2.1 Structure

X-ray Diffraction or XRD, considered as one of the most important characterization techniques, is used to identify crystalline phases in powder form for most adsorbents. It also gives valuable information on the size of individual crystallites from line-broadening peaks (Haber et al., 1995).

Figure 4.3 shows the XRD patterns of commercial GAC and Ag doped on GAC adsorbents. For both samples of 5% and 15% Ag/GAC, four peaks appeared at 2θ37.7°, 43.8°, 64.2°, and 77.1° corresponding to the (111), (200), (220), and (311) diffraction planes, respectively, of cubic silver (JCPDS No.4–0783). The diffraction peaks of adsorbents calcined at 480$^{o}$C can be certainly seen due to sufficient long–range and high peak sharpness peaks in the graphs, which indicate the order of the adsorbents. There were no traces of nitrate phase left after calcinations at 480°C which agrees with the result of Li et al. (2011).

The XRD pattern of GAC showed amorphous phases. 5%Ag/GAC line showed the peak of Ag was clearly crystalline. The effect of Ag–doping on the crystalline arrangement of GAC was visible. The adsorbents obtained showed satisfactory characteristics. Thus, these adsorbents, 5%Ag/GAC and 15%Ag/GAC, were successfully synthesized by using impregnation technique.

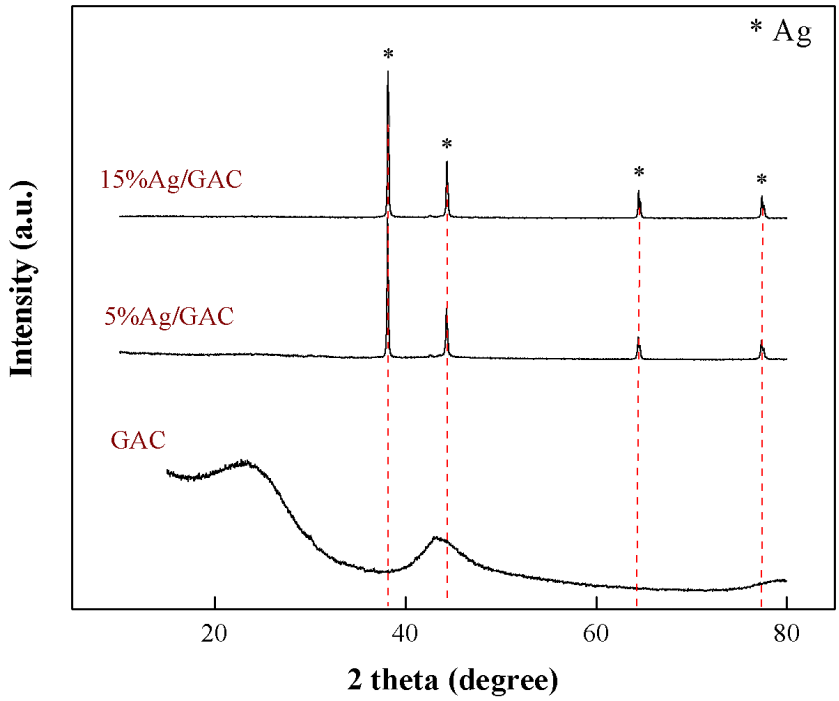


**Figure 4.3** XRD patterns of GAC with and without loading Ag.

The comparison of XRD patterns of the adsorbents with commercial $TiO_2$ were shown in Figure 4.4. Typically, $TiO_2$ crystals have two phases: anatase and rutile phases. The dominant peaks at $2\theta$ about 25.2°, 37.9°, 47.8°, 53.8°, 55.0°, 69.5° and 72.1° represented the indices of (101), (004), (200), (105), (211), (220) and (215) planes in standard JCPDS file No.21–1272. It conforms to the crystalline structure of anatase explained by Zhu et al., 2005.

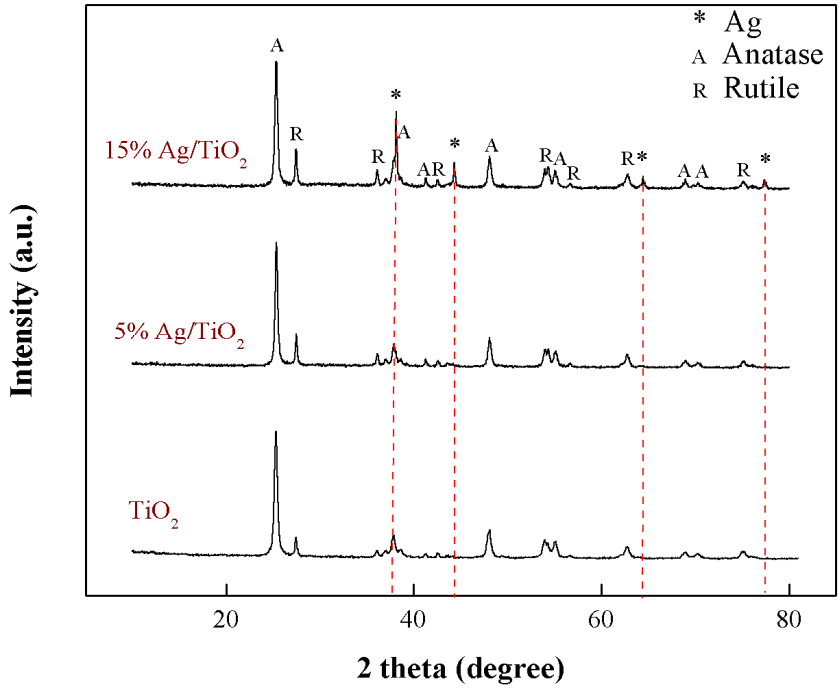


**Figure 4.4** XRD patterns of $TiO_2$ with and without loading Ag.

XRD spectra of the Ag–doped $TiO_2$ at different concentrations of precursor are shown above line of commercial $TiO_2$. The line of 5%Ag/$TiO_2$ spectra did not indicate significant presence of Ag metallic features. However, the intensity of anatase and rutile phase of $TiO_2$ was increased with increasing dropping Ag onto the pure $TiO_2$ as shown in line of 15%Ag/$TiO_2$. The peaks of Ag exhibit clearly appear in the XRD pattern.

### 4.2.2 Specific surface area

The surface area and pore size distribution of adsorbents were calculated by using Brunauer-Emmett-Teller method (BET). The surface area is used to assess potential active sites for adsorption and reaction occurring on adsorbent's surface. The pore size distribution, on the other hand, may help predict whether the adsorbate, which is Hg in this study, is adsorbed in the pores of adsorbent's surface.

The effects of chemical functionalization on specific surface area were calculated from nitrogen adsorption–desorption isotherms. The BET surface area of pure GAC and $TiO_2$ were 1,360 and 50 $m^2/g$, respectively. Both of these values decreased upon doping due to micropore blocking of Ag flakes distributed on the surface. However for the case of Ag doping on $TiO_2$, the blocking was not significant on $TiO_2$ since only mesopores were available. The BET surface areas of both supports with Ag doping are shown in Table 4.1.

**Table 4.1** Specific surface area and pore size of adsorbents.

| Adsorbents | Surface area ($m^2/g$) | Adsorbents | Surface area ($m^2/g$) |
|---|---|---|---|
| GAC | 1,360 | $TiO_2$ | 50 |
| 5% Ag/GAC | 907 | 5% Ag/$TiO_2$ | 34 |
| 15% Ag/GAC | 520 | 15% Ag/$TiO_2$ | 31 |

### 4.2.3 Morphology

Field Emission Scanning electron microscopy (FE–SEM) is a useful technique in characterizing the morphology of porous materials. FE–SEM images presented in Figure 4.5 shows surface morphology of GAC samples at 100, 1,000 and 10,000 magnitudes. The FE–SEM images of pure GAC (a–c) illustrates high porosity as well as absence of cracks in the surface. Upon doping of Ag onto GAC, significant changes in the porosity of GAC were observed. Figures 4.5(d–f) are the FE–SEM images of 5%Ag/GAC which shows layered structure of particles. It can also be observed that the porosity of GAC was reduced. The size of 5%Ag/GAC particles is approximately 1 µm to 2 µm. Figures 4.5(g–i) illustrates the morphology of 15%Ag/GAC in which porous clouds were observed.

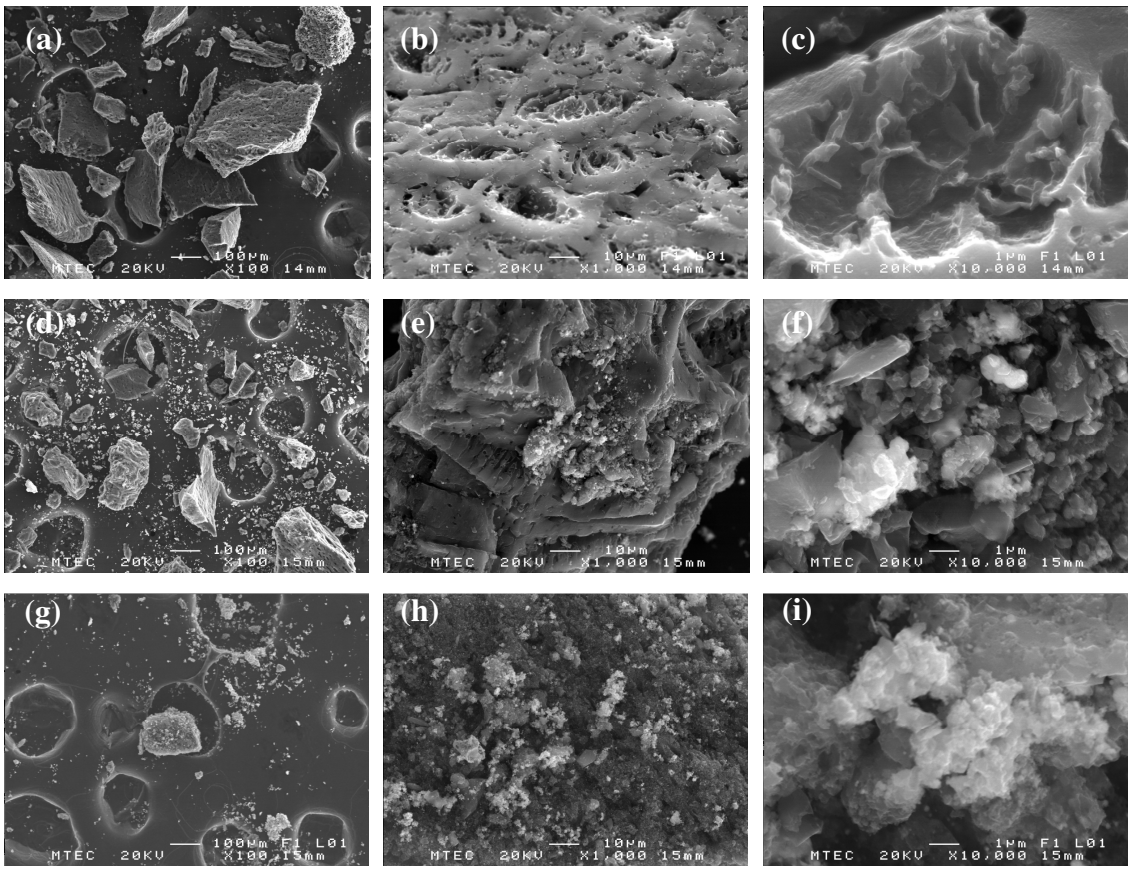


**Figure 4.5** FE–SEM photographs of fresh GAC (a–c), 5%Ag/GAC (d–f) and 15%Ag/GAC (g–i) samples while magnitude 100, 1,000 and 10,000 (left–right).

The size of 15%Ag/GAC particles is approximate 0.5 µmto 1 µm. The particles also exhibit a platelet structure. The FE–SEM images show the presence of bright metallic features on the surfaces of the samples. The Ag particles do not clearly appear in the images due to their penetration into the pores of GAC.

Figure 4.6 presents FE–SEM images for pure $TiO_2$, 5%Ag/$TiO_2$ and 15%Ag/$TiO_2$. Though there was no significant difference in surface morphology, FE–SEM revealed that the three samples are unique in both particle size and shape. It was found that the particle size ranged from around 25 nm to 50 nm.

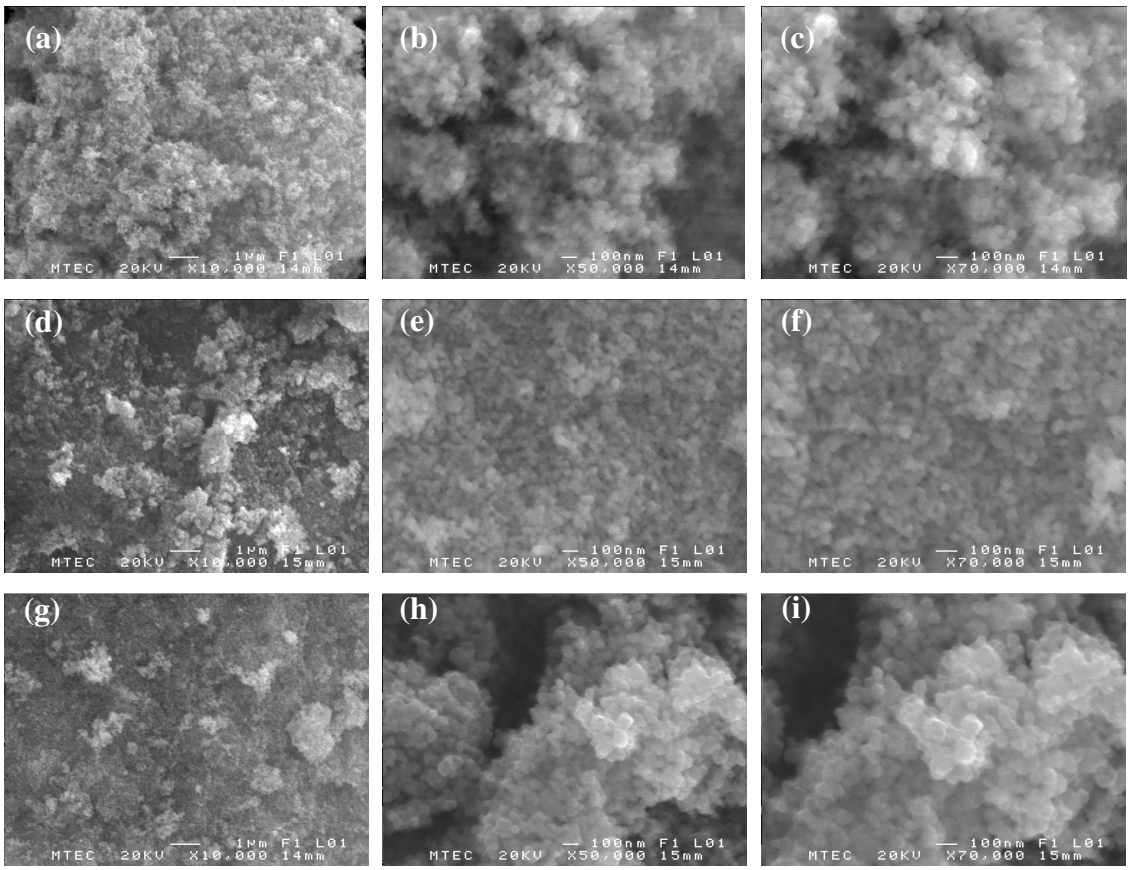


**Figure 4.6** FE–SEM photographs of fresh $TiO_2$ (a–c), 5%Ag/$TiO_2$ (d–f) and 15%Ag/$TiO_2$ (g–i) samples at magnitudes of 10,000, 50,000 and 70,000 (left–right).

The presence of bright metallic features on the surfaces of the samples can also be observed. This can be attributed to Ag having a greater atomic number than titanium and oxygen (Noberi et al., 2012). Ag particles adhered to the $TiO_2$ surfaces as can be clearly observed from Figures 4.6 (d and g).

### 4.2.4 Dispersion of Ag to the support

Wet impregnation method involves sonication of the adsorbents which aims to aid dispersion of Ag to the support.

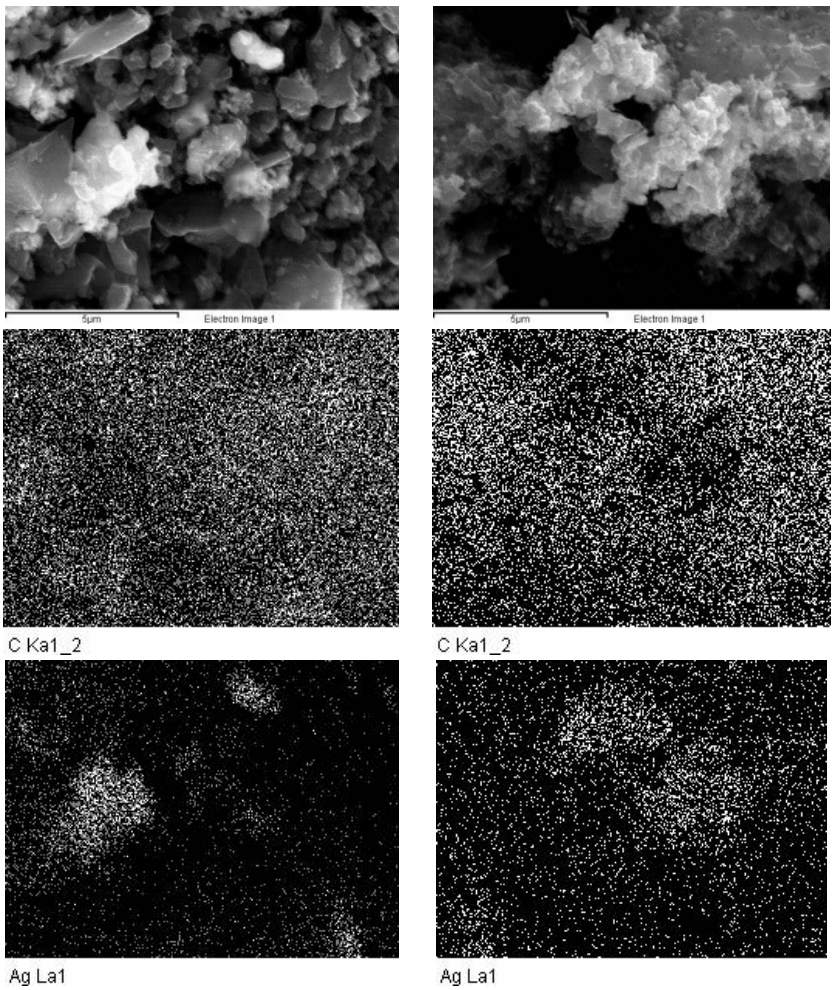


**Figure 4.7** FE–SEM and dot elemental mapping (C, Ag) of 5%Ag/GAC (left) and 15%Ag/GAC adsorbents (right).

For the case of Ag loaded to GAC the results of FESEM that Ag is dispersed poorly on the GAC surfaces. Most of the Ag particles are actually embedded within GAC and only few are on the surface (Noberi et al., 2012). This is also confirmed by dot elemental mapping which illustrates the presence of Ag in the GAC, as shown in Figure 4.7.

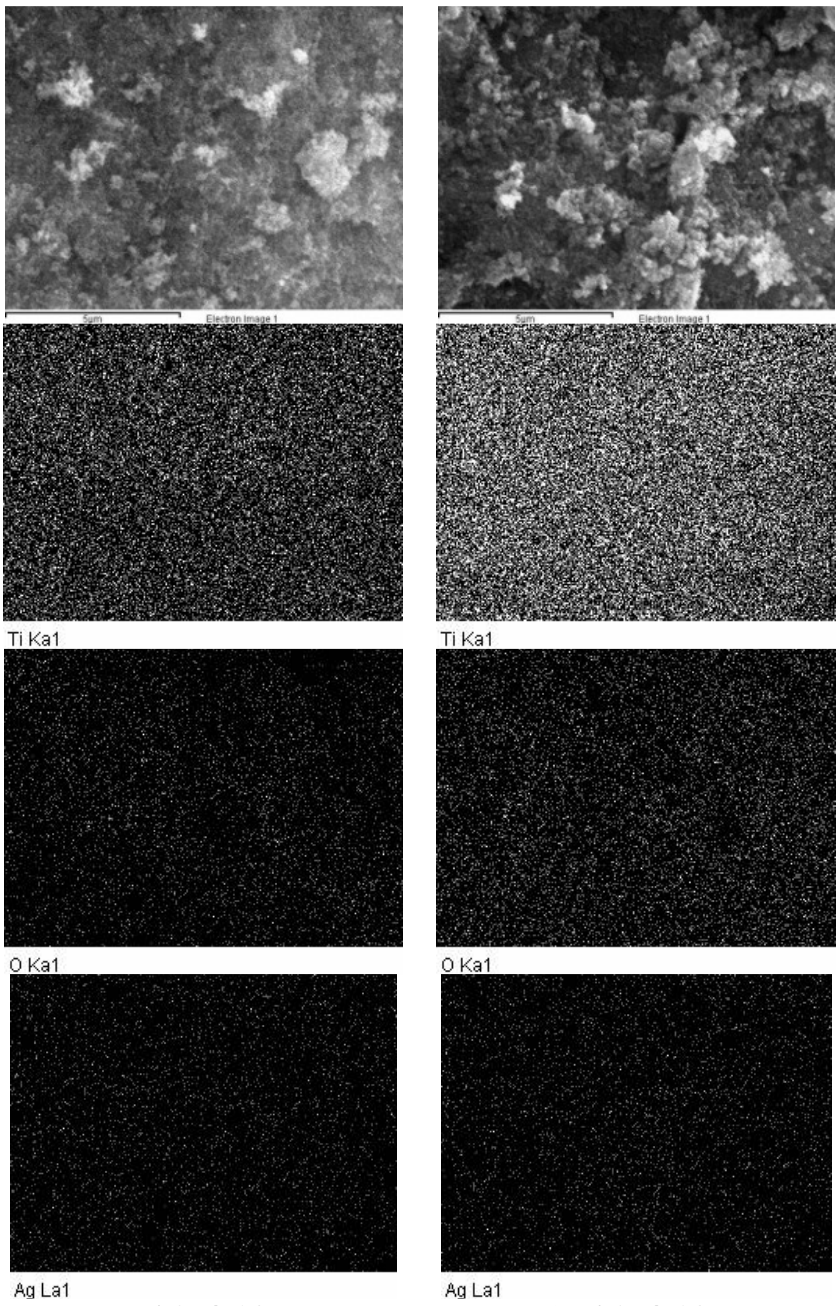


**Figure 4.8** FE–SEM and dot elemental mapping (Ti, O, Ag.) of 5%Ag/$TiO_2$ (left) and 15%Ag/$TiO_2$ adsorbents (right).

In comparison to $TiO_2$, adsorbents 5%Ag/$TiO_2$ and 15%Ag/$TiO_2$ indicated better distribution on GAC the surfaces. The small size of the $TiO_2$ particles may have caused high dispersion of Ag as shown in Figure 4.8.

## 4.3 Effect of Ag loading on Hg adsorption

After the adsorbents were characterized, each was tested in the preliminary adsorption system. The factor involved in the adsorption process was temperature and two tests were carried out at 40°C and 60°C of saturated Hg. The holder set was placed inside the heating bath throughout the test.

### 4.3.1 Adsorption capacity

The tests were carried out at 40°C and 60°Cwhich means that the vapor concentration was about its vapor pressure of 0.00085 and 0.0035 kPa, respectively. In these conditions mercury concentrations are equal to 8.4 and 34.6μg/$m^3$, respectively. The adsorption results from each adsorbent are presented in Figure 4.9.

Figures 4.9 (a) and (b) show the adsorption capacities at 40°C and 60°C, respectively. The results show that the adsorption of 15%Ag/GAC, 15%Ag/$TiO_2$ and Commercial has not yet achieved equilibrium at the 40th day. Therefore, the time for Hg adsorption test was extended until 60th day. However, adsorbents 15%Ag/GAC, 15%Ag/$TiO_2$ and Commercial showed only a slight improvement in Hg adsorption from 40 days to 60 days. The graph shows that on the 40th day, all the adsorbents either approached equilibrium or had a constant rate of adsorption.

The effect of temperature on the Hg adsorption was also studied. Results indicate that at lower temperature (40°C), there was not much change on Hg adsorption efficiency from 0 to 20th day. While at 60°C, there was significant difference on the adsorption capacities for all adsorbents at all points. This is because the higher temperature (60°C) provides better drying force than the lower temperature (40°C). With the aid of this drying force, the adsorption equilibrium can be achieved faster which is evident from the results at 60°C. Therefore the study focused on the adsorption at 60°C.

Since the commercial $TiO_2$ (bare $TiO_2$, □) was not loaded by Ag , it could scarcely adsorb significant amount of Hg as shown in Figure 4.9. The maximum

adsorption capacity of bare $TiO_2$ is 0.0146 mg Hg/g adsorbent. On the other hand, the commercial GAC (bare GAC, ○) derived from coconut shell was able to adsorb Hg at about 7.0553 mg Hg/ g adsorbent. The difference of their adsorption capacities may be accounted to the surface area and porosity of GAC being higher than $TiO_2$.

However bare GAC can only adsorb Hg but not react with it and form amalgams. Therefore the supports must be modified by Ag metal in order to adsorb more Hg vapor. The performance of 5%Ag/$TiO_2$ (⬒) is highly notable as it could adsorb Hg in vapor phases at very high rate of approximately 63.7914 mg Hg/ g adsorbent. GAC modified by Ag at the same loading (5%Ag/GAC, ◓) was able to adsorb Hg at around 23.2365 mg Hg/g adsorbent only, which was around 2.7 times less than 5%Ag/$TiO_2$. The results indicate, therefore, that $TiO_2$ was the more appropiate support because Ag metal could be dispersed all over its surface. On the other hand, the precursor was poorly distrubuted on the surface of GAC since most of the Ag passed through the pores of GAC, as confirmed by BET. The results indicated that there is very little difference between the surface area of bare GAC and GAC loaded with Ag. For $TiO_2$ loaded with 15% Ag (15%Ag/$TiO_2$, ■), the highest mercury adsorption for the whole experiment was observed as it was able to adsorb approximately 107.9368 mg Hg/g adsorbent, which is about 1.7 times higher than 5%Ag/$TiO_2$. Lastly, 15% by weight of Ag doped onto the GAC (15%Ag/GAC, ●) exhibited adsorption at around 78.7549 mg Hg/g adsorbent, which was three times higher than the adsorption capacity of 5%Ag/GAC. Even though modified GAC (with 5% and 15% of Ag) demonstrated high adsorption capacity, the total adsorpion capacity at final product of $TiO_2$ manifested that it is a better adsorbent than GAC. A commercial adsorbent obtained from petroleum research institute of Thailand was able to adsorb Hg vapor at a rate of 50.5138 mg Hg/g adsorbent at 60$^{o}$C.

Moreover, pure GAC has lower Hg removal than the commercial adsorbent but about 6–7 times higher than $TiO_2$ (at 40$^{o}$C and 60$^{o}$C). This is due to the higher surface area of GAC compared with $TiO_2$.

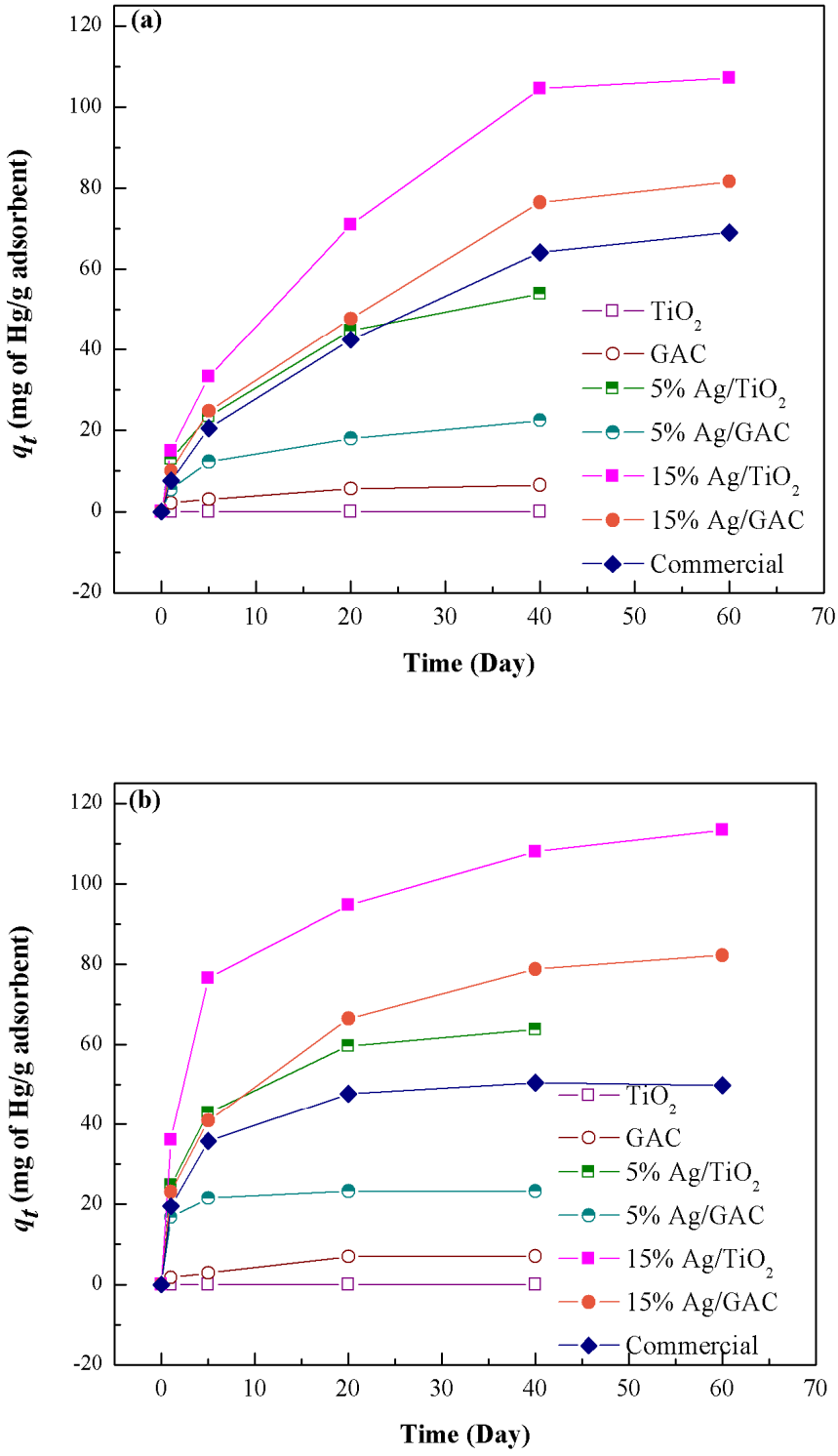


**Figure 4.9** Adsorption capacities of adsorbents (mg/g) at 40°C (a) and 60°C (b).

The Ag–modified adsorbents resulted in higher performance for both sorbents. Table 4.2 presents adsorption capacities during the adsorption of Hg in vapor phase.

**Table 4.2** Adsorption capacity of the adsorbents

| Symbols | Adsorbents | Adsorption capacity (mg Hg/g adsorbent) for 40 day | |
|---|---|---|---|
| | | Temperature = 40°C | Temperature = 60°C |
| □ | $TiO_2$ | 0.0078 | 0.0146 |
| ○ | GAC | 6.5611 | 7.0553 |
| ⬒ | 5%Ag/$TiO_2$ | 53.8962 | 63.7914 |
| ◓ | 5%Ag/GAC | 22.5080 | 23.2365 |
| ■ | 15%Ag/$TiO_2$ | 104.5149 | 107.9368 |
| ● | 15%Ag/GAC | 76.4878 | 78.7549 |
| ◆ | Commercial | 64.1329 | 50.5138 |

### 4.3.2 Kinetic adsorption

The results of the kinetic adsorption will not work on the isotherm adsorption system. Isotherm adsorption is the amount of adsorbate on the adsorbent as a function of its pressure or concentration at constant temperature. However, in this case concentration depends on the temperature. Therefore, Figure 4.10 simulate the isotherm adsorption were used to plot $q_e$ versus $c$ to obtain adsorption capacity at equilibrium. The $q_e$ originate the experimental for adsorption of Hg at 30°C–60°C for 40 day. However, the resulting plot shows that the equilibrium was not reached. Hg adsorption reached equilibrium adsorption by using commercial adsorbent at 34.6229 µg/$m^3$. On the other hand, 15%Ag/GAC and 15%Ag/$TiO_2$ adsorbents were not able to adsorb Hg until equilibrium. For further studies, it is recommended that higher concentration of Hg and longer adsorption time be utilized.

The value of $q_{max}$ for the rate of kinetic adsorption is suggested to be the $q_e$at 60°C presented in Table 4.3. The kinetics of Hg adsorption on the adsorbents was studied. The adsorption rates of 15%Ag/GAC, 15%Ag/$TiO_2$ and commercial can be obtained from Figures 4.11, 4.12 and 4.13, respectively.

**Table 4.3** The adsorption capacity for kinetics adsorption.

| Temperature (°C) | Concentration ($\mu g/m^3$) | $q_e$(mg Hg/g adsorbent) | | |
|---|---|---|---|---|
| | | 15%Ag/GAC | 15%Ag/$TiO_2$ | Commercial |
| 30 | 3.8800 | 24.2887 | 40.3252 | 29.7926 |
| 40 | 8.4389 | 48.1501 | 71.1946 | 44.9963 |
| 50 | 17.4777 | 57.1646 | 86.8074 | 46.8440 |
| 60 | 34.6229 | 66.4806 | 94.7150 | 47.7551 |

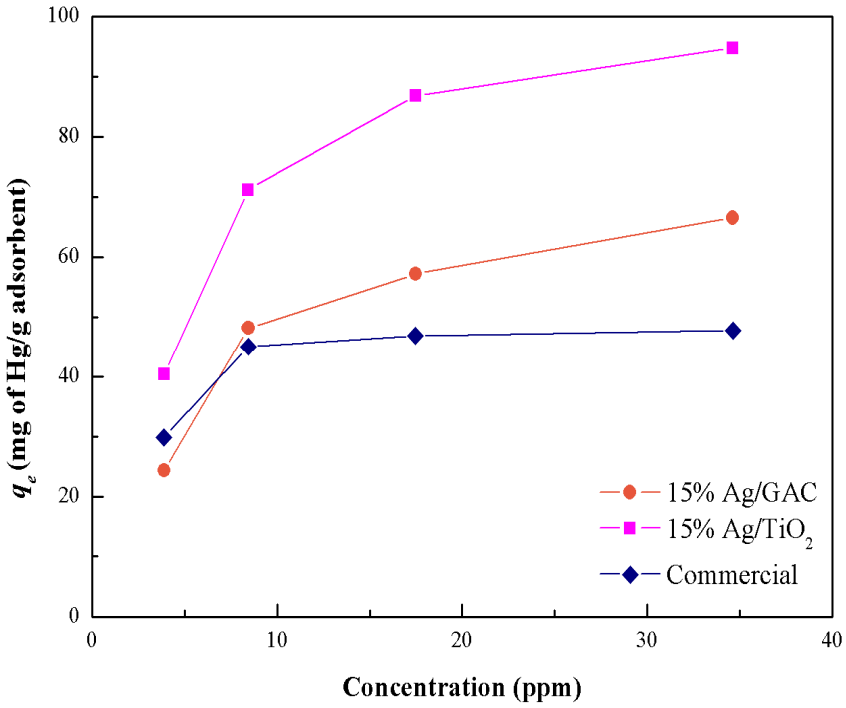


**Figure 4.10** Adsorption of Hg on 15%Ag/GAC, 15%Ag/$TiO_2$ and commercial at 30°C, 40°C, 50°,C 60°C.

The experimental data were fitted against the pseudo–first order, pseudo–second order and intra–particle diffusion models for the bare and modified adsorbents. Figures 4.11(a), 4.12(a) and 4.13(a) give a linear relationship between $\ln(q_e - q_t)$ and $t$ using the pseudo–first order model. The values of $k_1$ and $q_e$ can be calculated from the slope and intercept of the plot, respectively. Meanwhile, the relationship of $t/q_t$ and $t$ follows pseudo–second order model (Figures 4.11(b), 4.12(b) and 4.13(b)). The

values of $q_e$ and $k_2$ rate constants can also be obtained from the slope and intercept, respectively.

The result shows that 15%Ag/GAC, 15%Ag/$TiO_2$ and commercial adsorbent follows pseudo–first order model. The pseudo–first order rates ($k_1$) of Hg adsorbed on 15%Ag/GAC were found to be 0.020, 0.016, 0.015 and 0.012 $hour^{-1}$at 30°C, 40°C, 50°C and 60°C, respectively. It was observed that the rate of Hg adsorption on 15%Ag/GAC decreases with increasing temperature. On the other hand, 15%Ag/$TiO_2$ exhibited almost constant rate of kinetic adsorption at the four temperatures. The values of $k_1$ were 0.006, 0.007, 0.005 and 0.004 $hour^{-1}$ at 30°C, 40°C, 50°C and 60°C, respectively. This indicates that 15%Ag/$TiO_2$ adsorbent is independent on the temperature. Moreover, 15%Ag/$TiO_2$ demonstrated lesser rate of Hg vapor adsorption than Commercial. Adsorption rates of 0.018, 0.014, 0.015 and 0.015 $hour^{-1}$ were attained with the use of Commercial adsorbent.

The pseudo–first order rate of Hg adsorbed ($k_1$) of 15%Ag/GAC and 15%Ag/$TiO_2$ and Commercial adsorbents agrees to the result of Namasivayam and Periasamy (1993) (peanut hull cabon), Mishra et al. (1996) (hydrous zirconium oxide), Singh et al. (1996) (kaolinite) and Namasivayam and Senthilkumar (1997) ($Fe^{3+}$:$Cr^{3+}$ hydroxide). This is significant as it provides valuable insights into the reaction pathways and into the mechanism of sorption reactions. Moreover, the pseudo–first order model describes the solute uptake rate which in turn controls the residence time of sorbate uptake at the solid–solution interface (Ho and McKay, 1999). Thus, it is important to be able to predict the rate at which pollutant is removed in order to design appropriate sorption treatment plants.

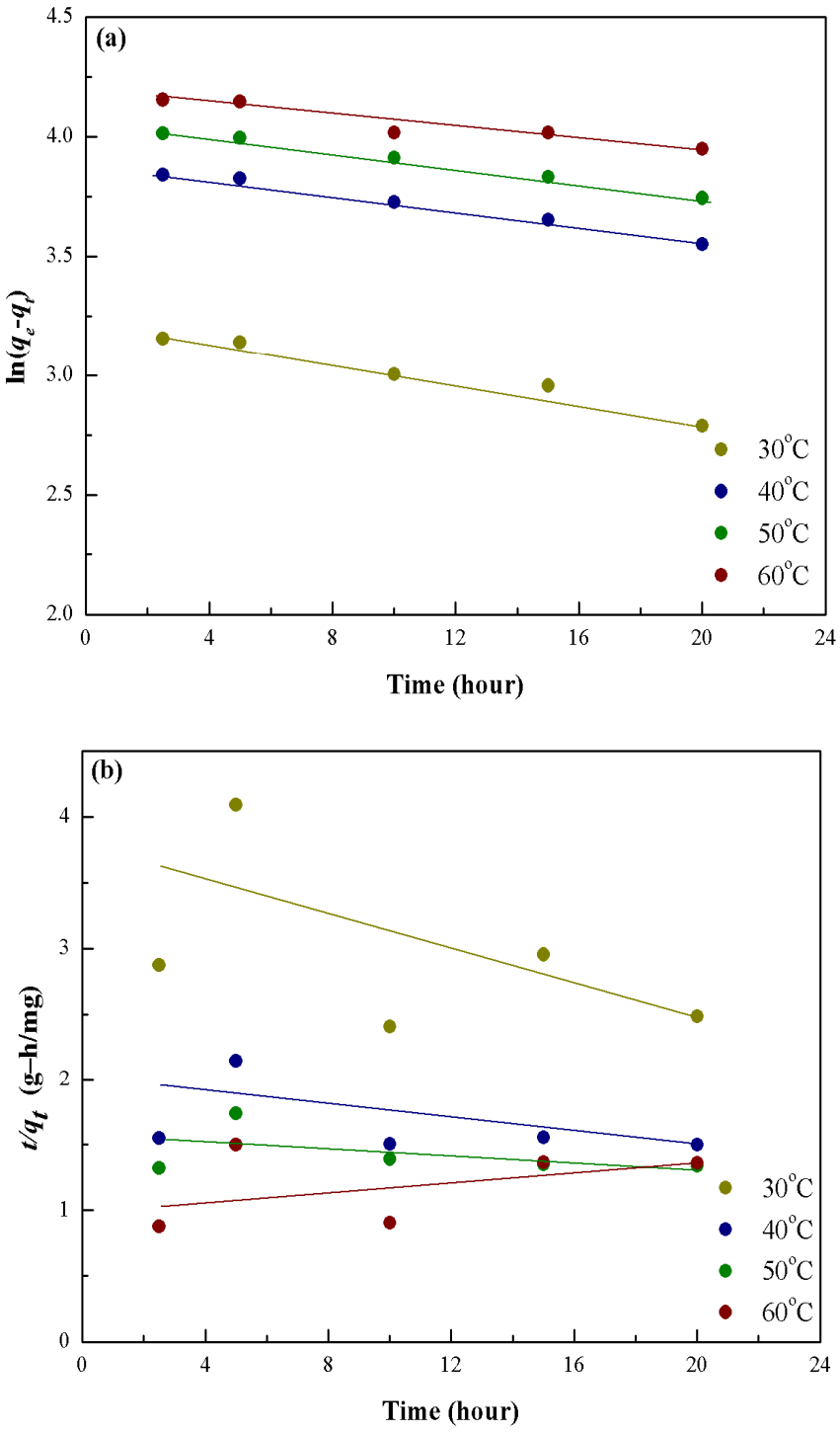


**Figure 4.11** Adsorption kinetic of Hg on15%Ag/GAC where pseudo–first order (a) and pseudo–second order (b).

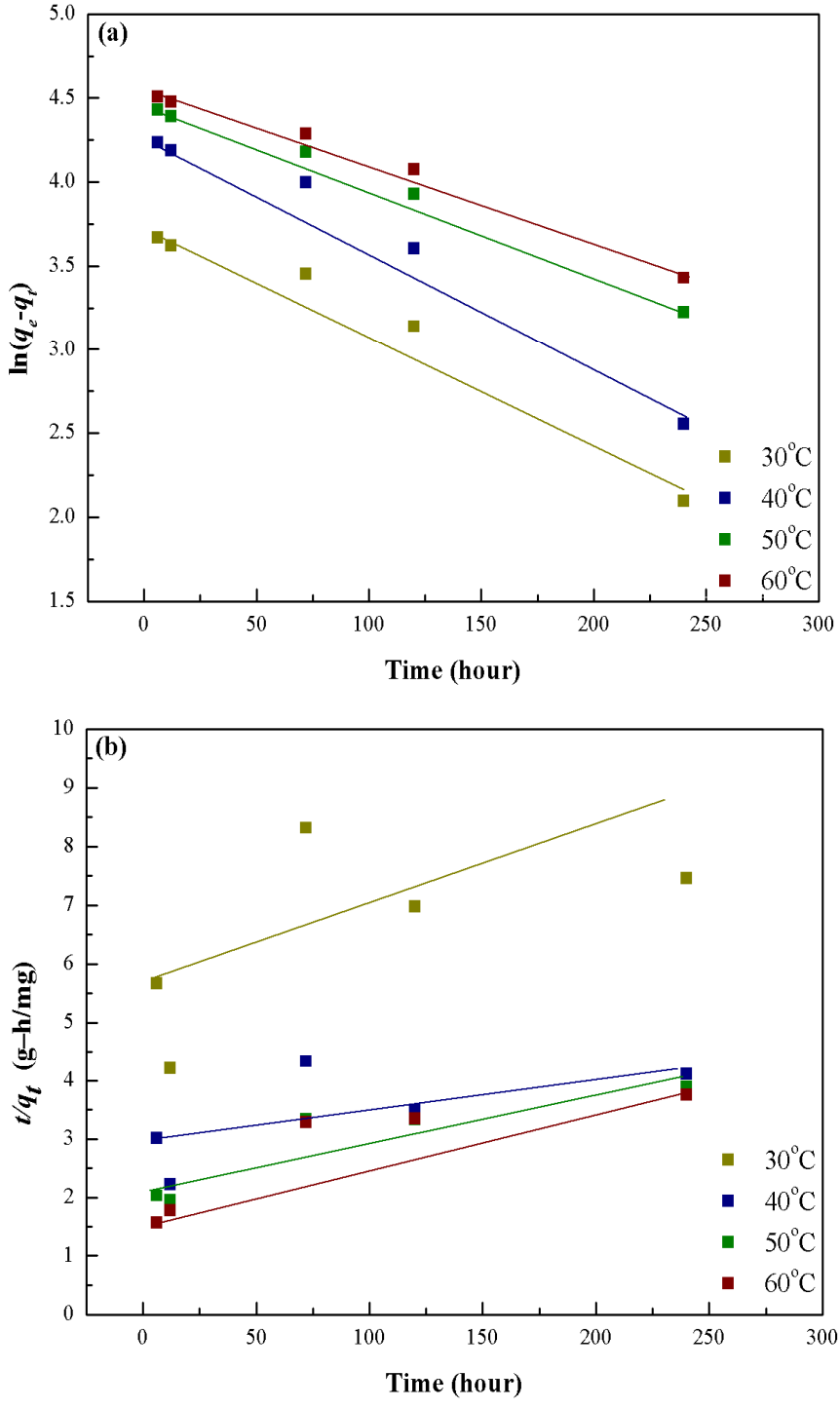


**Figure 4.12** Adsorption kinetic of Hg on15%Ag/$TiO_2$ where pseudo–first order (a) and pseudo–second order (b).

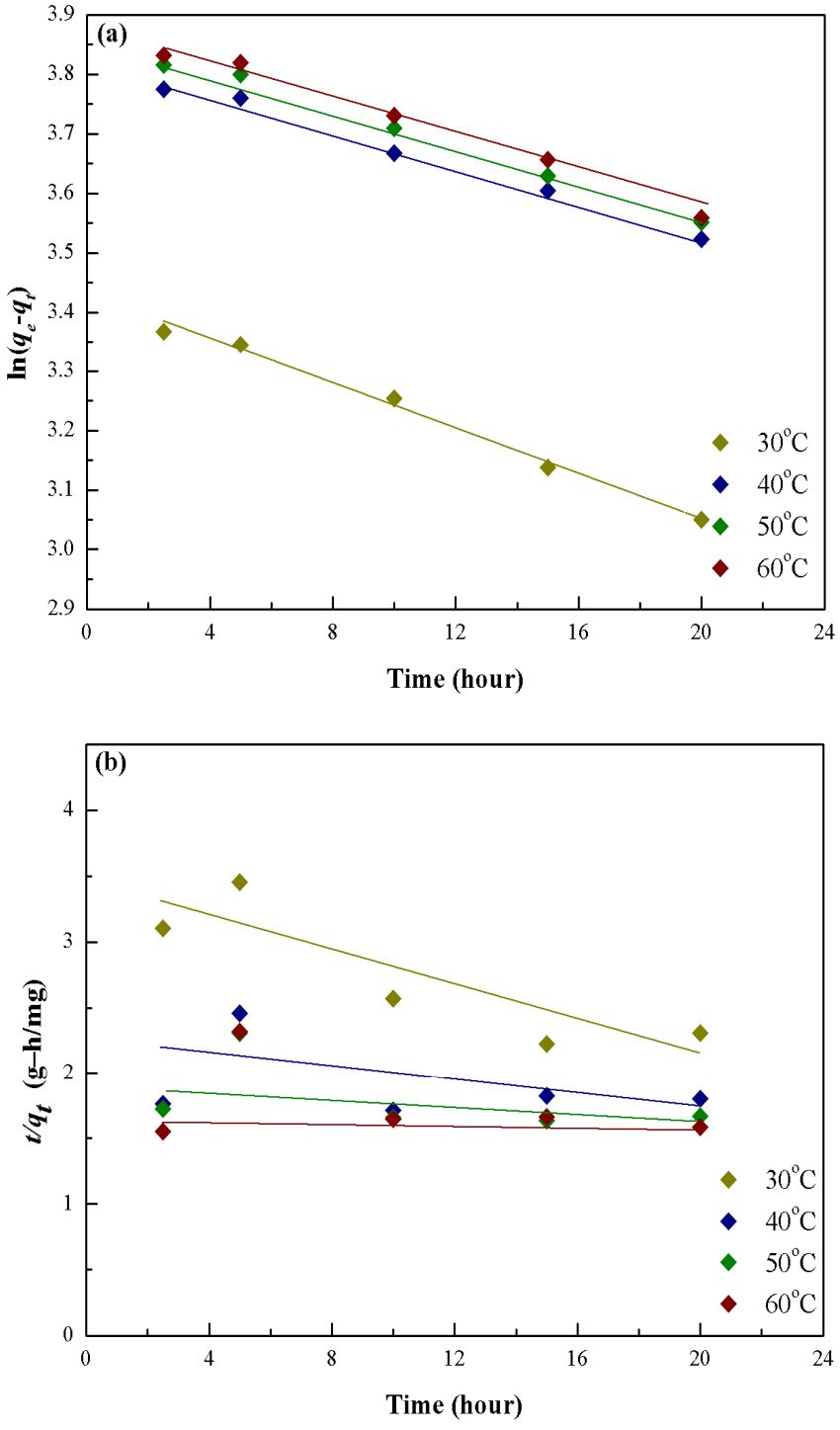


**Figure 4.13** Adsorption kinetic of Hg on commercial where pseudo–first order (a) and pseudo–second order (b).

**Table 4.4** The pseudo–first order rate constant at different temperature.

| Adsorbents | $k_1$ (hour$^{-1}$) at Temperature (°C) | | | |
|---|---|---|---|---|
| | 30 | 40 | 50 | 60 |
| 15%Ag/GAC | 0.020 | 0.016 | 0.015 | 0.012 |
| 15%Ag/$TiO_2$ | 0.006 | 0.007 | 0.005 | 0.004 |
| Commercial | 0.018 | 0.014 | 0.015 | 0.015 |

### 4.3.2 Activation energy of amalgam form

The effect of temperature on the transport of the Hg vapor through the adsorbents in batch set was examined at 30, 40, 50 and 60°C. The experimental results are collected in Table 4.4. The results suggest that the transport of the Hg vapor could be described by the kinetic laws of two consecutive irreversible first order reactions (Figures 4.11–4.13) (Shafey, 2010).

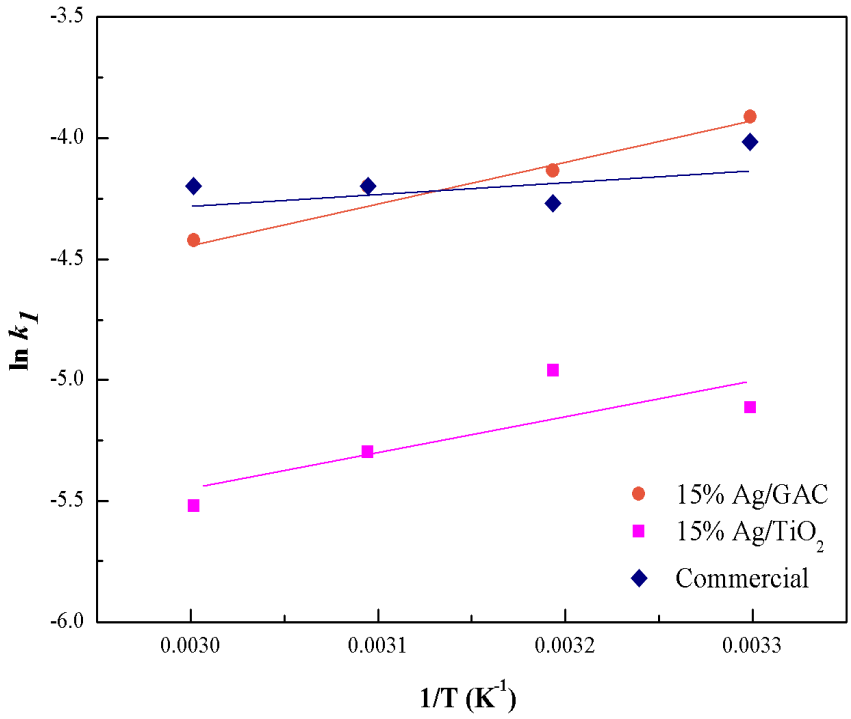


**Figure 4.14** Activation energy of amalgam form on 15%Ag/GAC, 15%Ag/$TiO_2$ and commercial.

An Arrhenius type plot is followed perfectly, as shown in Figure 4.14. The $E_A$ values of 15%Ag/GAC, 15%Ag/$TiO_2$ and Commercial were -193.983, -185.680 and -60.000 kJ/mol, respectively as shown in Table 4.5.

For many adsorbent in batch set, the distribution steps are rate determining at donor-adsorbents interfaces (Minhas et al., 2010). The overall transport kinetics in different adsorption processes is governed by chemical reaction kinetics.

**Table 4.5** The activation energy value of adsorbents.

| Adsorbents | $E_A$ (kJ/mol) |
|---|---|
| 15%Ag/GAC | -193.983 |
| 15%Ag/$TiO_2$ | -185.680 |
| Commercial | -60.000 |

The $E_A$ values of processes controlled by chemical reactions are high due to the strong effect of temperature on the actual speed constants. Thus, activation energy ($E_A$) is used as an indicator whether transport through adsorption processes is diffusion controlled or chemically controlled by reactions. In this research, the values of $E_A$ obtained specify that the transport of Hg vapor is diffusion controlled process.

### 4.3.4 Breakthrough curve

The breakthrough curve experimental set up involves of $N_2$ gas, as a carrier was flowed with the rate of 10 ml/min through Hg liquid and 110 ml/min for pure nitrogen. Hg vapor influence into bed column, adsorbent was packed in a glass reactor.

The concentration of Hg in the effluent is measured by a Lumex–RA915$^+$ mercury analyzer, then plotting the extraction ratio against the concentration of effluents. The extraction ration was equal to ($C/C_0$ = 0.012), where C was the concentration of the column effluents which petroleum require concentration less than 0.1 µg/$m^3$ or 100 ng/$m^3$ and $C_0$ was that of the column influent (Huang et al., 2009) which was 8.3 µg/$m^3$.Normally, the within the mass transfer zone (MTZ), the degree of saturation with adsorbate varies from 100% percent to effectively 0 (zero) which it look likes commercial sorbent (green line in Figure 4.15). Therefore, in this work

concentrated the data at break point that 15%Ag/$TiO_2$ was long time for adsorption.The breakthrough capacity curve for elemental Hg was illustrated in Figure 4.15. As shown, the mercury breakthrough ($t_b$) column started after 21st, 25th and 29th day for commercial, 15%Ag/GAC and 15%Ag/$TiO_2$, respectively. The result of 15%Ag/$TiO_2$ presented adsorption capacity at saturated point ($q_{sat}$) approximately 1.587 mg Hg/g of Ag/$TiO_2$ and adsorption capacity at break point ($q_b$) was 0.622 mg Hg/ g of Ag/$TiO_2$ that the bed capacity was around 0.392 as shown in APPENDIX C.4.

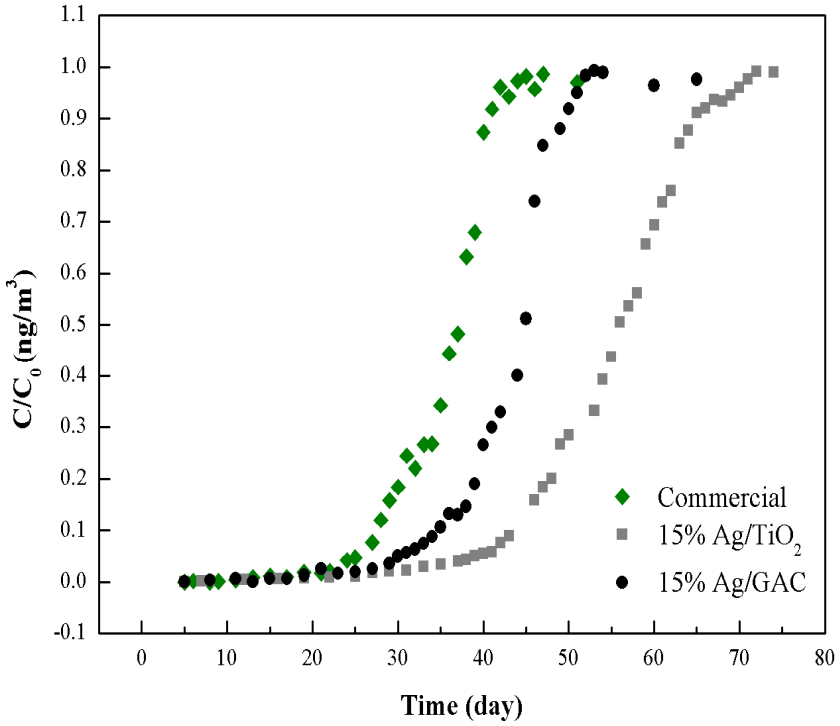


**Figure 4.15** Breakthrough curve of element Hg on 15%Ag/$TiO_2$, 15%Ag/GAC and commercial column.

There are many theoretical model equations have been proposed for describing the adsorption kinetics based on mass balance, pore diffusion rate and initial/boundary conditions (Tsai et al., 2006). However, these equations are not only complicated and impractically to use, but also require detailed data such as the characteristics of adsorbate and adsorbent.

## 4.4 Confirmatory tests

XRD and Elemental–Mapping were done to characterize the adsorbents after the Hg adsorption.

### 4.4.1 X–Ray Diffraction (XRD)

XRD confirmed the formation of amalgam. Figure 4.16 shows the XRD patterns of both pure and Ag-doped GAC and $TiO_2$ adsorbents.

We found that the XRD pattern of GAC (Figure 4.16) depicts amorphous phase and that Ag affects the crystalline arrangement of GAC. Similarly, in Figure 4.17 the altitude peak of $TiO_2$ was decreased when it was doped by Ag. After the adsorption tests, the XRD showed that peak of amalgam in adsorbent indicating that Hg was indeed adsorbed in both GAC and $TiO_2$ adsorbents.

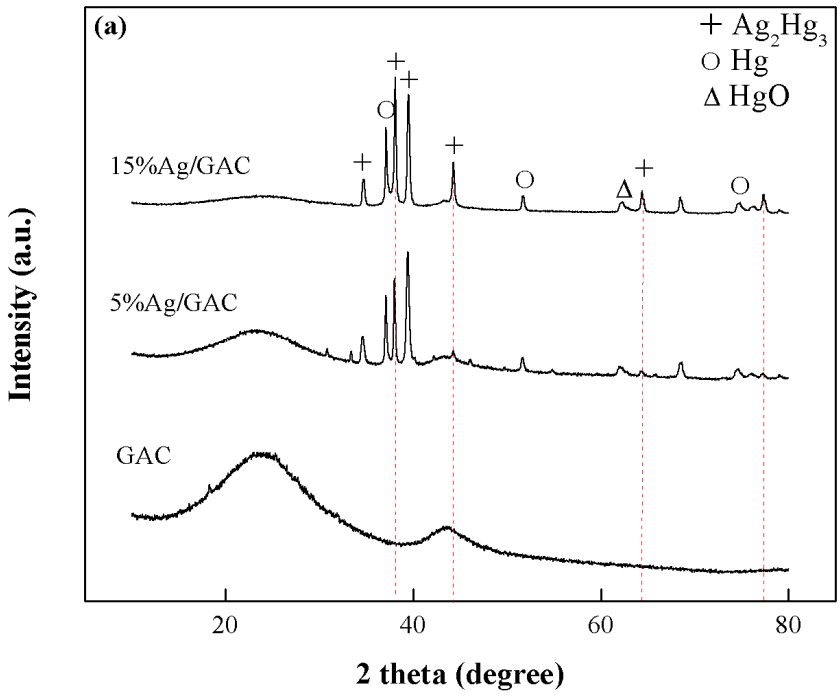


**Figure 4.16** XRD patterns of spent GAC adsorbents.

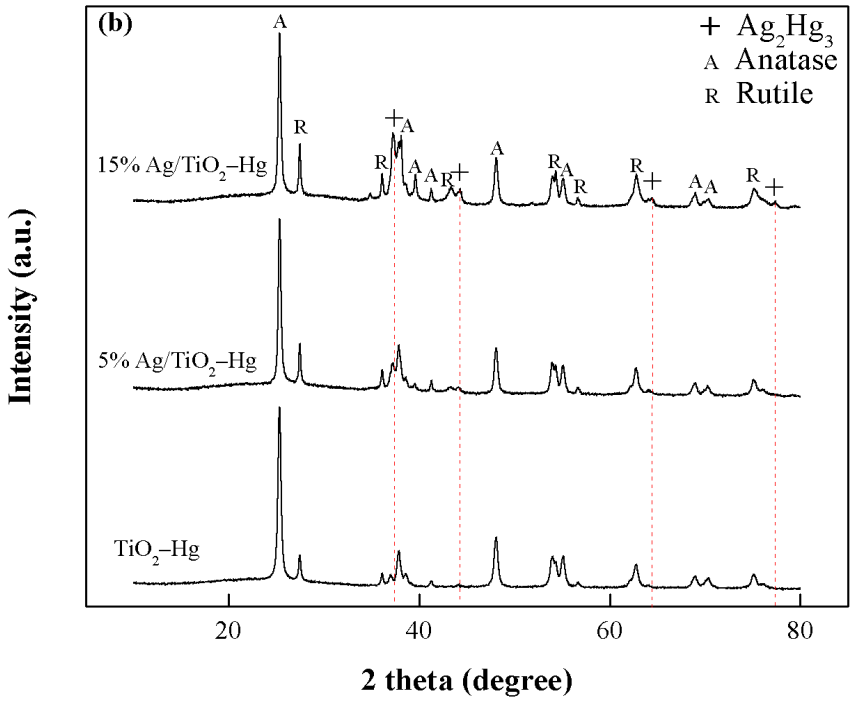


**Figure 4.17** XRD patterns of spent $TiO_2$ adsorbents.

### 4.4.2 Elemental–Mapping

SEM images of used 15%Ag/GAC adsorbent are shown in Figure 4.14. Elemental mapping for C, Ag and Hg affirm the presence of each element in the used adsorbent. Figure 4.8 confirms that the distribution of Ag was all over the GAC support and therefore Hg in amalgam was also dispersed on the surface (Han et al., 2002).

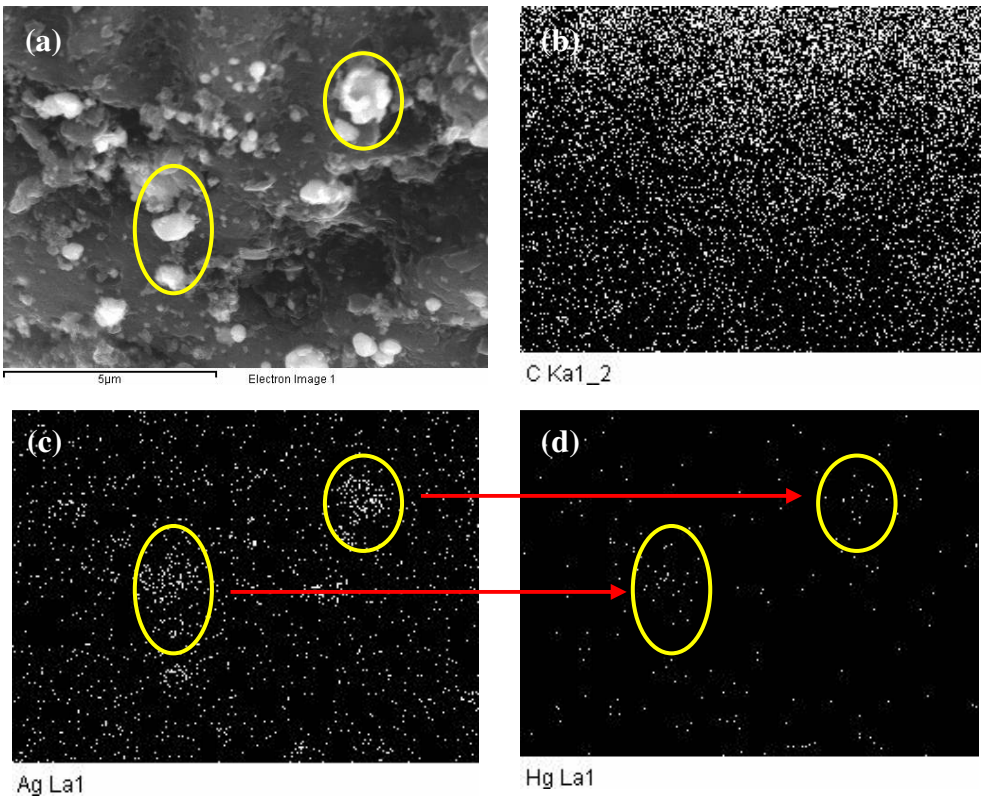


**Figure 4.18** FE–SEM (a) and elemental mappings of spent 15%Ag/GAC in Hg adsorption for 40 days; carbon (b), silver (c) and mercury (d).

# CHEPTER V

# CONCLUSIONS AND RECOMMENDATIONS

## 5.1 Conclusions

The effects of Ag modified adsorbents on Hg removal from contaminated natural gas were investigated in this study. The removal of Hg was carried out in static batchadsorption (at 40°C and 60°C) and flow adsorption (at 30°C) systems.

- Silver was dispersed onto supports (GAC and $TiO_2$) successfully under an impregnation method.
- Pure supports (without metal loading) presented no effect on Hg removal in terms of surface area.
- Supports doped with silver showed higher Hg vaporremoval than the commercial adsorbent under this study scope (flow and concentration).
- 15%Ag/$TiO_2$ and 15%Ag/GAC chemically adsorbed Hg vapor and formed a complex amalgam, approximately 107.9368 and 78.7549 mg Hg/gadsorbent, respectively.
- The kinetic adsorption model was corresponded to pseudo–first order, with *k* value of 0.0055 $hour^{-1}$. Under temperature range of 30–60$^{o}$C, activation energy for the adsorption was observed at -185.680 kJ/mol.

## 5.2 Recommendations

It may be difficult to use silver metal for actual application since the metal is expensive. Copper loaded can be used as an alternative because of its very low price. Furthermore, the flow system should be carried out at different temperatures. This work can be applied in the Mercury Removal Unit (MRU) of natural gas plants.

# REFERENCES


Agency for Toxic Substances and Disease Registry (ATSDR), **Public health statement: Mercury** [Online]. March 1999. Available from: http://www.atsdr.cdc.gov/ToxProfiles/tp46-c1-b.pdf [2013, January 29]

Al–Megren, H.A. Advances in natural gas technology. Rijeka, Croatia: InTech Publications, 2012.

BAXTER & WOODMAN, Calculations used in the daily operations of a water treatment plant [Online]. 2009. Available from http://www.baxterwoodman.com/documents/WaterCalcsBook.pdf [2013, February 23]

Bhattacharyya, K.G. and Sharma, A. Kinetics and thermodynamics of Methylene Blue adsorption on Neem (Azadirachta indica) leaf powder. Dyes and Pigments 65 (2005): 51–59.

Caliskan, N., Kul, A.R., Alkan, S., Sogut, E.G. and Alacabey, I. Adsorption of Zinc(II) on diatomite and manganese-oxide-modified diatomite: A kinetic and equilibrium study. Journal of Hazardous Materials 193 (2011): 27–36.

Díaz-Somoano, M., Unterberger., S. and Hein R.G.K. Mercury emission control in coal-fired plants: The role of wet scrubbers. Fuel Processing Technology 88 (2007): 259–263.

Earthworks, **Oil and gas pollution fact sheet** [Online]. January 17, 2006. Available from:http://www.earthworksaction.org/library/detail/oil_and_gas_pollution_fact_sheet#.UQo8JR03vEV [2013, January 29]

Eckersley, N. Advance mercury removal technologies. Hydrocarbon Processing: Gas processing developments (January 2010): 29–35.

Eisler, R. Mercury hazards to fish, wildlife, and invertebrates: A synoptic review. Biological Report 85 (April 1987).

Ghassabzadeh, H., Mohadespour, A., Torab, M., Zaheri, P., Maragheh, M.G. and Taheri, H. Adsorption of Ag, Cu, Hg from aqueous solutions using expandes perlite. Journal of Hazardous Materials 177 (2010): 950–955.

Ghorishi, S. and Sedman, C.B. Low concentration mercury sorption mechanisms and control by calcium–based sorbents: Application in coal–fired processes. Journal Air Waste Manage 12 (1998): 1191–1198.

Han, Y X., Zhu, Y Q., Tan, D S., Zhu, Y D. Treatment of waste gas containing mercury with adsorption method. Journal of Shanghai University (Natural Science) 8 (2002): 205–208.

Harada, M., Honjo, S., Suzaki, M., Ishida, K., Nagano, H. and Okino, S. Mercury Removal Method and System. United States Patent 6,770,119 (2004).

Henderson, D.C. Cilfford, R. and Young, D.M. Mercury–reactive lymphecytes in peripheral in blood are not a maker foe dental amalgam associate disease. Journal of Dentistry 29 (2001): 469–474.

Ho, Y.S. and McKay, G. Pseudo–second order model for sorption processes. Process Biochemistry 34 (1999): 451–465.

Horikawa, T. and Nicholson, D. Capillary condensation of adsorbates in porous materials. Advances in Colloid and Interface Science 169 (2011): 40–58.

Huang, X., Liao, X. and Shi, B. Hg(II) removal from aqueous solution by bayberry tannin-immobilized collagen fiber. Journal of Hazardous Materials 170 (2009): 1141–1148.

Huber, M.L., Laesecke, A. and Friend D.G. The vapor pressure of mercury. NISTIR 6643 (April 2006).

Hutchison, A., Atwood, D., and Santilliann–Jiminez, E. Q. The removal of mercury from water by open chain ligands containing multiple sulfurs. Journal of Hazardous Materials 156 (2008): 458–465.

Idris, A. S., Harvey, R. S. and Gibson, T. L. Selective extraction of mercury(II) from water samples using mercapto functionalised–MCM–41 and regeneration of the sorbent using microwave digestion. Journal of Hazardous Materials 193 (2011): 171–176.

Jose, C.P. Water and Purification and Management. The Nano Science for Peace and Security Programme (2009): 99–101.

Li, X., Zou, X., Qu, Z., Zhao, Q. and Wang, L. Photocatalytic degradation of gaseous toluene over Ag-doping TiO2 nanotube powder prepared by anodization coupled with impregnation method. Chemosphere 83 (2011): 674–679.

Louie, K.D. Handbook of sulphuric acid manufacturing, Second Edition, Thornhill, Ontario, Canada L3T 2C6: DKL Engineering Inc. Publications, 2008.

Ma, F., Qu, R., Sun, C., Wang, C. and Ji, C. Adsorption behaviors of Hg(II) on chitosan functionalized by amino-terminated. Journal of Hazardous Materials 172 (2009): 792–801.

Marsch, H.D. Synloop Ammonia Separator Accident. Summer National AIChE Ammonia Symposium (1990): 96b.

Manning, F.S. and Thompson, R.E. Oilfield processing of petroleum volume one natural gas, Tulsa, Oklahoma: Pennwell Publishing Company Publications, 1991.

Marayart Virakom. Mercury in natural gas. **Environmental journal** [Online]. 2010. Available from: http://web.ku.ac.th/schoolnet/snet6/envi3/parod/parodn.htm [2012, November 13]

McCurry, J. Japan remembers Minamata. The Lancet 367 (January 2006).

Minhas, F.T., Memon, S. and Bhanger, M.I. BhangerTransport of Hg(II) through bulk liquid membrane containing calix[4]arene thioalkyl derivative as a carrier. Desalination 262 (2010): 215–220.

Mokhatab, S., Poe, W. and Speight, J.G. Handbook of natural gas transmission and processing, Linacre House, Jordan Hill, Oxford OX2 8DP, UK: Gulf Professional Publishing: Elsevier Inc. Publications, 1991.

Mokhatab, S. and Poe, W. Handbook of natural gas transmission and processing, Second Edition, The Boulevard, Langford Lane, Kidlington, Oxford, OX5 1GB, UK: Gulf Professional Publishing: Elsevier Inc. Publications, 2012.

Morency, J. Zeolite sorbent that effectively removes mercury from flue gases. Feature article (2002): 24–26.

Mishra, S.P., Singh, V.K. and Tiwari, D. Radiotracer technique in adsorption study: Part XIV. Efficient removal of mercury from aqueous solutions by hydrous zirconium oxide. Applied Radiation and Isotopes 47 (1996): 15–21.

Namasivayam, C. and Periasamy, K. Bicarbonate–treated peanut hull carbon for mercury (II) removal from aqueous solution. Water Research 27 (1993): 1663–1668

Namasivayam, C. and Senthilkumar, S. Recycling of industrial solid waste for the removal of mercury(II) by adsorption process. Chemosphere 34 (1997): 357–375.

Nguyen–Phan, T.D., Kim, E.J., Hahn, S.H., Kim, W.J. and Shin, W. Synthesis of hierarchical rose bridal bouquet and humming–top–like $TiO_2$ nanostructures and their shape-dependent degradation efficiency of dye. Journal of Colloid and Interface Science 356 (2011): 138–144.

Nisakorn Saengprachum. Purification of Biodiesel Using Natural Diatomite and Diatomite Doped with $MnO_2$. Master's Thesis, Environmental Management and Hazardous waste: Chulalongkorn University, 2009.

NIST, SRM 2586 – Trace Elements in Soil (contains lead from paint) [Online]. Available from: https://www-s.nist.gov/srmors/view_detail.cfm?srm=2586 [2013, February 22]

Noberi, C., Zaman, A.C., Üstündağ, C.B. Kaya, F. and Kaya, C. Electrophoretic deposition of hydrothermally synthesised Ag–$TiO_2$ hybrid nanoparticles onto 3-D Ni filters. Materials Letters 67 (2012): 113–116.

Okabe, T. and Mitchell, R.J. Critical reviews in oral biology & medicine: Setting reactions in dental Amalgam Part 2. The kinetics of amalgamation [Online]. 1996. Available from: http://cro.sagepub.com/content/7/1/23 [2012, November 22]

Petersen, K.I., Dybkjær, I., Oversen, C.V., Schjødt, N.C., Sehested, J. and Thomsen, S.G. Natural gas to synthesis gas–Catalysts and catalytic processes, Journal of Natural Gas Science and Engineering 3 (2011):423–459.

Phothitontimongkol, T., Siebers, N., Sukpirom, N. and Unob, F. Preparation and characterization of novel organo-clay minerals for Hg(II) ions adsorption from aqueous solution. Applied Clay Science 43 (2009): 343–349.

Rahman, M. J., Bozadjiev, P., and Pelovski, Y. Studies on the effects of some additives on the physicomechanical properties of urea–ammonium sulphate (UAS) pellets. Fertilizer Research 38 (1994): 89–93.

Reilly, S.B-O', McCarty, K.M., Steckling, N. and Lettmeier, B. Mercury exposure and children's health. Current Problem in Pediatric and Adlescent Health Care 40 (2010): 186–215.

Schabron, J.F., Rovani, J.F. and Sorini, S.S. Mercury cem calibration: "Topical Report" WRI-07-R004R (March 2007).

Schnoor, J.L. Environmental Modeling: Fate and transport of pollutants in water, air, and soil, John Wiley & Sons, Inc. Publications, 1996.

Shafey, E.I. Removal of Zn(II) and Hg(II) from aqueous solution on a carbonaceous sorbent chemically prepared from rice husk. Journal of Hazardous Materials 175 (2010): 319–327.

Slotnick, S. Mercury: human exposure. **USEPA** [Online]. 2012. Available from: http://www.epa.gov/hg/exposure.htm [2012, November 13]

Singh, J. Huang, P.M., Hammer, U.T. and Liaw, W.K. Influence of Citric Acid and Glycine on the Adsorption of Mercury (II) by Kaolinite Under Various pH Conditions. Clays and Clay Minerals 44 (1996): 41–48.

Speight, J.G. Natural gas–A basic handbook, Houston, Texas: Gulf Publishing Company Publications, 2007.

Srinivasan, N.R., Shankar, P.A. and Bandyopadhyay, R. Plasma treated activated carbon impregnated with silver nanoparticles for improved antibacterial effect in water disinfection. Carbon (2013).

Thadani, R. **Mercury element facts** [Online] 2010. Available from: http://www.buzzle.com/articles/mercury-element-facts.html [2012, November 22]

The Linde, Group. **Natural gas processing plants** [Online]. Available from: http://www.the-linde-group.com/en/search.html [2013, January 29]

Tsai, W.T., Lai, C.W. and Su, T.Y. Adsorption of bisphenol–A from aqueous solution onto minerals and carbon adsorbents. Journal of Hazardous Materials B134 (2006): 169–175.

Varma. R.S. Ju, Y. Sikdar, S., Lee, J.Y. and Keener, T.C. Compositions and Methods for Removing Mercury from Mercury–Containing Fluids. United States Patent 7,858,061 2010

Wilhelm, S.M. and Bloom, N. Mercury in petroleum. Fuel Processing Technology 63 (2000): 1–27.

Willhelm M.S. Mercury in petroleum and natural gas: estimation of emissions from production, processing, and combustion. EPA/600/R-01-066 (September 2001): 24–34.

Wu, J., Zhang, Y., Pan, W., He, P., Ren, J., Guo, R., Pan, L. and Wang, P. Study on flyash characteristics and its effect on mercury removal in coal–fired derived flue gas. International Conference on Computure Engineering and Technology, IEEE 5 (2010): 429–432.

Yan, T.Y. and Philadelphia, P. Method for Removing Mercury from Hydrocarbon Oil by High Temperature Reactive Adsorption. United States Patent 4,909,926 (1990).

Yasushiro, S., and Takayuki, H. Selective organic transformations on titanium oxide-based photocatalysts. Journal of Photochemistry and Photobiology C: Photochemistry Reviews 9 (2008): 157–170.

Yaws, C. Chemical properties handbook. Hardcover Book. MrGraw–Hill Professional Publishing, 1998.

Zahir, F., Rizwi, S.J., Haq, S.K. and Khan, R.H. Low dose mercury toxicity and human health. Environmental Toxicology and Pharmacology 20 (2005): 351–360.

Zhu, K. R., Zhang, M. S., Hong, J. M., and Yin, Z. Size effect on phase transition sequence of $TiO_2$ nanocrystal. Materials Science and Engineering 403 (2005): 87–93.

# APPENDICES

# APPENDIX A

## Preparation of Adsorbent

### A.1 Calculation of Ag metal loading to the support (percent weight)

In this research, the adsorbents were synthesized by wet impregnation method. The metal loadings of Ag were 0%, 5% and 15% by weight. The precursor for Ag was silver nitrate ($AgNO_3$). The metal loading was calculated using this formula:

$$\mathbf{X} = \left( \frac{\mathbf{A} \times \mathbf{B}}{100} \right)$$

where X is mass faction of Ag (g), A is the amount of support (g) and B is percent loading of Ag

**Example:** Preparation of 5 g adsorbent with 5% Ag metal loading

Atomic weight:

Ag= 107.8682 g/mol

N = 14.0067 g/mol

O = 15.9994 g/mol

Molecular weight (MW) of $AgNO_3$ = (107.8682)+(14.0067)+(15.9994×3) g/mol

= 169.8727 g/mol

Mass faction ( **X** ) of 5% Ag $= \left( \frac{5 \text{ g} \times 5}{100} \right)$

= 0.25 g

To determine the amount of $AgNO_3$ needed to obtain 0.25 g Ag, given that the atomic weight of Ag is 107.8682 g/mol and the MW of $AgNO_3$ is 169.8727 g/mol, the following calculation was done.

$$\text{Mass of } AgNO_3 = \left( \frac{169.8727 \text{ g/mol} \times 0.25 \text{ g}}{107.8782 \text{ g/mol}} \right)$$

$$= 0.3937 \text{ g}$$

This means that 0.3937 g of $AgNO_3$ is needed to synthesize a 5 g adsorbent with metal loading of 5% Ag to the support. Table A.1 summarizes the amounts of $AgNO_3$ used during the experiment.

**Table A.1** Mass of Ag and $AgNO_3$ required for different metal loadings.

| Metal loading | Mass of support (g) | Mass of Ag (g) | Mass of $AgNO_3$ (g) |
|---|---|---|---|
| 5%Ag wt. | 5 | 0.25 | 0.3937 |
| 15%Ag wt. | 5 | 0.75 | 1.181 |

## A.2 Wet impregnation products

(a) GAC samples

(b) $TiO_2$ samples

**Figure A.1** GAC samples (a) and $TiO_2$ samples (b), in powder, grain and pellet form (from left to right).

# APPENDIX B

# Batch Adsorption

## B.1 Vapor pressure

The vapor pressure data of Hg is important in determining its feasible concentrations from triple point to critical point, as shown in Figure B.1.

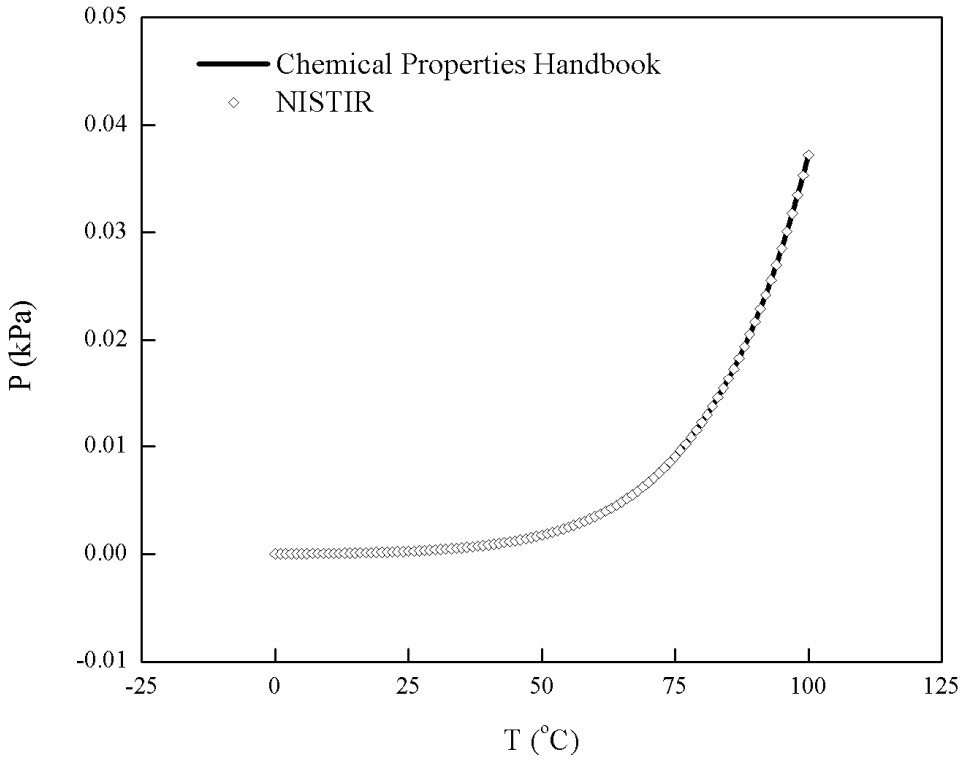


**Figure B.1** Temperature dependence of the vapor pressure of saturated liquid Hg. (Yaws, 2003 and Huber et al., 2006)

Using the vapor pressure data from Chemical Properties Handbook (Yaws C. L, 2003), the data in Table B.1 was calculated using the extended Antoine equation:

$$\log\ P = (A) + \frac{(B)}{T} + (C)\ \log\ T\ + (D)\ T + (E)T^2$$

Using the one from NISTIR, the data Table B.2 was calculated by this formula:

$$\ln\ (P/P_c) = \left(\frac{T_c}{T}\right)\left(a_1 t + a_2 t^{1.89} + a_3 t^2 + a_4 t^8 + a_5 t^{8.5} + a_6 t^9\right)$$

where P is vapor pressure (k Pa), T is temperature (C), Pc is constant of vapor pressure ($P_C$ = 167 M Pa), $T_C$ is constant of temperature ($T_C$ = 1764 K) and t is equation of 1-($T/T_C$)

**Table B.1** Vapor pressure of Hg (Chemical Properties Handbook).

| T [C] | T [K] | log P | P [mm Hg] | P [k Pa] |
|---|---|---|---|---|
| 0 | 273.15 | -3.69635 | 0.000201 | 2.68261E-05 |
| 1 | 274.15 | -3.65332 | 0.000222 | 2.962E-05 |
| 2 | 275.15 | -3.61061 | 0.000245 | 3.26809E-05 |
| 3 | 276.15 | -3.56822 | 0.000270 | 3.60319E-05 |
| 4 | 277.15 | -3.52613 | 0.000298 | 3.9698E-05 |
| 5 | 278.15 | -3.48436 | 0.000328 | 4.37062E-05 |
| 6 | 279.15 | -3.44289 | 0.000361 | 4.80852E-05 |
| 7 | 280.15 | -3.40172 | 0.000397 | 5.28662E-05 |
| 8 | 281.15 | -3.36086 | 0.000436 | 5.80827E-05 |
| 9 | 282.15 | -3.32028 | 0.000478 | 6.37706E-05 |
| 10 | 283.15 | -3.28000 | 0.000525 | 6.99684E-05 |
| 11 | 284.15 | -3.24001 | 0.000575 | 7.67176E-05 |
| 12 | 285.15 | -3.20030 | 0.000631 | 8.40624E-05 |
| 13 | 286.15 | -3.16088 | 0.00069 | 9.20504E-05 |
| 14 | 287.15 | -3.12173 | 0.000756 | 0.000100732 |
| 15 | 288.15 | -3.08287 | 0.000826 | 0.000110163 |
| 16 | 289.15 | -3.04427 | 0.000903 | 0.000120401 |
| 17 | 290.15 | -3.00595 | 0.000986 | 0.000131508 |
| 18 | 291.15 | -2.9679 | 0.001077 | 0.000143551 |
| 19 | 292.15 | -2.93011 | 0.001175 | 0.000156601 |
| 20 | 293.15 | -2.89258 | 0.001281 | 0.000170733 |
| 21 | 294.15 | -2.85532 | 0.001395 | 0.00018603 |
| 22 | 295.15 | -2.81831 | 0.001519 | 0.000202577 |
| 23 | 296.15 | -2.78156 | 0.001654 | 0.000220467 |

| T [C] | T [K] | log P | P [mm Hg] | P [k Pa] |
|---|---|---|---|---|
| 24 | 297.15 | -2.74506 | 0.001799 | 0.000239797 |
| 25 | 298.15 | -2.70881 | 0.001955 | 0.000260672 |
| 26 | 299.15 | -2.6728 | 0.002124 | 0.000283204 |
| 27 | 300.15 | -2.63705 | 0.002307 | 0.000307509 |
| 28 | 301.15 | -2.60153 | 0.002503 | 0.000333714 |
| 29 | 302.15 | -2.56625 | 0.002715 | 0.000361952 |
| 30 | 303.15 | -2.53121 | 0.002943 | 0.000392366 |
| 31 | 304.15 | -2.49641 | 0.003189 | 0.000425104 |
| 32 | 305.15 | -2.46184 | 0.003453 | 0.000460328 |
| 33 | 306.15 | -2.42749 | 0.003737 | 0.000498206 |
| 34 | 307.15 | -2.39338 | 0.004042 | 0.000538917 |
| 35 | 308.15 | -2.35949 | 0.00437 | 0.000582652 |
| 36 | 309.15 | -2.32583 | 0.004722 | 0.000629612 |
| 37 | 310.15 | -2.29239 | 0.0051 | 0.00068001 |
| 38 | 311.15 | -2.25916 | 0.005506 | 0.000734072 |
| 39 | 312.15 | -2.22616 | 0.005941 | 0.000792035 |
| 40 | 313.15 | -2.19337 | 0.006407 | 0.000854151 |
| 41 | 314.15 | -2.16079 | 0.006906 | 0.000920688 |
| 42 | 315.15 | -2.12842 | 0.00744 | 0.000991925 |
| 43 | 316.15 | -2.09627 | 0.008012 | 0.00106816 |
| 44 | 317.15 | -2.06432 | 0.008624 | 0.001149706 |
| 45 | 318.15 | -2.03257 | 0.009277 | 0.001236894 |
| 46 | 319.15 | -2.00103 | 0.009976 | 0.001330072 |
| 47 | 320.15 | -1.96969 | 0.010723 | 0.001429606 |
| 48 | 321.15 | -1.93854 | 0.01152 | 0.001535884 |
| 49 | 322.15 | -1.9076 | 0.012371 | 0.001649313 |
| 50 | 323.15 | -1.87685 | 0.013279 | 0.001770322 |
| 51 | 324.15 | -1.8463 | 0.014246 | 0.001899362 |
| 52 | 325.15 | -1.81593 | 0.015278 | 0.002036908 |
| 53 | 326.15 | -1.78576 | 0.016377 | 0.002183458 |
| 54 | 327.15 | -1.75577 | 0.017548 | 0.002339537 |
| 55 | 328.15 | -1.72597 | 0.018794 | 0.002505696 |
| 56 | 329.15 | -1.69636 | 0.020121 | 0.002682513 |
| 57 | 330.15 | -1.66693 | 0.021531 | 0.002870597 |
| 58 | 331.15 | -1.63768 | 0.023031 | 0.003070584 |
| 59 | 332.15 | -1.60861 | 0.024626 | 0.003283144 |
| 60 | 333.15 | -1.57972 | 0.02632 | 0.003508978 |
| 61 | 334.15 | -1.55101 | 0.028118 | 0.003748821 |
| 62 | 335.15 | -1.52247 | 0.030028 | 0.004003444 |
| 63 | 336.15 | -1.4941 | 0.032055 | 0.004273654 |
| 64 | 337.15 | -1.46591 | 0.034205 | 0.004560296 |
| 65 | 338.15 | -1.43789 | 0.036485 | 0.004864255 |
| 66 | 339.15 | -1.41003 | 0.038902 | 0.005186458 |

| T [C] | T [K] | log P | P [mm Hg] | P [k Pa] |
|---|---|---|---|---|
| 67 | 340.15 | -1.38235 | 0.041462 | 0.005527872 |
| 68 | 341.15 | -1.35482 | 0.044175 | 0.005889512 |
| 69 | 342.15 | -1.32747 | 0.047047 | 0.006272436 |
| 70 | 343.15 | -1.30027 | 0.050087 | 0.006677752 |
| 71 | 344.15 | -1.27324 | 0.053304 | 0.007106615 |
| 72 | 345.15 | -1.24637 | 0.056706 | 0.007560235 |
| 73 | 346.15 | -1.21965 | 0.060304 | 0.008039871 |
| 74 | 347.15 | -1.1931 | 0.064107 | 0.00854684 |
| 75 | 348.15 | -1.1667 | 0.068124 | 0.009082515 |
| 76 | 349.15 | -1.14045 | 0.072368 | 0.00964833 |
| 77 | 350.15 | -1.11436 | 0.07685 | 0.010245778 |
| 78 | 351.15 | -1.08842 | 0.08158 | 0.010876417 |
| 79 | 352.15 | -1.06263 | 0.086571 | 0.011541869 |
| 80 | 353.15 | -1.03699 | 0.091836 | 0.012243825 |
| 81 | 354.15 | -1.01149 | 0.097388 | 0.012984047 |
| 82 | 355.15 | -0.98615 | 0.103241 | 0.013764368 |
| 83 | 356.15 | -0.96095 | 0.109409 | 0.014586698 |
| 84 | 357.15 | -0.93589 | 0.115907 | 0.015453021 |
| 85 | 358.15 | -0.91098 | 0.122751 | 0.016365405 |
| 86 | 359.15 | -0.8862 | 0.129956 | 0.017325998 |
| 87 | 360.15 | -0.86157 | 0.137539 | 0.018337035 |
| 88 | 361.15 | -0.83708 | 0.145518 | 0.019400838 |
| 89 | 362.15 | -0.81273 | 0.153911 | 0.02051982 |
| 90 | 363.15 | -0.78851 | 0.162737 | 0.02169649 |
| 91 | 364.15 | -0.76443 | 0.172015 | 0.022933449 |
| 92 | 365.15 | -0.74049 | 0.181765 | 0.024233403 |
| 93 | 366.15 | -0.71668 | 0.192009 | 0.025599158 |
| 94 | 367.15 | -0.693 | 0.202769 | 0.027033625 |
| 95 | 368.15 | -0.66945 | 0.214066 | 0.028539827 |
| 96 | 369.15 | -0.64604 | 0.225925 | 0.030120896 |
| 97 | 370.15 | -0.62275 | 0.23837 | 0.031780084 |
| 98 | 371.15 | -0.59959 | 0.251426 | 0.033520758 |
| 99 | 372.15 | -0.57656 | 0.26512 | 0.035346409 |
| 100 | 373.15 | -0.55365 | 0.279478 | 0.037260657 |

**Table B.2** Vapor pressure of Hg (NISTIR).

| T [°C] | T [K] | t | ln ($P/P_C$) | P [k Pa] | Ideal gas density [ng/mL] | Concentration [$mg/m^3$] |
|---|---|---|---|---|---|---|
| 0 | 273.15 | 0.845153 | -22.5459 | 2.69883E-05 | 2.383673349 | 2.385173 |
| 1 | 274.15 | 0.844586 | -22.447 | 2.97939E-05 | 2.621875228 | 2.623525 |
| 2 | 275.15 | 0.844019 | -22.3488 | 3.28672E-05 | 2.881812836 | 2.883626 |
| 3 | 276.15 | 0.843452 | -22.2513 | 3.62313E-05 | 3.165274827 | 3.167267 |

| T [°C] | T [K] | t | ln ($P/P_C$) | P [k Pa] | Ideal gas density [ng/mL] | Concentration [mg/m$^3$] |
|---|---|---|---|---|---|---|
| 4 | 277.15 | 0.842885 | -22.1546 | 3.99112E-05 | 3.474180332 | 3.476367 |
| 5 | 278.15 | 0.842319 | -22.0586 | 4.39338E-05 | 3.810587184 | 3.812985 |
| 6 | 279.15 | 0.841752 | -21.9632 | 4.83279E-05 | 4.176700574 | 4.179329 |
| 7 | 280.15 | 0.841185 | -21.8686 | 5.31249E-05 | 4.574882152 | 4.577761 |
| 8 | 281.15 | 0.840618 | -21.7747 | 5.8358E-05 | 5.007659598 | 5.010811 |
| 9 | 282.15 | 0.840051 | -21.6814 | 6.40632E-05 | 5.477736665 | 5.481184 |
| 10 | 283.15 | 0.839484 | -21.5888 | 7.02791E-05 | 5.988003735 | 5.991772 |
| 11 | 284.15 | 0.838917 | -21.4968 | 7.7047E-05 | 6.541548884 | 6.545666 |
| 12 | 285.15 | 0.83835 | -21.4056 | 8.44113E-05 | 7.141669497 | 7.146164 |
| 13 | 286.15 | 0.837783 | -21.3149 | 9.24195E-05 | 7.79188443 | 7.796788 |
| 14 | 287.15 | 0.837217 | -21.2249 | 0.000101123 | 8.495946759 | 8.501294 |
| 15 | 288.15 | 0.83665 | -21.1356 | 0.000110575 | 9.257857124 | 9.263683 |
| 16 | 289.15 | 0.836083 | -21.0468 | 0.000120835 | 10.08187769 | 10.08822 |
| 17 | 290.15 | 0.835516 | -20.9587 | 0.000131965 | 10.97254678 | 10.97945 |
| 18 | 291.15 | 0.834949 | -20.8712 | 0.000144031 | 11.93469408 | 11.94221 |
| 19 | 292.15 | 0.834382 | -20.7843 | 0.000157105 | 12.97345667 | 12.98162 |
| 20 | 293.15 | 0.833815 | -20.6981 | 0.000171262 | 14.09429562 | 14.10317 |
| 21 | 294.15 | 0.833248 | -20.6124 | 0.000186583 | 15.30301343 | 15.31264 |
| 22 | 295.15 | 0.832681 | -20.5273 | 0.000203156 | 16.60577212 | 16.61622 |
| 23 | 296.15 | 0.832115 | -20.4428 | 0.000221071 | 18.00911219 | 18.02045 |
| 24 | 297.15 | 0.831548 | -20.3588 | 0.000240426 | 19.5199723 | 19.53226 |
| 25 | 298.15 | 0.830981 | -20.2755 | 0.000261327 | 21.14570986 | 21.15902 |
| 26 | 299.15 | 0.830414 | -20.1927 | 0.000283884 | 22.89412233 | 22.90853 |
| 27 | 300.15 | 0.829847 | -20.1105 | 0.000308214 | 24.77346959 | 24.78906 |
| 28 | 301.15 | 0.82928 | -20.0288 | 0.000334444 | 26.79249699 | 26.80936 |
| 29 | 302.15 | 0.828713 | -19.9477 | 0.000362707 | 28.96045949 | 28.97869 |
| 30 | 303.15 | 0.828146 | -19.8671 | 0.000393143 | 31.28714667 | 31.30684 |
| 31 | 304.15 | 0.827579 | -19.787 | 0.000425905 | 33.78290872 | 33.80417 |
| 32 | 305.15 | 0.827012 | -19.7075 | 0.000461149 | 36.45868343 | 36.48163 |
| 33 | 306.15 | 0.826446 | -19.6286 | 0.000499047 | 39.32602422 | 39.35077 |
| 34 | 307.15 | 0.825879 | -19.5501 | 0.000539777 | 42.39712921 | 42.42381 |
| 35 | 308.15 | 0.825312 | -19.4722 | 0.000583528 | 45.68487137 | 45.71362 |
| 36 | 309.15 | 0.824745 | -19.3947 | 0.000630502 | 49.20282974 | 49.2338 |
| 37 | 310.15 | 0.824178 | -19.3178 | 0.000680912 | 52.96532186 | 52.99866 |
| 38 | 311.15 | 0.823611 | -19.2414 | 0.000734981 | 56.98743727 | 57.0233 |
| 39 | 312.15 | 0.823044 | -19.1655 | 0.000792949 | 61.28507226 | 61.32364 |
| 40 | 313.15 | 0.822477 | -19.0901 | 0.000855067 | 65.87496577 | 65.91642 |
| 41 | 314.15 | 0.82191 | -19.0151 | 0.000921601 | 70.77473659 | 70.81928 |
| 42 | 315.15 | 0.821344 | -18.9407 | 0.00099283 | 76.00292179 | 76.05075 |
| 43 | 316.15 | 0.820777 | -18.8667 | 0.001069052 | 81.57901646 | 81.63036 |
| 44 | 317.15 | 0.82021 | -18.7932 | 0.00115058 | 87.52351472 | 87.5786 |
| 45 | 318.15 | 0.819643 | -18.7202 | 0.001237743 | 93.85795216 | 93.91702 |

| T [°C] | T [K] | t | ln ($P/P_C$) | P [k Pa] | Ideal gas density [ng/mL] | Concentration [$mg/m^3$] |
|---|---|---|---|---|---|---|
| 46 | 319.15 | 0.819076 | -18.6477 | 0.001330888 | 100.6049496 | 100.6683 |
| 47 | 320.15 | 0.818509 | -18.5756 | 0.001430383 | 107.7882583 | 107.8561 |
| 48 | 321.15 | 0.817942 | -18.5039 | 0.001536613 | 115.4328064 | 115.5055 |
| 49 | 322.15 | 0.817375 | -18.4327 | 0.001649985 | 123.5647473 | 123.6425 |
| 50 | 323.15 | 0.816808 | -18.362 | 0.001770928 | 132.2115087 | 132.2947 |
| 51 | 324.15 | 0.816241 | -18.2917 | 0.00189989 | 141.4018444 | 141.4908 |
| 52 | 325.15 | 0.815675 | -18.2219 | 0.002037347 | 151.1658859 | 151.261 |
| 53 | 326.15 | 0.815108 | -18.1524 | 0.002183795 | 161.5351976 | 161.6369 |
| 54 | 327.15 | 0.814541 | -18.0835 | 0.00233976 | 172.5428317 | 172.6514 |
| 55 | 328.15 | 0.813974 | -18.0149 | 0.002505789 | 184.223386 | 184.3393 |
| 56 | 329.15 | 0.813407 | -17.9468 | 0.002682462 | 196.6130629 | 196.7368 |
| 57 | 330.15 | 0.81284 | -17.8791 | 0.002870385 | 209.7497297 | 209.8817 |
| 58 | 331.15 | 0.812273 | -17.8118 | 0.003070193 | 223.6729814 | 223.8137 |
| 59 | 332.15 | 0.811706 | -17.7449 | 0.003282555 | 238.4242046 | 238.5743 |
| 60 | 333.15 | 0.811139 | -17.6784 | 0.00350817 | 254.0466433 | 254.2065 |
| 61 | 334.15 | 0.810573 | -17.6123 | 0.003747773 | 270.5854664 | 270.7558 |
| 62 | 335.15 | 0.810006 | -17.5467 | 0.004002133 | 288.0878373 | 288.2691 |
| 63 | 336.15 | 0.809439 | -17.4814 | 0.004272055 | 306.602985 | 306.7959 |
| 64 | 337.15 | 0.808872 | -17.4165 | 0.004558384 | 326.1822769 | 326.3876 |
| 65 | 338.15 | 0.808305 | -17.3521 | 0.004862002 | 346.8792944 | 347.0976 |
| 66 | 339.15 | 0.807738 | -17.288 | 0.005183834 | 368.7499086 | 368.982 |
| 67 | 340.15 | 0.807171 | -17.2242 | 0.005524848 | 391.8523602 | 392.099 |
| 68 | 341.15 | 0.806604 | -17.1609 | 0.005886054 | 416.247339 | 416.5093 |
| 69 | 342.15 | 0.806037 | -17.098 | 0.00626851 | 441.9980675 | 442.2762 |
| 70 | 343.15 | 0.805471 | -17.0354 | 0.00667332 | 469.1703846 | 469.4657 |
| 71 | 344.15 | 0.804904 | -16.9732 | 0.007101641 | 497.8328325 | 498.1461 |
| 72 | 345.15 | 0.804337 | -16.9113 | 0.007554676 | 528.0567456 | 528.3891 |
| 73 | 346.15 | 0.80377 | -16.8499 | 0.008033686 | 559.9163403 | 560.2687 |
| 74 | 347.15 | 0.803203 | -16.7887 | 0.008539985 | 593.4888082 | 593.8623 |
| 75 | 348.15 | 0.802636 | -16.728 | 0.009074943 | 628.8544108 | 629.2502 |
| 76 | 349.15 | 0.802069 | -16.6676 | 0.009639991 | 666.096576 | 666.5158 |
| 77 | 350.15 | 0.801502 | -16.6075 | 0.010236621 | 705.3019971 | 705.7459 |
| 78 | 351.15 | 0.800935 | -16.5478 | 0.010866388 | 746.560734 | 747.0306 |
| 79 | 352.15 | 0.800368 | -16.4885 | 0.011530912 | 789.9663158 | 790.4635 |
| 80 | 353.15 | 0.799802 | -16.4295 | 0.012231881 | 835.615847 | 836.1417 |
| 81 | 354.15 | 0.799235 | -16.3708 | 0.012971055 | 883.6101138 | 884.1662 |
| 82 | 355.15 | 0.798668 | -16.3124 | 0.013750264 | 934.0536948 | 934.6415 |
| 83 | 356.15 | 0.798101 | -16.2544 | 0.014571415 | 987.055072 | 987.6763 |
| 84 | 357.15 | 0.797534 | -16.1968 | 0.01543649 | 1042.726745 | 1043.383 |
| 85 | 358.15 | 0.796967 | -16.1394 | 0.016347553 | 1101.185348 | 1101.878 |
| 86 | 359.15 | 0.7964 | -16.0824 | 0.017306751 | 1162.551767 | 1163.283 |
| 87 | 360.15 | 0.795833 | -16.0257 | 0.018316315 | 1226.951262 | 1227.723 |

| T [°C] | T [K] | t | ln ($P/P_C$) | P [k Pa] | Ideal gas density [ng/mL] | Concentration [$mg/m^3$] |
|---|---|---|---|---|---|---|
| 88 | 361.15 | 0.795266 | -15.9693 | 0.019378565 | 1294.513587 | 1295.328 |
| 89 | 362.15 | 0.7947 | -15.9133 | 0.020495911 | 1365.373118 | 1366.232 |
| 90 | 363.15 | 0.794133 | -15.8575 | 0.021670857 | 1439.668982 | 1440.575 |
| 91 | 364.15 | 0.793566 | -15.8021 | 0.022906004 | 1517.54518 | 1518.5 |
| 92 | 365.15 | 0.792999 | -15.747 | 0.024204052 | 1599.150726 | 1600.157 |
| 93 | 366.15 | 0.792432 | -15.6922 | 0.025567807 | 1684.639777 | 1685.7 |
| 94 | 367.15 | 0.791865 | -15.6377 | 0.027000175 | 1774.171772 | 1775.288 |
| 95 | 368.15 | 0.791298 | -15.5835 | 0.028504176 | 1867.911568 | 1869.087 |
| 96 | 369.15 | 0.790731 | -15.5295 | 0.030082942 | 1966.029585 | 1967.267 |
| 97 | 370.15 | 0.790164 | -15.4759 | 0.031739718 | 2068.701944 | 2070.004 |
| 98 | 371.15 | 0.789598 | -15.4226 | 0.03347787 | 2176.110618 | 2177.48 |
| 99 | 372.15 | 0.789031 | -15.3696 | 0.035300887 | 2288.443576 | 2289.884 |
| 100 | 373.15 | 0.788464 | -15.3169 | 0.037212383 | 2405.894934 | 2407.409 |

## B.2 Quantitative analysis of trace Hg

The soil standard sample (Standard Reference Material (SRM) ® 2586 Trace Elements in Soil which contains lead from paint) used for Hg quantitative analysis was obtained from National Institute of Standards and Technology (NIST), as shown in Figure B.2 Table B.3 summarizes its concentration details. This sample is tested quantitatively for the presence of solid Hg using Lumex–$RA915^+$ mercury analyzer (Ohio Lumex) shown in Figure B.3.


**Figure B.2** Soil standard of SRM ® 2586

**Table B.3** Measurand* data of SRM ® 2586 (NIST, 2012).

| **Concentrations**** | |
|---|---|
| **Parameter** | **Value** |
| Aluminum | 6.652% |
| Arsenic | 8.700 |
| Barium | 413 |
| Beryllium | (1.4) |
| Cadmium | 2.71 |
| Calcium | 2.218 % |
| Cerium | 58 |
| Chromium | 301 |
| Cobalt | (35) |
| Copper | (81) |
| Dysprosium | (5.4) |
| Erbium | 3.3 |
| Europium | (1.5) |
| Gadolinium | 5.8 |
| Gallium | (14) |
| Holmium | (1.1) |
| Iron (total) | 5.161 % |
| Lanthanum | 29.7 |
| Lead | 432 |
| Lithium | (25) |
| Magnesium | 1.707 % |
| Manganese | 1000 |
| **Mercury** | **0.367** |
| Neodymium | 26.4 |
| Nickel | (75) |
| Niobium | 6 |
| Phosphorus | 1001 |
| Potassium | 0.976 % |
| Praseodymium | 7.3 |
| Samarium | (6.1) |

| | |
|---|---|
| Scandium | 24 |
| Selenium | 0.6 |
| Silicon | 29.15 % |
| Sodium | 0.468 % |
| Strontium | 84.1 |
| Terbium | 0.9 |
| Thorium | (7) |
| Thulium | 0.5 |
| Titanium | 0.605 % |
| Vanadium | (160) |
| Ytterbium | 2.64 |
| Yttrium | (21) |
| Zinc | 352 |

Notes * Measurand is defined by the measurement method, characterization of test methods and simple calibration.

** Concentrations are in mass fractions, in mg/kg, unless noted as % and (powder form).

**Figure B.3** Lumex–RA915$^{+}$ mercury analyzer apparatus.

## B.3 Calibration

The mass fraction of Hg in the soil sample (0.367 mg/kg) was obtained from Table B.4. Assuming that the mass of the soil sample is 10 mg, the calibration data was calculated as follows:

$$\text{Amount of Hg in the soil sample} = \frac{(0.367\ mg \times 10\ mg)}{1\ x\ 10^{6}\ mg}$$

$$= 3.67\times10^{-6}\ \text{mg}$$

**Table B.4** Standard samples of known area and their corresponding Hg amount

| Tests | Mass soil std. (mg) | Area | Amount of Hg (mg) |
|---|---|---|---|
| 1 | 10.0 | 1880 | 3.670E-06 |
| 2 | 30.2 | 5120 | 1.108E-05 |
| 3 | 50.1 | 10800 | 1.839E-05 |
| 4 | 100.0 | 21300 | 3.670E-05 |
| 5 | 150.0 | 27200 | 5.505E-05 |
| 6 | 200.0 | 39995 | 7.340E-05 |

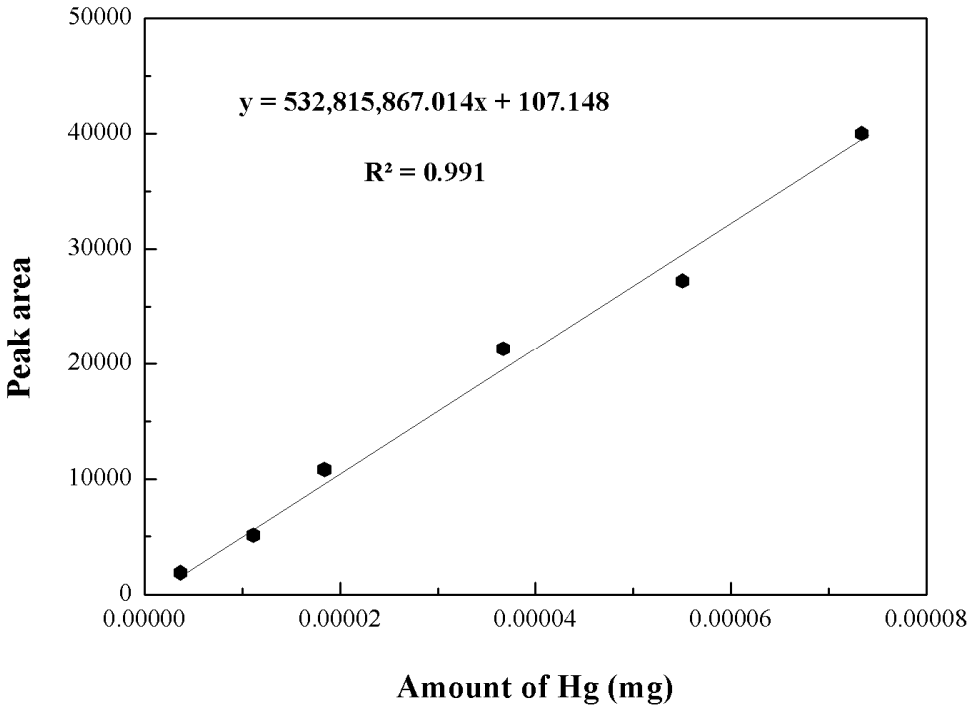


**Figure B.4** Calibration curve for Hg (solid).

## B.4 Adsorption capacity

The quantity of Hg was measured by using the mercury analyzer equipped with a Pyro 915 attachment (Figure B.4). A plot of PMT Current vs. time was obtained.

The plot shows maximum values or peak, as shown in Figure B.5. Adsorption capacity ($q_t$) data was calculated as follows:

Example; Hg adsorbed by GAC at 40°C for 1 Day (Trial 1).

From Figure B.3, the equation of calibration curve is y = 532,815,867.014x + 107.148

$$\text{Amount of Hg} = \frac{(\text{Area} - \text{y Intercept})}{\text{Slope}}$$

$$= \frac{(28{,}800 - 107.148)}{532{,}815867.014}$$

$$= 5.\ 39\times10^{-5}\ \text{mg}$$

Thus,

$$q_t = \frac{(\text{Amount of Hg} \times \text{y Dilutions})}{\text{Mass Samples}}$$

$$= \frac{(5.39\times10^{-5}\ \text{mg}_{\text{Hg}})\times 197.14}{5\ \text{mg}_{\text{adsorbent}}}$$

$$= 2.123\times10^{-3}\ \text{mg of Hg/mg adsorbent}$$

Or,

$$= 2.123\ \text{mg of Hg/g adsorbent}$$


**Figure B.5** Lumex–RA915$^{+}$ mercury analyzer with Pyro 915 apparatus

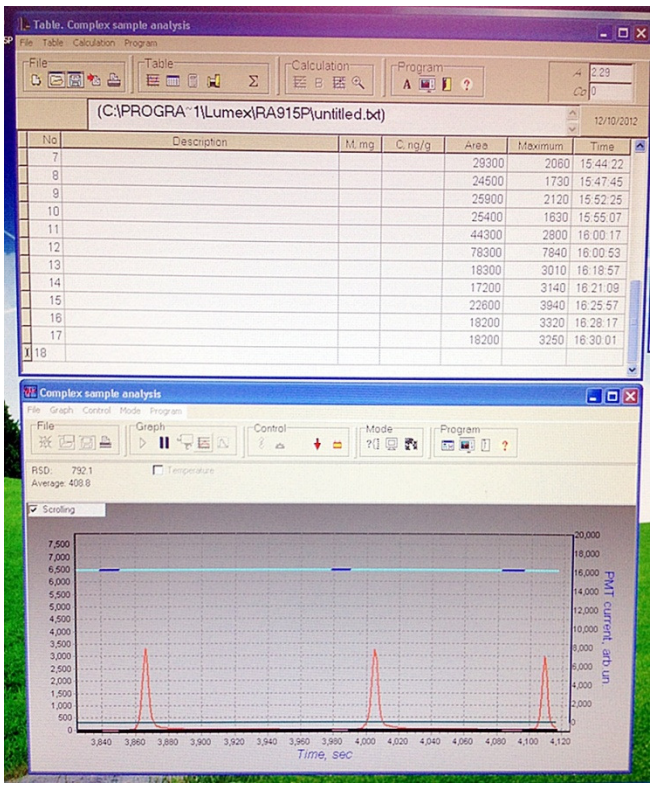


**Figure B.6** Monitoring of peak area.

Tables B.5 to B6 sum up the information needed to obtain $q_t$ data for the adsorption of Hg at 40°C and 60°C for 1, 5, 20, 40 and 60 days. The values of $q_t$ at 40°C and 60°C are summarized in Tables B.7 and B.8, respectively. Table B.9 shown the data of adsorption.

**Table B.5** Adsorption of Hg at 40°C

**1 Day**

| Adsorbent | Test | Mass of sample (mg) | Dilution (times) | Area | Amount of Hg (mg) | $q_t$ (mg Hg/g adsorbent) |
|---|---|---|---|---|---|---|
| $TiO_2$ | 1 | 1.0 | 1 | 4,600 | 8.43E-06 | 0.0087 |
| | 2 | 1.0 | 1 | 4,910 | 9.01E-06 | |
| GAC | 1 | 5.0 | 197.14 | 28,800 | 5.39E-05 | 2.1565 |
| | 2 | 5.0 | 197.14 | 29,700 | 5.55E-05 | |
| 5%Ag/$TiO_2$ | 1 | 2.0 | 511.35 | 28,000 | 5.23E-05 | 13.0201 |
| | 2 | 2.1 | 511.35 | 27,800 | 5.20E-05 | |
| 5%Ag/GAC | 1 | 4.9 | 1021.29 | 13,100 | 2.44E-05 | 5.4151 |
| | 2 | 5.1 | 1021.29 | 15,400 | 2.87E-05 | |
| 15%Ag/$TiO_2$ | 1 | 2.2 | 1021.31 | 16,300 | 3.04E-05 | 15.0535 |
| | 2 | 2.0 | 1021.31 | 16,800 | 3.13E-05 | |
| 15%Ag/GAC | 1 | 2.1 | 1001.06 | 11,600 | 2.16E-05 | 10.1034 |
| | 2 | 2.1 | 1001.06 | 11,200 | 2.08E-05 | |
| Commercial | 1 | 5.2 | 981.43 | 21,600 | 4.03E-05 | 7.6396 |
| | 2 | 4.9 | 981.43 | 20,500 | 3.83E-05 | |

**5 Day**

| Adsorbent | Test | Mass of sample (mg) | Dilution (times) | Area | Amount of Hg (mg) | $q_t$ (mg Hg/g adsorbent) |
|---|---|---|---|---|---|---|
| $TiO_2$ | 1 | 2.1 | 1 | 3,220 | 5.82E-06 | 0.0033 |
| | 2 | 2.1 | 1 | 4,340 | 7.91E-06 | |
| GAC | 1 | 2.2 | 205.24 | 16,300 | 3.03E-05 | 2.9813 |
| | 2 | 2.2 | 205.24 | 18,100 | 3.36E-05 | |
| 5%Ag/$TiO_2$ | 1 | 1.5 | 1001.12 | 18,800 | 3.49E-05 | 23.5737 |
| | 2 | 1.5 | 1001.12 | 19,200 | 3.57E-05 | |
| 5%Ag/GAC | 1 | 5.0 | 2001.36 | 18,500 | 3.44E-05 | 12.3007 |
| | 2 | 4.9 | 2001.36 | 14,300 | 2.65E-05 | |
| 15%Ag/$TiO_2$ | 1 | 2.1 | 2000.68 | 19,700 | 3.66E-05 | 33.2942 |
| | 2 | 2.1 | 2000.68 | 17,900 | 3.33E-05 | |
| 15%Ag/GAC | 1 | 5.1 | 2001.40 | 32,600 | 6.07E-05 | 24.8218 |
| | 2 | 4.9 | 2001.40 | 33,900 | 6.32E-05 | |
| Commercial | 1 | 4.9 | 2001.28 | 26,900 | 5.01E-05 | 20.5726 |
| | 2 | 4.9 | 2001.28 | 27,200 | 5.07E-05 | |

**20 Day**

| Adsorbent | Test | Mass of sample (mg) | Dilution (times) | Area | Amount of Hg (mg) | $q_t$ (mg Hg/g adsorbent) |
|---|---|---|---|---|---|---|
| $TiO_2$ | 1 | 49.9 | 197.22 | 2,930 | 5.28E-06 | 0.0185 |
| | 2 | 50.1 | 197.22 | 2,310 | 4.12E-06 | |
| GAC | 1 | 2.0 | 205.20 | 29,000 | 5.40E-05 | 5.6477 |
| | 2 | 2.1 | 205.20 | 31,600 | 5.89E-05 | |
| 5%Ag/$TiO_2$ | 1 | 2.2 | 2084.31 | 23,200 | 4.32E-05 | 44.7528 |
| | 2 | 2.1 | 2084.31 | 26,300 | 4.90E-05 | |
| 5%Ag/GAC | 1 | 2.1 | 1001.04 | 21,200 | 3.94E-05 | 17.9955 |
| | 2 | 2.1 | 1001.04 | 19,400 | 3.61E-05 | |
| 15%Ag/$TiO_2$ | 1 | 2.1 | 4001.36 | 20,600 | 3.83E-05 | 71.0013 |
| | 2 | 2.2 | 4001.36 | 20,400 | 3.79E-05 | |
| 15%Ag/GAC | 1 | 2.2 | 4001.24 | 14,900 | 2.77E-05 | 47.7645 |
| | 2 | 2.0 | 4001.24 | 12,200 | 2.26E-05 | |
| Commercial | 1 | 1.9 | 3000.88 | 15,200 | 2.82E-05 | 42.4698 |
| | 2 | 2.0 | 3000.88 | 14,500 | 2.69E-05 | |

**40 Day**

| Adsorbents | Tests | Mass of sample (mg) | Dilution (times) | Area | Amount of Hg (mg) | $q_t$ (mg Hg/g adsorbent) |
|---|---|---|---|---|---|---|
| $TiO_2$ | 1 | 50.0 | 102.12 | 2,200 | 3.91E-06 | 0.0078 |
| | 2 | 49.0 | 102.12 | 2,080 | 3.69E-06 | |
| GAC | 1 | 5.0 | 1042.65 | 15,600 | 2.90E-05 | 6.5611 |
| | 2 | 5.2 | 1042.65 | 19,000 | 3.53E-05 | |
| 5%Ag/$TiO_2$ | 1 | 2.1 | 1725.14 | 37,900 | 7.07E-05 | 53.8962 |
| | 2 | 2.1 | 1725.14 | 32,500 | 6.06E-05 | |
| 5%Ag/GAC | 1 | 2.0 | 1001.06 | 23,800 | 4.43E-05 | 22.5080 |
| | 2 | 1.9 | 1001.06 | 23,300 | 4.34E-05 | |
| 15%Ag/$TiO_2$ | 1 | 2.1 | 3001.28 | 39,000 | 7.27E-05 | 104.5149 |
| | 2 | 1.9 | 3001.28 | 35,700 | 6.65E-05 | |
| 15%Ag/GAC | 1 | 2.0 | 3126.21 | 27,700 | 5.16E-05 | 76.4878 |
| | 2 | 2.1 | 3126.21 | 26,100 | 4.86E-05 | |
| Commercial | 1 | 2.9 | 2885.65 | 33,200 | 6.19E-05 | 64.1329 |
| | 2 | 3.0 | 2885.65 | 37,200 | 6.93E-05 | |

**60 Day**

| Adsorbents | Tests | Mass of sample (mg) | Dilution (times) | Area | Amount of Hg (mg) | $q_t$ (mg Hg/g adsorbent) |
|---|---|---|---|---|---|---|
| 15%Ag/$TiO_2$ | 1 | 2.0 | 3001.32 | 38,700 | 7.22E-05 | 107.1517 |
| | 2 | 2.0 | 3001.32 | 37,900 | 7.07E-05 | |
| 15%Ag/GAC | 1 | 2.1 | 2886.00 | 33,900 | 6.32E-05 | 81.5752 |
| | 2 | 2.0 | 2886.00 | 28,400 | 5.29E-05 | |
| Commercial | 1 | 2.2 | 3126.33 | 27,000 | 5.03E-05 | 69.0560 |
| | 2 | 2.2 | 3126.33 | 25,200 | 4.69E-05 | |

**Table B.6** Adsorption of Hg at 60°C

**1 Day**

| Adsorbents | Tests | Mass of sample (mg) | Dilution (times) | Area | Amount of Hg (mg) | $q_t$ (mg Hg/g adsorbent) |
|---|---|---|---|---|---|---|
| $TiO_2$ | 1 | 5.1 | 1.00 | 18,600 | 3.47E-05 | 0.0061 |
| | 2 | 5.0 | 1.00 | 18,860 | 3.52E-05 | |
| | 3 | 4.9 | 1.00 | 14,000 | 2.61E-05 | |
| | 4 | 4.9 | 1.00 | 14,400 | 2.68E-05 | |
| | 5 | 5.1 | 1.00 | 16,400 | 3.06E-05 | |
| | 6 | 4.9 | 1.00 | 16,400 | 3.06E-05 | |
| GAC | 1 | 1.9 | 197.18 | 8,640 | 1.60E-05 | 1.7074 |
| | 2 | 1.9 | 197.18 | 8,430 | 1.56E-05 | |
| | 3 | 2.7 | 197.18 | 12,300 | 2.29E-05 | |
| | 4 | 2.6 | 197.18 | 12,700 | 2.36E-05 | |
| | 5 | 2.4 | 197.18 | 11,600 | 2.16E-05 | |
| | 6 | 2.4 | 197.18 | 11,300 | 2.10E-05 | |
| 5%Ag/$TiO_2$ | 1 | 2.0 | 962.40 | 27,700 | 5.18E-05 | 24.7518 |
| | 2 | 2.0 | 962.40 | 30,200 | 5.65E-05 | |
| | 3 | 1.9 | 962.40 | 24,700 | 4.62E-05 | |
| | 4 | 1.9 | 962.40 | 24,500 | 4.58E-05 | |
| | 5 | 2.0 | 962.40 | 27,200 | 5.08E-05 | |
| | 6 | 1.9 | 962.40 | 26,800 | 5.01E-05 | |
| 5%Ag/GAC | 1 | 2.1 | 1000.98 | 21,200 | 3.96E-05 | 16.7880 |
| | 2 | 2.1 | 1000.98 | 21,100 | 3.94E-05 | |
| | 3 | 1.8 | 1000.98 | 16,100 | 3.00E-05 | |
| | 4 | 1.6 | 1000.98 | 14,100 | 2.63E-05 | |
| | 5 | 2.1 | 1000.98 | 18,600 | 3.47E-05 | |
| | 6 | 2.1 | 1000.98 | 15,100 | 2.81E-05 | |
| 15%Ag/$TiO_2$ | 1 | 2.3 | 1021.57 | 41,400 | 7.75E-05 | 36.1686 |
| | 2 | 2.1 | 1021.57 | 40,100 | 7.51E-05 | |
| | 3 | 2.1 | 1021.57 | 40,800 | 7.64E-05 | |
| | 4 | 2.1 | 1021.57 | 40,100 | 7.51E-05 | |
| | 5 | 2.2 | 1021.57 | 40,500 | 7.58E-05 | |
| | 6 | 2.2 | 1021.57 | 42,800 | 8.01E-05 | |
| 15%Ag/GAC | 1 | 2.3 | 962.63 | 26,800 | 5.01E-05 | 23.0885 |
| | 2 | 2.3 | 962.63 | 36,400 | 6.81E-05 | |
| | 3 | 1.8 | 962.63 | 20,200 | 3.77E-05 | |
| | 4 | 2.4 | 962.63 | 30,000 | 5.61E-05 | |
| | 5 | 1.9 | 962.63 | 21,000 | 3.92E-05 | |
| | 6 | 2.5 | 962.63 | 36,800 | 6.89E-05 | |
| Commercial | 1 | 2.2 | 1021.41 | 25,600 | 4.78E-05 | 19.5335 |
| | 2 | 2.0 | 1021.41 | 18,300 | 3.41E-05 | |
| | 3 | 2.1 | 1021.41 | 26,100 | 4.88E-05 | |
| | 4 | 2.0 | 1021.41 | 18,900 | 3.53E-05 | |
| | 5 | 2.4 | 1021.41 | 22,900 | 4.28E-05 | |
| | 6 | 2.7 | 1021.41 | 24,900 | 4.65E-05 | |

**5 Day**

| Adsorbent | Test | Mass of sample (mg) | Dilution (times) | Area | Amount of Hg (mg) | $q_t$ (mg Hg/g adsorbent) |
|---|---|---|---|---|---|---|
| $TiO_2$ | 1 | 2.0 | 1.00 | 7,140 | 1.32E-05 | 0.0061 |
| | 2 | 2.0 | 1.00 | 6,800 | 1.26E-05 | |
| | 3 | 2.0 | 1.00 | 5,600 | 1.03E-05 | |
| | 4 | 2.0 | 1.00 | 6,850 | 1.27E-05 | |
| | 5 | 1.9 | 1.00 | 6,630 | 1.22E-05 | |
| | 6 | 1.9 | 1.00 | 6,250 | 1.15E-05 | |
| GAC | 1 | 2.0 | 205.04 | 12,500 | 2.33E-05 | 2.8585 |
| | 2 | 2.0 | 205.04 | 14,700 | 2.74E-05 | |
| | 3 | 2.3 | 205.04 | 17,900 | 3.34E-05 | |
| | 4 | 1.9 | 205.04 | 12,600 | 2.34E-05 | |
| | 5 | 2.3 | 205.04 | 18,700 | 3.49E-05 | |
| | 6 | 1.9 | 205.04 | 16,600 | 3.10E-05 | |
| 5%Ag/$TiO_2$ | 1 | 1.7 | 1563.56 | 25,000 | 4.67E-05 | 42.9322 |
| | 2 | 1.9 | 1563.56 | 23,600 | 4.41E-05 | |
| | 3 | 1.8 | 1563.56 | 25,000 | 4.67E-05 | |
| | 4 | 1.8 | 1563.56 | 28,700 | 5.37E-05 | |
| | 5 | 2.2 | 1563.56 | 34,500 | 6.45E-05 | |
| | 6 | 2.1 | 1563.56 | 32,500 | 6.08E-05 | |
| 5%Ag/GAC | 1 | 1.9 | 1501.10 | 15,600 | 2.91E-05 | 21.5134 |
| | 2 | 2.0 | 1501.10 | 16,300 | 3.04E-05 | |
| | 3 | 1.9 | 1501.10 | 15,200 | 2.83E-05 | |
| | 4 | 1.7 | 1501.10 | 12,900 | 2.40E-05 | |
| | 5 | 1.9 | 1501.10 | 13,200 | 2.46E-05 | |
| | 6 | 1.9 | 1501.10 | 13,800 | 2.57E-05 | |
| 15%Ag/$TiO_2$ | 1 | 1.1 | 1471.75 | 30,200 | 5.65E-05 | 76.4988 |
| | 2 | 0.9 | 1471.75 | 25,100 | 4.69E-05 | |
| | 3 | 1.1 | 1471.75 | 29,100 | 5.44E-05 | |
| | 4 | 1.0 | 1471.75 | 27,100 | 5.07E-05 | |
| | 5 | 1.2 | 1471.75 | 34,000 | 6.36E-05 | |
| | 6 | 1.1 | 1471.75 | 32,500 | 6.08E-05 | |
| 15%Ag/GAC | 1 | 1.9 | 1531.76 | 26,900 | 5.03E-05 | 40.9722 |
| | 2 | 1.9 | 1531.76 | 28,900 | 5.40E-05 | |
| | 3 | 2.1 | 1531.76 | 31,000 | 5.80E-05 | |
| | 4 | 1.9 | 1531.76 | 24,500 | 4.58E-05 | |
| | 5 | 2.1 | 1531.76 | 31,900 | 5.97E-05 | |
| | 6 | 2.1 | 1531.76 | 28,600 | 5.35E-05 | |
| Commercial | 1 | 1.3 | 1531.53 | 14,400 | 2.68E-05 | 35.8130 |
| | 2 | 1.2 | 1531.53 | 15,300 | 2.85E-05 | |
| | 3 | 1.6 | 1531.53 | 20,600 | 3.85E-05 | |
| | 4 | 2.1 | 1531.53 | 25,900 | 4.84E-05 | |
| | 5 | 2.1 | 1531.53 | 25,600 | 4.78E-05 | |
| | 6 | 1.6 | 1531.53 | 22,300 | 4.17E-05 | |

**20 Day**

| Adsorbent | Test | Mass of sample (mg) | Dilution (times) | Area | Amount of Hg (mg) | $q_t$ (mg Hg/g adsorbent) |
|---|---|---|---|---|---|---|
| $TiO_2$ | 1 | 1.9 | 1.00 | 18,000 | 3.36E-05 | 0.0175 |
| | 2 | 1.9 | 1.00 | 16,700 | 3.11E-05 | |
| | 3 | 1.8 | 1.00 | 17,600 | 3.28E-05 | |
| | 4 | 2.0 | 1.00 | 13,600 | 2.53E-05 | |
| | 5 | 1.9 | 1.00 | 22,500 | 4.20E-05 | |
| | 6 | 2.0 | 1.00 | 18,900 | 3.53E-05 | |
| GAC | 1 | 2.1 | 201.14 | 39,400 | 7.37E-05 | 6.9853 |
| | 2 | 2.1 | 201.14 | 39,400 | 7.37E-05 | |
| | 3 | 2.0 | 201.14 | 39,100 | 7.32E-05 | |
| | 4 | 1.8 | 201.14 | 32,600 | 6.10E-05 | |
| | 5 | 1.9 | 201.14 | 32,800 | 6.14E-05 | |
| | 6 | 2.0 | 201.14 | 37,800 | 7.07E-05 | |
| 5%Ag/$TiO_2$ | 1 | 2.4 | 2041.78 | 36,200 | 6.77E-05 | 59.7016 |
| | 2 | 2.2 | 2041.78 | 31,200 | 5.84E-05 | |
| | 3 | 2.5 | 2041.78 | 38,300 | 7.17E-05 | |
| | 4 | 2.3 | 2041.78 | 38,000 | 7.11E-05 | |
| | 5 | 2.3 | 2041.78 | 38,700 | 7.24E-05 | |
| | 6 | 1.8 | 2041.78 | 28,500 | 5.33E-05 | |
| 5%Ag/GAC | 1 | 1.9 | 1500.92 | 9,680 | 1.80E-05 | 23.3053 |
| | 2 | 2.3 | 1500.92 | 20,200 | 3.77E-05 | |
| | 3 | 2.3 | 1500.92 | 20,400 | 3.81E-05 | |
| | 4 | 2.3 | 1500.92 | 20,400 | 3.81E-05 | |
| | 5 | 2.3 | 1500.92 | 20,900 | 3.90E-05 | |
| | 6 | 2.2 | 1500.92 | 20,300 | 3.79E-05 | |
| 15%Ag/$TiO_2$ | 1 | 1.8 | 3704.56 | 25,000 | 4.67E-05 | 94.7150 |
| | 2 | 1.9 | 3704.56 | 25,000 | 4.67E-05 | |
| | 3 | 1.8 | 3704.56 | 26,900 | 5.03E-05 | |
| | 4 | 1.9 | 3704.56 | 26,300 | 4.92E-05 | |
| | 5 | 2.1 | 3704.56 | 27,600 | 5.16E-05 | |
| | 6 | 2.2 | 3704.56 | 28,800 | 5.39E-05 | |
| 15%Ag/GAC | 1 | 2.1 | 2858.20 | 29,300 | 5.48E-05 | 66.4806 |
| | 2 | 2.2 | 2858.20 | 24,500 | 4.58E-05 | |
| | 3 | 2.1 | 2858.20 | 25,900 | 4.84E-05 | |
| | 4 | 2.1 | 2858.20 | 25,400 | 4.75E-05 | |
| | 5 | 2.1 | 2858.20 | 24,300 | 4.54E-05 | |
| | 6 | 1.9 | 2858.20 | 25,800 | 4.82E-05 | |
| Commercial | 1 | 2.0 | 2778.89 | 18,300 | 3.41E-05 | 47.7551 |
| | 2 | 1.8 | 2778.89 | 17,200 | 3.21E-05 | |
| | 3 | 2.4 | 2778.89 | 22,600 | 4.22E-05 | |
| | 4 | 2.1 | 2778.89 | 18,200 | 3.40E-05 | |
| | 5 | 2.0 | 2778.89 | 18,200 | 3.40E-05 | |
| | 6 | 1.9 | 2778.89 | 17,800 | 3.32E-05 | |

**40 Day**

| Adsorbent | Test | Mass of sample (mg) | Dilution (times) | Area | Amount of Hg (mg) | $q_t$ (mg Hg/g adsorbent) |
|---|---|---|---|---|---|---|
| $TiO_2$ | 1 | 1.9 | 1.00 | 15,500 | 2.89E-05 | 0.0146 |
| | 2 | 1.8 | 1.00 | 13,000 | 2.42E-05 | |
| | 3 | 1.9 | 1.00 | 16,300 | 3.04E-05 | |
| | 4 | 1.9 | 1.00 | 15,300 | 2.85E-05 | |
| | 5 | 1.9 | 1.00 | 15,200 | 2.83E-05 | |
| | 6 | 2.0 | 1.00 | 14,100 | 2.63E-05 | |
| GAC | 1 | 2.0 | 401.16 | 19,200 | 3.58E-05 | 7.0553 |
| | 2 | 1.8 | 401.16 | 16,400 | 3.06E-05 | |
| | 3 | 1.8 | 401.16 | 16,600 | 3.10E-05 | |
| | 4 | 2.3 | 401.16 | 21,600 | 4.03E-05 | |
| | 5 | 2.1 | 401.16 | 20,000 | 3.73E-05 | |
| | 6 | 2.0 | 401.16 | 19,400 | 3.62E-05 | |
| 5%Ag/$TiO_2$ | 1 | 2.6 | 2679.50 | 33,000 | 6.17E-05 | 63.7914 |
| | 2 | 2.4 | 2679.50 | 30,300 | 5.67E-05 | |
| | 3 | 2.3 | 2679.50 | 29,700 | 5.55E-05 | |
| | 4 | 2.1 | 2679.50 | 27,100 | 5.07E-05 | |
| | 5 | 2.6 | 2679.50 | 33,700 | 6.30E-05 | |
| | 6 | 2.5 | 2679.50 | 30,700 | 5.74E-05 | |
| 5%Ag/GAC | 1 | 2.5 | 1974.95 | 13,500 | 2.51E-05 | 23.2365 |
| | 2 | 2.5 | 1974.95 | 14,100 | 2.63E-05 | |
| | 3 | 2.2 | 1974.95 | 13,900 | 2.59E-05 | |
| | 4 | 2.0 | 1974.95 | 14,900 | 2.78E-05 | |
| | 5 | 2.2 | 1974.95 | 15,500 | 2.89E-05 | |
| | 6 | 2.1 | 1974.95 | 12,700 | 2.36E-05 | |
| 15%Ag/$TiO_2$ | 1 | 1.3 | 2501.73 | 31,100 | 5.82E-05 | 107.9368 |
| | 2 | 1.3 | 2501.73 | 31,700 | 5.93E-05 | |
| | 3 | 1.4 | 2501.73 | 31,100 | 5.82E-05 | |
| | 4 | 1.2 | 2501.73 | 28,300 | 5.29E-05 | |
| | 5 | 1.2 | 2501.73 | 26,300 | 4.92E-05 | |
| | 6 | 1.2 | 2501.73 | 26,900 | 5.03E-05 | |
| 15%Ag/GAC | 1 | 1.7 | 2500.90 | 28,800 | 5.39E-05 | 78.7549 |
| | 2 | 1.7 | 2500.90 | 27,300 | 5.10E-05 | |
| | 3 | 1.7 | 2500.90 | 29,800 | 5.57E-05 | |
| | 4 | 1.7 | 2500.90 | 29,200 | 5.46E-05 | |
| | 5 | 1.5 | 2500.90 | 25,500 | 4.77E-05 | |
| | 6 | 1.7 | 2500.90 | 27,800 | 5.20E-05 | |
| Commercial | 1 | 2.0 | 2501.97 | 22,000 | 4.11E-05 | 50.5138 |
| | 2 | 1.6 | 2501.97 | 20,800 | 3.88E-05 | |
| | 3 | 2.1 | 2501.97 | 20,500 | 3.83E-05 | |
| | 4 | 1.7 | 2501.97 | 18,000 | 3.36E-05 | |
| | 5 | 1.6 | 2501.97 | 17,700 | 3.30E-05 | |
| | 6 | 1.6 | 2501.97 | 15,200 | 2.83E-05 | |

**60 Day**

| Adsorbent | Test | Mass of sample (mg) | Dilution (times) | Area | Amount of Hg (mg) | $q_t$ (mg Hg/g adsorbent) |
|---|---|---|---|---|---|---|
| 15%Ag/$TiO_2$ | 1 | 1.7 | 2679.86 | 39,400 | 7.37E-05 | 113.4002 |
| | 2 | 1.5 | 2679.86 | 34,200 | 6.40E-05 | |
| | 3 | 1.5 | 2679.86 | 35,500 | 6.64E-05 | |
| | 4 | 1.4 | 2679.86 | 29,800 | 5.57E-05 | |
| | 5 | 1.4 | 2679.86 | 31,400 | 5.87E-05 | |
| | 6 | 1.4 | 2679.86 | 31,300 | 5.85E-05 | |
| 15%Ag/GAC | 1 | 1.5 | 2501.13 | 26,600 | 4.97E-05 | 82.2122 |
| | 2 | 2.1 | 2501.13 | 36,900 | 6.91E-05 | |
| | 3 | 2.1 | 2501.13 | 35,800 | 6.70E-05 | |
| | 4 | 2.2 | 2501.13 | 39,300 | 7.36E-05 | |
| | 5 | 1.9 | 2501.13 | 33,700 | 6.30E-05 | |
| | 6 | 1.7 | 2501.13 | 29,700 | 5.55E-05 | |
| Commercial | 1 | 2.2 | 2501.37 | 24,600 | 4.60E-05 | 49.8664 |
| | 2 | 1.9 | 2501.37 | 20,100 | 3.75E-05 | |
| | 3 | 2.0 | 2501.37 | 20,600 | 3.85E-05 | |
| | 4 | 2.0 | 2501.37 | 19,400 | 3.62E-05 | |
| | 5 | 2.1 | 2501.37 | 22,800 | 4.26E-05 | |
| | 6 | 2.1 | 2501.37 | 24,000 | 4.48E-05 | |

The performance of each adsorbent is calculated from the plot of $q_t$ versus $t$ which depicts the Hg removal rate.

**Table B.7** Adsorption capacity ($q_t$) for Hg adsorbed by adsorbents at 40°C

| Time (Days) | $q_t$ (mg Hg/g adsorbent) at 40°C | | | | | | |
|---|---|---|---|---|---|---|---|
| | $TiO_2$ | GAC | 5%Ag/$TiO_2$ | 5%Ag/GAC | 15%Ag/$TiO_2$ | 15%Ag/GAC | PTT Commercial |
| 0 | 0 | 0 | 0 | 0 | 0 | 0 | 0 |
| 1 | 0.0087 | 2.1565 | 13.0201 | 5.4151 | 15.0535 | 10.1034 | 7.6396 |
| 5 | 0.0033 | 2.9813 | 23.5737 | 12.3007 | 33.2942 | 24.8218 | 20.5726 |
| 20 | 0.0185 | 5.6477 | 44.7528 | 17.9955 | 71.0013 | 47.7645 | 42.4698 |
| 40 | 0.0078 | 6.5611 | 53.8962 | 22.5080 | 104.5149 | 76.4878 | 64.1329 |
| 60 | – | – | – | – | 107.1517 | 81.5752 | 69.0560 |

**Table B.8** Adsorption capacity ($q_t$) for Hg adsorbed by adsorbents at 60°C

| Time (Days) | $q_t$ (mg Hg/g adsorbent) at 60°C | | | | | | |
|---|---|---|---|---|---|---|---|
| | $TiO_2$ | GAC | 5%Ag/$TiO_2$ | 5%Ag/GAC | 15%Ag/$TiO_2$ | 15%Ag/GAC | PTT Commercial |
| 0 | 0.0000 | 0.0000 | 0.0000 | 0.0000 | 0.0000 | 0.0000 | 0.0000 |
| 1 | 0.0061 | 1.7074 | 24.7518 | 16.7880 | 36.1686 | 23.0885 | 19.5335 |
| 5 | 0.0061 | 2.8585 | 42.9322 | 21.5134 | 76.4988 | 40.9722 | 35.8130 |
| 20 | 0.0175 | 6.9853 | 59.7016 | 23.3053 | 94.7150 | 66.4806 | 47.7551 |
| 40 | 0.0146 | 7.0553 | 63.7914 | 23.2365 | 107.9368 | 78.7549 | 50.5138 |
| 60 | – | – | – | – | 113.4002 | 82.2122 | 49.8664 |

**Table B.9** Adsorption of Hg at differences temperatures.

**15%Ag/GAC**

| Temperature (°C) | Test | Mass of sample (mg) | Dilution (times) | Area | Amount of Hg (mg) | $q_e$ (mg Hg/g adsorbent) |
|---|---|---|---|---|---|---|
| 30 | 1 | 2.6 | 1501.12 | 23,700 | 4.43E-05 | 24.2887 |
| | 2 | 2.9 | 1501.12 | 24,700 | 4.62E-05 | |
| | 3 | 2.7 | 1501.12 | 24,100 | 4.50E-05 | |
| | 4 | 3.0 | 1501.12 | 25,900 | 4.84E-05 | |
| | 5 | 3.1 | 1416.30 | 25,500 | 4.77E-05 | |
| | 6 | 2.2 | 1416.30 | 20,400 | 3.81E-05 | |
| 40 | 1 | 2.6 | 1416.30 | 23,800 | 4.45E-05 | 48.1501 |
| | 2 | 3.2 | 1416.30 | 30,300 | 5.67E-05 | |
| | 3 | 2.2 | 4001.24 | 14,900 | 2.78E-05 | |
| | 4 | 2.0 | 4001.24 | 12,200 | 2.27E-05 | |
| | 5 | 2.6 | 4001.24 | 18,800 | 3.51E-05 | |
| | 6 | 1.9 | 4001.24 | 10,400 | 1.93E-05 | |
| 50 | 1 | 2.2 | 4001.24 | 14,100 | 2.63E-05 | 47.1646 |
| | 2 | 1.9 | 4001.24 | 12,900 | 2.40E-05 | |
| | 3 | 1.2 | 1563.35 | 27,400 | 5.12E-05 | |
| | 4 | 2.0 | 1563.35 | 31,500 | 5.89E-05 | |
| | 5 | 2.3 | 1563.35 | 32,500 | 6.08E-05 | |
| | 6 | 1.7 | 1563.35 | 28,700 | 5.37E-05 | |
| 60 | 1 | 1.8 | 1501.22 | 30,100 | 5.63E-05 | 66.4806 |
| | 2 | 1.9 | 1501.22 | 28,500 | 5.33E-05 | |
| | 3 | 1.8 | 1501.22 | 28,100 | 5.25E-05 | |
| | 4 | 2.0 | 1501.22 | 29,200 | 5.46E-05 | |
| | 5 | 2.1 | 2858.20 | 29,300 | 5.48E-05 | |
| | 6 | 2.2 | 2858.20 | 24,500 | 4.58E-05 | |

**15% Ag/$TiO_2$**

| Temperature (°C) | Test | Mass of sample (mg) | Dilution (times) | Area | Amount of Hg (mg) | $q_e$ (mg Hg/g adsorbent) |
|---|---|---|---|---|---|---|
| 30 | 1 | 2.2 | 1531.49 | 30,100 | 5.63E-05 | 40.3252 |
| | 2 | 2.3 | 1531.49 | 30,900 | 5.78E-05 | |
| | 3 | 2.6 | 1531.49 | 31,000 | 5.80E-05 | |
| | 4 | 1.9 | 1531.49 | 27,900 | 5.22E-05 | |
| | 5 | 2.4 | 1563.50 | 31,300 | 5.85E-05 | |
| | 6 | 2.3 | 1563.50 | 29,600 | 5.54E-05 | |
| 40 | 1 | 1.7 | 1563.50 | 27,400 | 5.12E-05 | 71.1946 |
| | 2 | 1.9 | 1563.50 | 29,800 | 5.57E-05 | |
| | 3 | 2.1 | 4001.36 | 20,600 | 3.85E-05 | |
| | 4 | 2.2 | 4001.36 | 20,400 | 3.81E-05 | |
| | 5 | 2.2 | 4001.36 | 21,500 | 4.02E-05 | |
| | 6 | 1.9 | 4001.36 | 16,600 | 3.10E-05 | |
| 50 | 1 | 2.4 | 4001.36 | 23,400 | 4.37E-05 | 66.8074 |
| | 2 | 2.4 | 4001.36 | 23,600 | 4.41E-05 | |
| | 3 | 1.5 | 1531.69 | 32,900 | 6.15E-05 | |
| | 4 | 1.2 | 1531.69 | 28,700 | 5.37E-05 | |
| | 5 | 1.2 | 1531.69 | 29,300 | 5.48E-05 | |
| | 6 | 0.9 | 1531.69 | 24,600 | 4.60E-05 | |
| 60 | 1 | 1.5 | 1501.26 | 32,300 | 6.04E-05 | 94.7150 |
| | 2 | 1.1 | 1501.26 | 25,900 | 4.84E-05 | |
| | 3 | 1.3 | 1501.26 | 30,500 | 5.70E-05 | |
| | 4 | 1.5 | 1501.26 | 33,400 | 6.25E-05 | |
| | 5 | 1.8 | 3704.56 | 25,000 | 4.67E-05 | |
| | 6 | 1.9 | 3704.56 | 25,000 | 4.67E-05 | |

**Commercial**

| Temperature (°C) | Test | Mass of sample (mg) | Dilution (times) | Area | Amount of Hg (mg) | $q_e$ (mg Hg/g adsorbent) |
|---|---|---|---|---|---|---|
| 30 | 1 | 2.9 | 1443.42 | 30,700 | 5.74E-05 | 29.7926 |
| | 2 | 2.8 | 1443.42 | 30,600 | 5.72E-05 | |
| | 3 | 2.8 | 1443.42 | 30,000 | 5.61E-05 | |
| | 4 | 2.6 | 1443.42 | 29,500 | 5.52E-05 | |
| | 5 | 3.2 | 1416.13 | 34,000 | 6.36E-05 | |
| | 6 | 2.6 | 1416.13 | 30,300 | 5.67E-05 | |
| 40 | 1 | 2.7 | 1416.13 | 33,000 | 6.17E-05 | 44.9963 |
| | 2 | 3.0 | 1416.13 | 33,200 | 6.21E-05 | |
| | 3 | 1.9 | 3000.88 | 15,200 | 2.83E-05 | |
| | 4 | 2.0 | 3000.88 | 14,500 | 2.70E-05 | |
| | 5 | 1.7 | 3000.88 | 12,700 | 2.36E-05 | |
| | 6 | 2.1 | 3000.88 | 17,300 | 3.23E-05 | |
| 50 | 1 | 2.1 | 3000.88 | 17,900 | 3.34E-05 | 39.8440 |
| | 2 | 2.6 | 3000.88 | 22,800 | 4.26E-05 | |
| | 3 | 2.1 | 1501.00 | 31,600 | 5.91E-05 | |
| | 4 | 2.1 | 1501.00 | 33,600 | 6.29E-05 | |
| | 5 | 3.0 | 1501.00 | 36,200 | 6.77E-05 | |
| | 6 | 2.5 | 1501.00 | 33,800 | 6.32E-05 | |
| 60 | 1 | 2.8 | 1596.72 | 34,900 | 6.53E-05 | 47.7551 |
| | 2 | 3.2 | 1596.72 | 38,800 | 7.26E-05 | |
| | 3 | 2.5 | 1596.72 | 32,700 | 6.12E-05 | |
| | 4 | 2.4 | 1596.72 | 32,500 | 6.08E-05 | |
| | 5 | 2.0 | 2778.89 | 18,300 | 3.41E-05 | |
| | 6 | 1.8 | 2778.89 | 17,200 | 3.21E-05 | |

## B.5 Kinetic adsorption

The kinetic adsorption data showing the rate adsorption of Hg in 15%Ag/GAC 15%Ag/$TiO_2$ and Commercial adsorbents at 30, 40, 50 and 60°C was obtained, as shown in Table B.10 to B.13.

**Table B.10** Kinetic adsorption of Hg at 30°C

**15%Ag/GAC**

| Time (hour) | Test | Mass of sample (mg) | Dilution (times) | Area | Amount of Hg (mg) | $q_t$ (mg Hg/g adsorbent) |
|---|---|---|---|---|---|---|
| 2.5 | 1 | 2.0 | 511.14 | 3,900 | 7.12E-06 | 1.6138 |
| | 2 | 2.1 | 511.14 | 3,840 | 7.01E-06 | |
| | 3 | 2.1 | 511.14 | 4,660 | 8.54E-06 | |
| | 4 | 2.2 | 491.35 | 3,210 | 5.82E-06 | |
| | 5 | 2.0 | 491.35 | 2,620 | 4.72E-06 | |
| | 6 | 2.2 | 491.35 | 3,970 | 7.25E-06 | |
| 5 | 1 | 4.9 | 533.00 | 11,640 | 2.16E-05 | 2.3288 |
| | 2 | 4.9 | 533.00 | 11,520 | 2.14E-05 | |
| | 3 | 4.9 | 533.00 | 11,840 | 2.20E-05 | |
| | 4 | 5.1 | 501.08 | 12,100 | 2.25E-05 | |
| | 5 | 5.3 | 501.08 | 13,300 | 2.48E-05 | |
| | 6 | 5.3 | 501.08 | 13,300 | 2.48E-05 | |
| 10 | 1 | 5.0 | 501.04 | 37,200 | 6.96E-05 | 6.6347 |
| | 2 | 4.6 | 501.04 | 33,000 | 6.17E-05 | |
| | 3 | 4.7 | 501.04 | 35,400 | 6.62E-05 | |
| | 4 | 4.6 | 491.43 | 30,900 | 5.78E-05 | |
| | 5 | 4.9 | 491.43 | 34,100 | 6.38E-05 | |
| | 6 | 4.9 | 491.43 | 34,500 | 6.45E-05 | |
| 15 | 1 | 2.1 | 491.14 | 22,300 | 4.17E-05 | 9.6348 |
| | 2 | 2.5 | 491.14 | 25,500 | 4.77E-05 | |
| | 3 | 2.5 | 491.14 | 26,600 | 4.97E-05 | |
| | 4 | 3.0 | 491.12 | 30,000 | 5.61E-05 | |
| | 5 | 2.7 | 491.12 | 29,000 | 5.42E-05 | |
| | 6 | 2.6 | 491.12 | 28,000 | 5.23E-05 | |
| 20 | 1 | 1.9 | 482.02 | 25,300 | 4.73E-05 | 13.3422 |
| | 2 | 1.6 | 482.02 | 24,500 | 4.58E-05 | |
| | 3 | 2.2 | 482.02 | 30,800 | 5.76E-05 | |
| | 4 | 2.0 | 511.37 | 29,700 | 5.55E-05 | |
| | 5 | 2.4 | 511.37 | 35,600 | 6.66E-05 | |
| | 6 | 2.1 | 511.37 | 29,100 | 5.44E-05 | |

**15% Ag/$TiO_2$**

| Time (hour) | Tests | Mass of sample (mg) | Dilution (times) | Area | Amount of Hg (mg) | $q_t$ (mg Hg/g adsorbent) |
|---|---|---|---|---|---|---|
| 6 | 1 | 2.3 | 1042.58 | 2,510 | 4.51E-06 | 1.9902 |
| | 2 | 2.3 | 1042.58 | 2,380 | 4.27E-06 | |
| | 3 | 2.2 | 1042.58 | 2,360 | 4.23E-06 | |
| | 4 | 2.3 | 962.60 | 2,720 | 4.90E-06 | |
| | 5 | 2.0 | 962.60 | 2,130 | 3.80E-06 | |
| | 6 | 2.0 | 962.60 | 2,410 | 4.32E-06 | |
| 12 | 1 | 2.2 | 981.57 | 6,220 | 1.15E-05 | 5.3949 |
| | 2 | 2.4 | 981.57 | 6,480 | 1.20E-05 | |
| | 3 | 2.0 | 981.57 | 6,140 | 1.13E-05 | |
| | 4 | 2.9 | 1042.88 | 7,060 | 1.30E-05 | |
| | 5 | 2.2 | 1042.88 | 7,890 | 1.46E-05 | |
| | 6 | 2.5 | 1042.88 | 6,730 | 1.24E-05 | |
| 72 | 1 | 2.5 | 2000.72 | 12,500 | 2.33E-05 | 16.6160 |
| | 2 | 2.2 | 2000.72 | 10,900 | 2.03E-05 | |
| | 3 | 2.7 | 2000.72 | 13,100 | 2.44E-05 | |
| | 4 | 2.7 | 1924.00 | 10,700 | 1.99E-05 | |
| | 5 | 2.5 | 1924.00 | 10,200 | 1.89E-05 | |
| | 6 | 2.3 | 1924.00 | 10,200 | 1.89E-05 | |
| 120 | 1 | 2.4 | 2001.44 | 20,800 | 3.88E-05 | 34.3629 |
| | 2 | 2.3 | 2001.44 | 20,200 | 3.77E-05 | |
| | 3 | 3.0 | 2001.44 | 27,000 | 5.05E-05 | |
| | 4 | 2.2 | 1924.42 | 20,700 | 3.86E-05 | |
| | 5 | 2.5 | 1924.42 | 23,100 | 4.32E-05 | |
| | 6 | 2.6 | 1924.42 | 29,100 | 5.44E-05 | |
| 240 | 1 | 1.6 | 2001.08 | 22,000 | 4.11E-05 | 58.3208 |
| | 2 | 1.9 | 2001.08 | 25,100 | 4.69E-05 | |
| | 3 | 1.7 | 2001.08 | 22,000 | 4.11E-05 | |
| | 4 | 1.8 | 2084.25 | 31,500 | 5.89E-05 | |
| | 5 | 2.1 | 2084.25 | 36,200 | 6.77E-05 | |
| | 6 | 2.0 | 2084.25 | 33,500 | 6.27E-05 | |

**Commercial**

| Time (hour) | Test | Mass of sample (mg) | Dilution (times) | Area | Amount of Hg (mg) | $q_t$ (mg Hg/g adsorbent) |
|---|---|---|---|---|---|---|
| 2.5 | 1 | 2.0 | 511.14 | 2,100 | 3.74E-06 | 0.8052 |
| | 2 | 2.1 | 511.14 | 2,040 | 3.63E-06 | |
| | 3 | 2.1 | 511.14 | 2,260 | 4.04E-06 | |
| | 4 | 2.2 | 491.35 | 1,910 | 3.38E-06 | |
| | 5 | 2.0 | 491.35 | 1,350 | 2.33E-06 | |
| | 6 | 2.2 | 491.35 | 1,730 | 3.05E-06 | |
| 5 | 1 | 4.9 | 533.00 | 6,320 | 1.17E-05 | 1.4481 |
| | 2 | 4.9 | 533.00 | 6,370 | 1.18E-05 | |
| | 3 | 4.9 | 533.00 | 7,810 | 1.45E-05 | |
| | 4 | 5.1 | 501.08 | 8,800 | 1.63E-05 | |
| | 5 | 5.3 | 501.08 | 8,500 | 1.58E-05 | |
| | 6 | 5.3 | 501.08 | 8,430 | 1.56E-05 | |
| 10 | 1 | 5.0 | 501.04 | 20,200 | 3.77E-05 | 3.8884 |
| | 2 | 4.6 | 501.04 | 22,000 | 4.11E-05 | |
| | 3 | 4.7 | 501.04 | 20,200 | 3.77E-05 | |
| | 4 | 4.6 | 491.43 | 19,400 | 3.62E-05 | |
| | 5 | 4.9 | 491.43 | 19,900 | 3.71E-05 | |
| | 6 | 4.9 | 491.43 | 18,500 | 3.45E-05 | |
| 15 | 1 | 2.1 | 491.14 | 19,400 | 3.62E-05 | 6.7351 |
| | 2 | 2.5 | 491.14 | 16,400 | 3.06E-05 | |
| | 3 | 2.5 | 491.14 | 17,800 | 3.32E-05 | |
| | 4 | 3.0 | 491.12 | 20,100 | 3.75E-05 | |
| | 5 | 2.7 | 491.12 | 17,900 | 3.34E-05 | |
| | 6 | 2.6 | 491.12 | 20,400 | 3.81E-05 | |
| 20 | 1 | 1.9 | 482.02 | 20,000 | 3.73E-05 | 8.6683 |
| | 2 | 1.6 | 482.02 | 18,300 | 3.41E-05 | |
| | 3 | 2.2 | 482.02 | 17,900 | 3.34E-05 | |
| | 4 | 2.0 | 511.37 | 19,200 | 3.58E-05 | |
| | 5 | 2.4 | 511.37 | 15,900 | 2.96E-05 | |
| | 6 | 2.1 | 511.37 | 20,800 | 3.88E-05 | |

**Table B.11** Kinetic adsorption of Hg at 40°C

**15%Ag/GAC**

| Time (hour) | Test | Mass of sample (mg) | Dilution (times) | Area | Amount of Hg (mg) | $q_t$ (mg Hg/g adsorbent) |
|---|---|---|---|---|---|---|
| 2.5 | 1 | 2.0 | 511.14 | 3,900 | 7.12E-06 | 1.6138 |
| | 2 | 2.1 | 511.14 | 3,840 | 7.01E-06 | |
| | 3 | 2.1 | 511.14 | 4,660 | 8.54E-06 | |
| | 4 | 2.2 | 491.35 | 3,210 | 5.82E-06 | |
| | 5 | 2.0 | 491.35 | 2,620 | 4.72E-06 | |
| | 6 | 2.2 | 491.35 | 3,970 | 7.25E-06 | |
| 5 | 1 | 4.9 | 533.00 | 11,640 | 2.16E-05 | 2.3288 |
| | 2 | 4.9 | 533.00 | 11,520 | 2.14E-05 | |
| | 3 | 4.9 | 533.00 | 11,840 | 2.20E-05 | |
| | 4 | 5.1 | 501.08 | 12,100 | 2.25E-05 | |
| | 5 | 5.3 | 501.08 | 13,300 | 2.48E-05 | |
| | 6 | 5.3 | 501.08 | 13,300 | 2.48E-05 | |
| 10 | 1 | 5.0 | 501.04 | 37,200 | 6.96E-05 | 6.6347 |
| | 2 | 4.6 | 501.04 | 33,000 | 6.17E-05 | |
| | 3 | 4.7 | 501.04 | 35,400 | 6.62E-05 | |
| | 4 | 4.6 | 491.43 | 30,900 | 5.78E-05 | |
| | 5 | 4.9 | 491.43 | 34,100 | 6.38E-05 | |
| | 6 | 4.9 | 491.43 | 34,500 | 6.45E-05 | |
| 15 | 1 | 2.1 | 491.14 | 22,300 | 4.17E-05 | 9.6348 |
| | 2 | 2.5 | 491.14 | 25,500 | 4.77E-05 | |
| | 3 | 2.5 | 491.14 | 26,600 | 4.97E-05 | |
| | 4 | 3.0 | 491.12 | 30,000 | 5.61E-05 | |
| | 5 | 2.7 | 491.12 | 29,000 | 5.42E-05 | |
| | 6 | 2.6 | 491.12 | 28,000 | 5.23E-05 | |
| 20 | 1 | 1.9 | 482.02 | 25,300 | 4.73E-05 | 13.3422 |
| | 2 | 1.6 | 482.02 | 24,500 | 4.58E-05 | |
| | 3 | 2.2 | 482.02 | 30,800 | 5.76E-05 | |
| | 4 | 2.0 | 511.37 | 29,700 | 5.55E-05 | |
| | 5 | 2.4 | 511.37 | 35,600 | 6.66E-05 | |
| | 6 | 2.1 | 511.37 | 29,100 | 5.44E-05 | |

**15% Ag/$TiO_2$**

| Time (hour) | Tests | Mass of sample (mg) | Dilution (times) | Area | Amount of Hg (mg) | $q_t$ (mg Hg/g adsorbent) |
|---|---|---|---|---|---|---|
| 6 | 1 | 2.3 | 1042.58 | 2,510 | 4.51E-06 | 1.9902 |
| | 2 | 2.3 | 1042.58 | 2,380 | 4.27E-06 | |
| | 3 | 2.2 | 1042.58 | 2,360 | 4.23E-06 | |
| | 4 | 2.3 | 962.60 | 2,720 | 4.90E-06 | |
| | 5 | 2.0 | 962.60 | 2,130 | 3.80E-06 | |
| | 6 | 2.0 | 962.60 | 2,410 | 4.32E-06 | |
| 12 | 1 | 2.2 | 981.57 | 6,220 | 1.15E-05 | 5.3949 |
| | 2 | 2.4 | 981.57 | 6,480 | 1.20E-05 | |
| | 3 | 2.0 | 981.57 | 6,140 | 1.13E-05 | |
| | 4 | 2.9 | 1042.88 | 7,060 | 1.30E-05 | |
| | 5 | 2.2 | 1042.88 | 7,890 | 1.46E-05 | |
| | 6 | 2.5 | 1042.88 | 6,730 | 1.24E-05 | |
| 72 | 1 | 2.5 | 2000.72 | 12,500 | 2.33E-05 | 16.6160 |
| | 2 | 2.2 | 2000.72 | 10,900 | 2.03E-05 | |
| | 3 | 2.7 | 2000.72 | 13,100 | 2.44E-05 | |
| | 4 | 2.7 | 1924.00 | 10,700 | 1.99E-05 | |
| | 5 | 2.5 | 1924.00 | 10,200 | 1.89E-05 | |
| | 6 | 2.3 | 1924.00 | 10,200 | 1.89E-05 | |
| 120 | 1 | 2.4 | 2001.44 | 20,800 | 3.88E-05 | 34.3629 |
| | 2 | 2.3 | 2001.44 | 20,200 | 3.77E-05 | |
| | 3 | 3.0 | 2001.44 | 27,000 | 5.05E-05 | |
| | 4 | 2.2 | 1924.42 | 20,700 | 3.86E-05 | |
| | 5 | 2.5 | 1924.42 | 23,100 | 4.32E-05 | |
| | 6 | 2.6 | 1924.42 | 29,100 | 5.44E-05 | |
| 240 | 1 | 1.6 | 2001.08 | 22,000 | 4.11E-05 | 58.3208 |
| | 2 | 1.9 | 2001.08 | 25,100 | 4.69E-05 | |
| | 3 | 1.7 | 2001.08 | 22,000 | 4.11E-05 | |
| | 4 | 1.8 | 2084.25 | 31,500 | 5.89E-05 | |
| | 5 | 2.1 | 2084.25 | 36,200 | 6.77E-05 | |
| | 6 | 2.0 | 2084.25 | 33,500 | 6.27E-05 | |

**Commercial**

| Time (hour) | Test | Mass of sample (mg) | Dilution (times) | Area | Amount of Hg (mg) | $q_t$ (mg Hg/g adsorbent) |
|---|---|---|---|---|---|---|
| 2.5 | 1 | 2.0 | 511.14 | 3,300 | 5.99E-06 | 1.4182 |
| | 2 | 2.1 | 511.14 | 3,540 | 6.44E-06 | |
| | 3 | 2.1 | 511.14 | 4,260 | 7.79E-06 | |
| | 4 | 2.2 | 491.35 | 2,910 | 5.26E-06 | |
| | 5 | 2.0 | 491.35 | 2,120 | 3.78E-06 | |
| | 6 | 2.2 | 491.35 | 3,470 | 6.31E-06 | |
| 5 | 1 | 4.9 | 533.00 | 9,640 | 1.79E-05 | 2.0348 |
| | 2 | 4.9 | 533.00 | 9,520 | 1.77E-05 | |
| | 3 | 4.9 | 533.00 | 9,840 | 1.83E-05 | |
| | 4 | 5.1 | 501.08 | 11,100 | 2.06E-05 | |
| | 5 | 5.3 | 501.08 | 12,300 | 2.29E-05 | |
| | 6 | 5.3 | 501.08 | 12,300 | 2.29E-05 | |
| 10 | 1 | 5.0 | 501.04 | 32,200 | 6.02E-05 | 5.8298 |
| | 2 | 4.6 | 501.04 | 32,000 | 5.99E-05 | |
| | 3 | 4.7 | 501.04 | 30,400 | 5.69E-05 | |
| | 4 | 4.6 | 491.43 | 26,900 | 5.03E-05 | |
| | 5 | 4.9 | 491.43 | 29,100 | 5.44E-05 | |
| | 6 | 4.9 | 491.43 | 29,500 | 5.52E-05 | |
| 15 | 1 | 2.1 | 491.14 | 21,300 | 3.98E-05 | 8.2258 |
| | 2 | 2.5 | 491.14 | 20,500 | 3.83E-05 | |
| | 3 | 2.5 | 491.14 | 21,600 | 4.03E-05 | |
| | 4 | 3.0 | 491.12 | 26,000 | 4.86E-05 | |
| | 5 | 2.7 | 491.12 | 22,000 | 4.11E-05 | |
| | 6 | 2.6 | 491.12 | 26,000 | 4.86E-05 | |
| 20 | 1 | 1.9 | 482.02 | 22,300 | 4.17E-05 | 11.1020 |
| | 2 | 1.6 | 482.02 | 21,500 | 4.02E-05 | |
| | 3 | 2.2 | 482.02 | 20,800 | 3.88E-05 | |
| | 4 | 2.0 | 511.37 | 25,700 | 4.80E-05 | |
| | 5 | 2.4 | 511.37 | 30,600 | 5.72E-05 | |
| | 6 | 2.1 | 511.37 | 24,100 | 4.50E-05 | |

**Table B.12** Kinetic adsorption of Hg at 50°C

**15%Ag/GAC**

| Time (hour) | Test | Mass of sample (mg) | Dilution (times) | Area | Amount of Hg (mg) | $q_t$ (mg Hg/g adsorbent) |
|---|---|---|---|---|---|---|
| 2.5 | 1 | 2.0 | 511.14 | 4,200 | 7.68E-06 | 1.8916 |
| | 2 | 2.1 | 511.14 | 4,010 | 7.32E-06 | |
| | 3 | 2.1 | 511.14 | 5,490 | 1.01E-05 | |
| | 4 | 2.2 | 491.35 | 4,280 | 7.83E-06 | |
| | 5 | 2.0 | 491.35 | 3,550 | 6.46E-06 | |
| | 6 | 2.2 | 491.35 | 4,420 | 8.09E-06 | |
| 5 | 1 | 4.9 | 533.00 | 13,640 | 2.54E-05 | 2.8717 |
| | 2 | 4.9 | 533.00 | 15,420 | 2.87E-05 | |
| | 3 | 4.9 | 533.00 | 14,840 | 2.77E-05 | |
| | 4 | 5.1 | 501.08 | 15,100 | 2.81E-05 | |
| | 5 | 5.3 | 501.08 | 16,300 | 3.04E-05 | |
| | 6 | 5.3 | 501.08 | 15,300 | 2.85E-05 | |
| 10 | 1 | 5.0 | 501.04 | 39,200 | 7.34E-05 | 7.1865 |
| | 2 | 4.6 | 501.04 | 38,100 | 7.13E-05 | |
| | 3 | 4.7 | 501.04 | 37,900 | 7.09E-05 | |
| | 4 | 4.6 | 491.43 | 33,900 | 6.34E-05 | |
| | 5 | 4.9 | 491.43 | 35,600 | 6.66E-05 | |
| | 6 | 4.9 | 491.43 | 37,200 | 6.96E-05 | |
| 15 | 1 | 2.1 | 491.14 | 28,300 | 5.29E-05 | 11.1162 |
| | 2 | 2.5 | 491.14 | 29,300 | 5.48E-05 | |
| | 3 | 2.5 | 491.14 | 29,900 | 5.59E-05 | |
| | 4 | 3.0 | 491.12 | 34,000 | 6.36E-05 | |
| | 5 | 2.7 | 491.12 | 31,900 | 5.97E-05 | |
| | 6 | 2.6 | 491.12 | 32,000 | 5.99E-05 | |
| 20 | 1 | 1.9 | 482.02 | 29,800 | 5.57E-05 | 14.9611 |
| | 2 | 1.6 | 482.02 | 27,900 | 5.22E-05 | |
| | 3 | 2.2 | 482.02 | 33,100 | 6.19E-05 | |
| | 4 | 2.0 | 511.37 | 35,000 | 6.55E-05 | |
| | 5 | 2.4 | 511.37 | 37,000 | 6.92E-05 | |
| | 6 | 2.1 | 511.37 | 32,600 | 6.10E-05 | |

**15% Ag/$TiO_2$**

| Time (hour) | Tests | Mass of sample (mg) | Dilution (times) | Area | Amount of Hg (mg) | $q_t$ (mg Hg/g adsorbent) |
|---|---|---|---|---|---|---|
| 6 | 1 | 2.3 | 1042.58 | 3,610 | 6.57E-06 | 2.9553 |
| | 2 | 2.3 | 1042.58 | 3,480 | 6.33E-06 | |
| | 3 | 2.2 | 1042.58 | 3,560 | 6.48E-06 | |
| | 4 | 2.3 | 962.60 | 3,820 | 6.97E-06 | |
| | 5 | 2.0 | 962.60 | 3,230 | 5.86E-06 | |
| | 6 | 2.0 | 962.60 | 3,510 | 6.39E-06 | |
| 12 | 1 | 2.2 | 981.57 | 7,320 | 1.35E-05 | 6.1550 |
| | 2 | 2.4 | 981.57 | 7,580 | 1.40E-05 | |
| | 3 | 2.0 | 981.57 | 7,240 | 1.34E-05 | |
| | 4 | 2.9 | 1042.88 | 8,160 | 1.51E-05 | |
| | 5 | 2.2 | 1042.88 | 8,090 | 1.50E-05 | |
| | 6 | 2.5 | 1042.88 | 7,830 | 1.45E-05 | |
| 72 | 1 | 2.5 | 2000.72 | 14,400 | 2.68E-05 | 21.5583 |
| | 2 | 2.2 | 2000.72 | 13,100 | 2.44E-05 | |
| | 3 | 2.7 | 2000.72 | 15,300 | 2.85E-05 | |
| | 4 | 2.7 | 1924.00 | 13,200 | 2.46E-05 | |
| | 5 | 2.5 | 1924.00 | 15,200 | 2.83E-05 | |
| | 6 | 2.3 | 1924.00 | 16,200 | 3.02E-05 | |
| 120 | 1 | 2.4 | 2001.44 | 22,900 | 4.28E-05 | 35.9874 |
| | 2 | 2.3 | 2001.44 | 22,800 | 4.26E-05 | |
| | 3 | 3.0 | 2001.44 | 28,200 | 5.27E-05 | |
| | 4 | 2.2 | 1924.42 | 22,900 | 4.28E-05 | |
| | 5 | 2.5 | 1924.42 | 25,900 | 4.84E-05 | |
| | 6 | 2.6 | 1924.42 | 24,100 | 4.50E-05 | |
| 240 | 1 | 1.6 | 2001.08 | 24,200 | 4.52E-05 | 61.7038 |
| | 2 | 1.9 | 2001.08 | 26,300 | 4.92E-05 | |
| | 3 | 1.7 | 2001.08 | 24,300 | 4.54E-05 | |
| | 4 | 1.8 | 2084.25 | 32,600 | 6.10E-05 | |
| | 5 | 2.1 | 2084.25 | 38,200 | 7.15E-05 | |
| | 6 | 2.0 | 2084.25 | 34,300 | 6.42E-05 | |

**Commercial**

| Time (hour) | Test | Mass of sample (mg) | Dilution (times) | Area | Amount of Hg (mg) | $q_t$ (mg Hg/g adsorbent) |
|---|---|---|---|---|---|---|
| 2.5 | 1 | 2.0 | 511.14 | 3,000 | 5.43E-06 | 1.4465 |
| | 2 | 2.1 | 511.14 | 3,140 | 5.69E-06 | |
| | 3 | 2.1 | 511.14 | 3,860 | 7.04E-06 | |
| | 4 | 2.2 | 491.35 | 4,110 | 7.51E-06 | |
| | 5 | 2.0 | 491.35 | 2,320 | 4.15E-06 | |
| | 6 | 2.2 | 491.35 | 3,670 | 6.69E-06 | |
| 5 | 1 | 4.9 | 533.00 | 10,040 | 1.86E-05 | 2.1646 |
| | 2 | 4.9 | 533.00 | 10,520 | 1.95E-05 | |
| | 3 | 4.9 | 533.00 | 10,840 | 2.01E-05 | |
| | 4 | 5.1 | 501.08 | 11,800 | 2.19E-05 | |
| | 5 | 5.3 | 501.08 | 12,600 | 2.34E-05 | |
| | 6 | 5.3 | 501.08 | 12,900 | 2.40E-05 | |
| 10 | 1 | 5.0 | 501.04 | 32,900 | 6.15E-05 | 6.0185 |
| | 2 | 4.6 | 501.04 | 30,500 | 5.70E-05 | |
| | 3 | 4.7 | 501.04 | 34,100 | 6.38E-05 | |
| | 4 | 4.6 | 491.43 | 27,100 | 5.07E-05 | |
| | 5 | 4.9 | 491.43 | 30,000 | 5.61E-05 | |
| | 6 | 4.9 | 491.43 | 31,400 | 5.87E-05 | |
| 15 | 1 | 2.1 | 491.14 | 24,100 | 4.50E-05 | 9.1758 |
| | 2 | 2.5 | 491.14 | 23,500 | 4.39E-05 | |
| | 3 | 2.5 | 491.14 | 23,600 | 4.41E-05 | |
| | 4 | 3.0 | 491.12 | 29,000 | 5.42E-05 | |
| | 5 | 2.7 | 491.12 | 24,400 | 4.56E-05 | |
| | 6 | 2.6 | 491.12 | 28,500 | 5.33E-05 | |
| 20 | 1 | 1.9 | 482.02 | 24,300 | 4.54E-05 | 11.9738 |
| | 2 | 1.6 | 482.02 | 24,500 | 4.58E-05 | |
| | 3 | 2.2 | 482.02 | 22,800 | 4.26E-05 | |
| | 4 | 2.0 | 511.37 | 29,700 | 5.55E-05 | |
| | 5 | 2.4 | 511.37 | 24,600 | 4.60E-05 | |
| | 6 | 2.1 | 511.37 | 29,000 | 5.42E-05 | |

**Table B.13** Kinetic adsorption of Hg at 60°C

**15%Ag/GAC**

| Time (hour) | Test | Mass of sample (mg) | Dilution (times) | Area | Amount of Hg (mg) | $q_t$ (mg Hg/g adsorbent) |
|---|---|---|---|---|---|---|
| 2.5 | 1 | 2.0 | 511.14 | 6,700 | 1.24E-05 | 2.8522 |
| | 2 | 2.1 | 511.14 | 6,540 | 1.21E-05 | |
| | 3 | 2.1 | 511.14 | 6,660 | 1.23E-05 | |
| | 4 | 2.2 | 491.35 | 6,210 | 1.15E-05 | |
| | 5 | 2.0 | 491.35 | 6,620 | 1.22E-05 | |
| | 6 | 2.2 | 491.35 | 5,970 | 1.10E-05 | |
| 5 | 1 | 4.9 | 533.00 | 17,600 | 3.28E-05 | 3.3282 |
| | 2 | 4.9 | 533.00 | 17,500 | 3.26E-05 | |
| | 3 | 4.9 | 533.00 | 17,800 | 3.32E-05 | |
| | 4 | 5.1 | 501.08 | 17,100 | 3.19E-05 | |
| | 5 | 5.3 | 501.08 | 17,300 | 3.23E-05 | |
| | 6 | 5.3 | 501.08 | 17,300 | 3.23E-05 | |
| 10 | 1 | 5.0 | 501.04 | 30,200 | 5.65E-05 | 11.0254 |
| | 2 | 4.6 | 501.04 | 30,000 | 5.61E-05 | |
| | 3 | 4.7 | 501.04 | 31,400 | 5.87E-05 | |
| | 4 | 4.6 | 491.43 | 31,900 | 5.97E-05 | |
| | 5 | 4.9 | 491.43 | 29,900 | 5.59E-05 | |
| | 6 | 4.9 | 491.43 | 28,100 | 5.25E-05 | |
| 15 | 1 | 2.1 | 491.14 | 27,300 | 5.10E-05 | 10.9767 |
| | 2 | 2.5 | 491.14 | 29,500 | 5.52E-05 | |
| | 3 | 2.5 | 491.14 | 30,600 | 5.72E-05 | |
| | 4 | 3.0 | 491.12 | 32,000 | 5.99E-05 | |
| | 5 | 2.7 | 491.12 | 32,600 | 6.10E-05 | |
| | 6 | 2.6 | 491.12 | 31,000 | 5.80E-05 | |
| 20 | 1 | 1.9 | 482.02 | 31,300 | 5.85E-05 | 14.6750 |
| | 2 | 1.6 | 482.02 | 32,500 | 6.08E-05 | |
| | 3 | 2.2 | 482.02 | 30,800 | 5.76E-05 | |
| | 4 | 2.0 | 511.37 | 31,700 | 5.93E-05 | |
| | 5 | 2.4 | 511.37 | 33,600 | 6.29E-05 | |
| | 6 | 2.1 | 511.37 | 30,100 | 5.63E-05 | |

**15% Ag/$TiO_2$**

| Time (hour) | Tests | Mass of sample (mg) | Dilution (times) | Area | Amount of Hg (mg) | $q_t$ (mg Hg/g adsorbent) |
|---|---|---|---|---|---|---|
| 6 | 1 | 2.3 | 1042.58 | 4,110 | 7.51E-06 | 3.8118 |
| | 2 | 2.3 | 1042.58 | 4,380 | 8.02E-06 | |
| | 3 | 2.2 | 1042.58 | 4,360 | 7.98E-06 | |
| | 4 | 2.3 | 962.60 | 4,720 | 8.66E-06 | |
| | 5 | 2.0 | 962.60 | 4,130 | 7.55E-06 | |
| | 6 | 2.0 | 962.60 | 5,410 | 9.95E-06 | |
| 12 | 1 | 2.2 | 981.57 | 8,220 | 1.52E-05 | 6.7587 |
| | 2 | 2.4 | 981.57 | 8,480 | 1.57E-05 | |
| | 3 | 2.0 | 981.57 | 8,140 | 1.51E-05 | |
| | 4 | 2.9 | 1042.88 | 8,060 | 1.49E-05 | |
| | 5 | 2.2 | 1042.88 | 8,890 | 1.65E-05 | |
| | 6 | 2.5 | 1042.88 | 8,730 | 1.62E-05 | |
| 72 | 1 | 2.5 | 2000.72 | 16,500 | 3.08E-05 | 21.8971 |
| | 2 | 2.2 | 2000.72 | 14,900 | 2.78E-05 | |
| | 3 | 2.7 | 2000.72 | 15,100 | 2.81E-05 | |
| | 4 | 2.7 | 1924.00 | 13,700 | 2.55E-05 | |
| | 5 | 2.5 | 1924.00 | 14,200 | 2.64E-05 | |
| | 6 | 2.3 | 1924.00 | 14,200 | 2.64E-05 | |
| 120 | 1 | 2.4 | 2001.44 | 23,800 | 4.45E-05 | 35.7923 |
| | 2 | 2.3 | 2001.44 | 22,200 | 4.15E-05 | |
| | 3 | 3.0 | 2001.44 | 22,000 | 4.11E-05 | |
| | 4 | 2.2 | 1924.42 | 25,700 | 4.80E-05 | |
| | 5 | 2.5 | 1924.42 | 24,100 | 4.50E-05 | |
| | 6 | 2.6 | 1924.42 | 27,100 | 5.07E-05 | |
| 240 | 1 | 1.6 | 2001.08 | 27,000 | 5.05E-05 | 63.8426 |
| | 2 | 1.9 | 2001.08 | 28,100 | 5.25E-05 | |
| | 3 | 1.7 | 2001.08 | 29,000 | 5.42E-05 | |
| | 4 | 1.8 | 2084.25 | 31,500 | 5.89E-05 | |
| | 5 | 2.1 | 2084.25 | 36,200 | 6.77E-05 | |
| | 6 | 2.0 | 2084.25 | 33,500 | 6.27E-05 | |

**Commercial**

| Time (hour) | Test | Mass of sample (mg) | Dilution (times) | Area | Amount of Hg (mg) | $q_t$ (mg Hg/g adsorbent) |
|---|---|---|---|---|---|---|
| 2.5 | 1 | 2.0 | 511.14 | 3,500 | 6.37E-06 | 1.6076 |
| | 2 | 2.1 | 511.14 | 3,740 | 6.82E-06 | |
| | 3 | 2.1 | 511.14 | 4,860 | 8.92E-06 | |
| | 4 | 2.2 | 491.35 | 3,110 | 5.64E-06 | |
| | 5 | 2.0 | 491.35 | 3,220 | 5.84E-06 | |
| | 6 | 2.2 | 491.35 | 3,670 | 6.69E-06 | |
| 5 | 1 | 4.9 | 533.00 | 10,640 | 1.98E-05 | 2.1557 |
| | 2 | 4.9 | 533.00 | 10,520 | 1.95E-05 | |
| | 3 | 4.9 | 533.00 | 10,840 | 2.01E-05 | |
| | 4 | 5.1 | 501.08 | 12,000 | 2.23E-05 | |
| | 5 | 5.3 | 501.08 | 12,100 | 2.25E-05 | |
| | 6 | 5.3 | 501.08 | 12,200 | 2.27E-05 | |
| 10 | 1 | 5.0 | 501.04 | 33,200 | 6.21E-05 | 6.0614 |
| | 2 | 4.6 | 501.04 | 33,100 | 6.19E-05 | |
| | 3 | 4.7 | 501.04 | 32,400 | 6.06E-05 | |
| | 4 | 4.6 | 491.43 | 27,900 | 5.22E-05 | |
| | 5 | 4.9 | 491.43 | 30,100 | 5.63E-05 | |
| | 6 | 4.9 | 491.43 | 30,500 | 5.70E-05 | |
| 15 | 1 | 2.1 | 491.14 | 24,300 | 4.54E-05 | 9.0235 |
| | 2 | 2.5 | 491.14 | 23,500 | 4.39E-05 | |
| | 3 | 2.5 | 491.14 | 23,600 | 4.41E-05 | |
| | 4 | 3.0 | 491.12 | 28,000 | 5.23E-05 | |
| | 5 | 2.7 | 491.12 | 26,000 | 4.86E-05 | |
| | 6 | 2.6 | 491.12 | 25,000 | 4.67E-05 | |
| 20 | 1 | 1.9 | 482.02 | 24,300 | 4.54E-05 | 12.6193 |
| | 2 | 1.6 | 482.02 | 24,500 | 4.58E-05 | |
| | 3 | 2.2 | 482.02 | 23,800 | 4.45E-05 | |
| | 4 | 2.0 | 511.37 | 31,700 | 5.93E-05 | |
| | 5 | 2.4 | 511.37 | 29,600 | 5.54E-05 | |
| | 6 | 2.1 | 511.37 | 30,100 | 5.63E-05 | |

The relevant parameters in the kinetic adsorption are presented in Table B.14.Then, the plot of ln ($q_e$-$q_t$) versus $t$ and $t/q_t$ versus $t$ were obtained. The first plot depicts a Pseudo–first order model. The second one, on the other hand, portrays a Pseudo–second order model

**Table B.14** Parameters of kinetic adsorption

15%Ag/GAC

| Time (hour) | Temperature (°C) | | | | | | | |
|---|---|---|---|---|---|---|---|---|
| | 30 | | 40 | | 50 | | 60 | |
| | ln ($q_e$-$q_t$) | $t/q_t$ | ln ($q_e$-$q_t$) | $t/q_t$ | ln ($q_e$-$q_t$) | $t/q_t$ | ln ($q_e$-$q_t$) | $t/q_t$ |
| 2.5 | 3.1535 | 2.8712 | 3.8402 | 1.5491 | 4.0123 | 1.3216 | 4.1531 | 0.8765 |
| 5.0 | 3.1384 | 4.0903 | 3.8247 | 2.1470 | 3.9944 | 1.7411 | 4.1456 | 1.5023 |
| 10.0 | 3.0024 | 2.4070 | 3.7261 | 1.5072 | 3.9116 | 1.3915 | 4.0156 | 0.9070 |
| 15.0 | 2.9555 | 2.9539 | 3.6511 | 1.5569 | 3.8297 | 1.3494 | 4.0165 | 1.3665 |
| 20.0 | 2.7874 | 2.4846 | 3.5498 | 1.4990 | 3.7425 | 1.3368 | 3.9475 | 1.3629 |

15%Ag/$TiO_2$

| Time (hour) | Temperature (°C) | | | | | | | |
|---|---|---|---|---|---|---|---|---|
| | 30 | | 40 | | 50 | | 60 | |
| | ln ($q_e$-$q_t$) | $t/q_t$ | ln ($q_e$-$q_t$) | $t/q_t$ | ln ($q_e$-$q_t$) | $t/q_t$ | ln ($q_e$-$q_t$) | $t/q_t$ |
| 6 | 3.6704 | 5.6689 | 4.2371 | 3.0147 | 4.4291 | 2.0303 | 4.5098 | 1.5741 |
| 12 | 3.6238 | 4.2154 | 4.1866 | 2.2243 | 4.3901 | 1.9497 | 4.4768 | 1.7755 |
| 72 | 3.4553 | 8.3176 | 3.9996 | 4.3332 | 4.1782 | 3.3398 | 4.2880 | 3.2881 |
| 120 | 3.1408 | 6.9753 | 3.6064 | 3.4921 | 3.9283 | 3.3345 | 4.0762 | 3.3527 |
| 240 | 2.0959 | 7.4551 | 2.5552 | 4.1152 | 3.2230 | 3.8896 | 3.4299 | 3.7592 |

Commercial

| Time (hour) | Temperature (°C) | | | | | | | |
|---|---|---|---|---|---|---|---|---|
| | 30 | | 40 | | 50 | | 60 | |
| | ln ($q_e$-$q_t$) | $t/q_t$ | ln ($q_e$-$q_t$) | $t/q_t$ | ln ($q_e$-$q_t$) | $t/q_t$ | ln ($q_e$-$q_t$) | $t/q_t$ |
| 2.5 | 3.3669 | 3.1047 | 3.7746 | 1.7628 | 3.8155 | 1.7283 | 3.8318 | 1.5551 |
| 5.0 | 3.3444 | 3.4528 | 3.7603 | 2.4572 | 3.7995 | 2.3099 | 3.8199 | 2.3195 |
| 10.0 | 3.2544 | 2.5717 | 3.6678 | 1.7153 | 3.7093 | 1.6615 | 3.7303 | 1.6498 |
| 15.0 | 3.1380 | 2.2271 | 3.6047 | 1.8235 | 3.6288 | 1.6347 | 3.6567 | 1.6623 |
| 20.0 | 3.0504 | 2.3073 | 3.5232 | 1.8015 | 3.5516 | 1.6703 | 3.5592 | 1.5849 |

The kinetic batch experimental data was calculated as follows:

Pseudo–first order kinetic equation

$$\ln(q_e - q_t) = \ln q_e - k_1 t$$

Pseudo–second order kinetic equation

$$\frac{t}{q_t} = \frac{1}{k_2 q_e^2} + \frac{t}{q_e}$$

The graph (Figure. 4.5) was obtained by using Pseudo–first order and Pseudo–second order model kinetic equations. Table B.15 summarizes the results of the kinetic adsorption modeling. The activation energy data presented the result on the Table B.16

**Table B.15** Result of kinetic adsorption modeling.

15%Ag/GAC

| **Pseudo first-order** | | | | | **Pseudo second-order** | | | | |
|---|---|---|---|---|---|---|---|---|---|
| **Parameters** | **Temperature (°C)** | | | | **Parameters** | **Temperature (°C)** | | | |
| | **30** | **40** | **50** | **60** | | **30** | **40** | **50** | **60** |
| $R^2$ | 0.964 | 0.991 | 0.994 | 0.909 | $R^2$ | 0.256 | 0.217 | 0.167 | 0.264 |
| Slope | -0.020 | -0.016 | -0.015 | -0.012 | Slope | -0.047 | -0.018 | -0.010 | 0.016 |
| $k_1$ | 0.020 | 0.016 | 0.015 | 0.012 | $q_t$ | -21.27 | -55.55 | -100.0 | 62.50 |
| y Intercept | 3.223 | 3.896 | 4.063 | 4.181 | y Intercept | 3.462 | 1.841 | 1.534 | 1.030 |
| $q_e$ | 25.103 | 49.205 | 58.148 | 65.431 | $k_2$ | 0.0006 | 0.0002 | 0.0001 | 0.0002 |

15%Ag/$TiO_2$

| Pseudo first-order | | | | | Pseudo second-order | | | | |
|---|---|---|---|---|---|---|---|---|---|
| Parameters | Temperature (°C) | | | | Parameters | Temperature (°C) | | | |
| | 30 | 40 | 50 | 60 | | 30 | 40 | 50 | 60 |
| $R^2$ | 0.960 | 0.970 | 0.989 | 0.987 | $R^2$ | 0.364 | 0.439 | 0.812 | 0.758 |
| Slope | -0.006 | -0.007 | -0.005 | -0.004 | Slope | 0.010 | 0.005 | 0.008 | 0.009 |
| $k_1$ | 0.006 | 0.007 | 0.005 | 0.004 | $q_t$ | 100.0 | 200.0 | 125.0 | 111.1 |
| y Intercept | 3.794 | 4.359 | 4.489 | 4.567 | y Intercept | 5.616 | 2.905 | 2.174 | 1.933 |
| $q_e$ | 44.434 | 78.179 | 89.032 | 96.255 | $k_2$ | 0.0006 | 0.0002 | 0.0001 | 0.0002 |

Commercial

| Pseudo first-order | | | | | Pseudo second-order | | | | |
|---|---|---|---|---|---|---|---|---|---|
| Parameters | Temperature (°C) | | | | Parameters | Temperature (°C) | | | |
| | 30 | 40 | 50 | 60 | | 30 | 40 | 50 | 60 |
| $R^2$ | 0.992 | 0.992 | 0.994 | 0.989 | $R^2$ | 0.756 | 0.128 | 0.254 | 0.145 |
| Slope | -0.018 | -0.014 | -0.015 | -0.015 | Slope | -0.064 | -0.015 | -0.020 | -0.017 |
| $k_1$ | 0.018 | 0.014 | 0.015 | 0.015 | $q_t$ | -15.62 | -66.67 | -50.0 | -58.82 |
| y Intercept | 3.428 | 3.829 | 3.865 | 3.886 | y Intercept | 3.407 | 2.073 | 2.012 | 1.932 |
| $q_e$ | 30.815 | 46.016 | 47.703 | 48.716 | $k_2$ | 0.0012 | 0.0001 | 0.0002 | 0.0001 |

## B.6 Activation energy of amalgam form

$$\ln k = \frac{-E_A}{R}\left(\frac{1}{T(K)}\right) + \ln A$$

**Table B.16** Data of activation energy of amalgam form plot.

| Temp. (°C) | Temp. (K) | 1/T | k | ln k | k | ln k | k | ln k |
|---|---|---|---|---|---|---|---|---|
| | | | 15%Ag/GAC | | 15%Ag/$TiO_2$ | | Commercial | |
| 30 | 303.15 | 0.00330 | 0.0200 | -3.9120 | 0.0060 | -5.1160 | 0.0180 | -4.0174 |
| 40 | 313.15 | 0.00319 | 0.0160 | -4.1352 | 0.0070 | -4.9618 | 0.0140 | -4.2687 |
| 50 | 323.15 | 0.00309 | 0.0150 | -4.1997 | 0.0050 | -5.2983 | 0.0150 | -4.1997 |
| 60 | 333.15 | 0.00300 | 0.0120 | -4.4228 | 0.0040 | -5.5215 | 0.0150 | -4.1997 |

**Table B.17** The result of activation energy of amalgam form

| Parameter | 15%Ag/GAC | 15%Ag/$TiO_2$ | Commercial |
|---|---|---|---|
| $R^2$ | 0.961 | 0.669 | 0.350 |
| $-E_A/R$ | 1612 | 1543 | 498.6 |
| ln A | -9.240 | -10.080 | -5.740 |
| $-E_A$ | -193.938 | -185.680 | -60.000 |

# APPENDIX C

# Flow Adsorption

## C.1 Experimental set up

In this research, the flow adsorptions set-up consists of several apparatus such as $N_2$ gas, rotameter, monitoring control, box PVC, column reactor, Hg filter, water bath etc. as shows in Figure C.1.


**Figure C.1** Experimental Set-up for flow adsorption studies.

## C.2 System design of Hg removal units

Dynamic adsorption columns are used to enable continuous intimate contact between solid and dispersed gas. The simplest design of this column involves a column reactor which consists of (a) a vertical cylindrical vessel filled with

adsorbents and (b) a gas distributor at the top. Figure C.2 shows the dimensions (ID) of the Hg adsorption column which was used in this research.

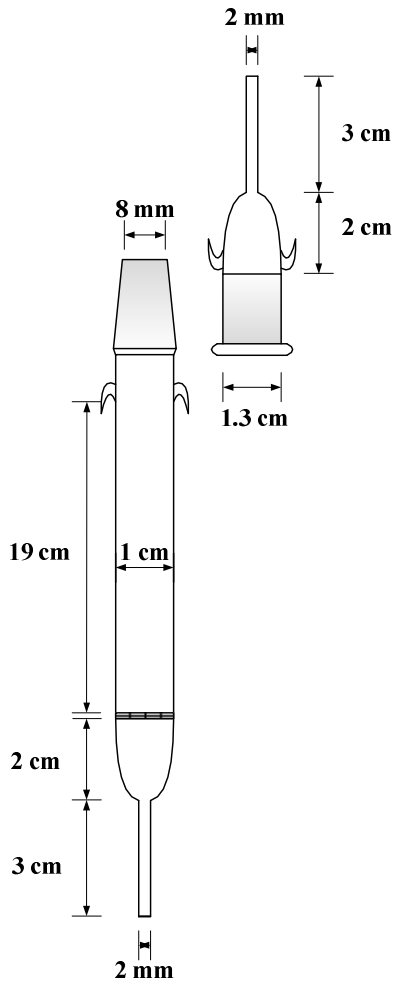


**Figure C.2** ID of adsorption column.

To be able to describe the daily operation of the dynamic adsorption system, parameters such as flow rate, pipe volume and chemical closing must be determined (BAXTER & WOODMAN, 2009). These parameters require calculation of the column's bed volume, bed surface area and slenderness ratio first. The relevant formulas are found below, along with sample calculation. The results of the calculations were summarized in Table C.1.

Bed volume (BV)

$$BV = \frac{\pi d^2 h}{4}$$

where, $\pi$ = constant rate (22/7), d = bed diameter (cm), and h = bed high (cm)

$$BV = \frac{\left(22/7\right)(1\ cm)^2(16.5\ cm)}{4}$$

$$= 12.96\ cm^3$$

Bed surface area (BSA)

$$BSA = \frac{\pi d^2}{4}$$

$$BV = \frac{\left(22/7\right)(1\ cm)^2}{4}$$

$$= 0.79\ cm^3$$

Slenderness ratio (L/D)

$$\mathbf{L/D} = \frac{\text{Bed high}}{\text{Bed diameter}}$$

$$BV = \frac{16.5\ cm}{1\ cm}$$

$$= 16.5$$

**Table C.1** Column specifications.

| Properties | Dimensions | Unit | Calculation |
|---|---|---|---|
| Bed diameter (BD) | 1 | cm | – |
| Bed high (BH) | 16.50 | cm | – |
| Bed volume (BV) | 12.96 | $cm^3$ | √ |
| Bed surface area (BSA) | 0.79 | $cm^2$ | √ |
| Slenderness ratio (L/D) | 16.5 | – | √ |
| Sorbent size | 1 (0.5–1 mm) | mm | – |

After identifying the specifications of the column, the calculations for parameters such gas hourly space velocity, superficial velocity and contact time were done, as follows.

Gas hourly space velocity (GHSV)

$$\text{GHSV} = \frac{\text{Reactant gas flow rate}}{\text{Reactor volume}}$$

$$\text{GHSV} = \frac{\left(0.00012\ \text{m}^3/\text{min}\right)}{\left(12.96\times10^{-6}\ \text{m}^3\right)}$$

$$= 9\ \text{min}^{-1}$$

Superficial velocity

$$\text{Superficial velocity} = \frac{\text{Flow rate}}{\text{Bed surface area}}$$

$$\text{Superficial velocity} = \frac{\left(0.00012\ \text{m}^3/\text{min}\right)}{\left(0.79\times10^{-4}\ \text{m}^2\right)}$$

$$= 0.025\ \text{m/s}$$

Contact time

$$\text{Contact time} = \frac{\text{Bed high}}{\text{Superficial velocity}}$$

$$\text{Contact time} = \frac{16.5 \text{ cm}}{0.025 \text{ m/s}}$$
$$= 6.482 \text{ s}$$

The data on operating conditions for the dynamic adsorption were then summarized and presented in Table C.3.

**Table C.2** Operating conditions

| Properties | Dimensions | Unit | Calculation |
|---|---|---|---|
| Flow Rate , ml/min | 110 | ml/min | – |
| | 0.00012 | $m^3$/min | – |
| Pressure (P) | 1.75 | barg | – |
| Temperature (T) | 30 | Deg C | – |
| Gas hourly space velocity (GHSV) | 9 | $min^{-1}$ | √ |
| Superficial velocity | 0.025 | m/s | √ |
| Contact time | 6.482 | S | √ |

## C.3 Breakthrough curve

The results show that the adsorbents which demonstrated the highest of adsorption capacities were 15%Ag/$TiO_2$ and 15%Ag/GAC with particles size of about 0.5–1 mm., as shown in Figure C.3.

(a) (b) (c)

**Figure C.3** Commercial (a), 15%Ag/GAC (b) and 15%Ag/$TiO_2$ (c) sample.

## C.4 The calculation of Hg adsorption capacity

The Hg adsorption capacity by equation was calculated by equation;

$$q_{sat} = \frac{F_A \times \text{Area above the breakthrough curve graph}}{\text{Mass of adsorbent per unit cross section area of bed}}$$

$$q_b = \frac{F_A \times \text{Area above the breakthrough curve graph at breakpoint}}{\text{Mass of adsorbent per unit cross section area of bed}}$$

$$\text{Bed capacity} = \frac{q_b}{q_{sat}}$$

where; $F_A$ = solute feed rate ($g/cm^2h$),

$$F_A = U_0C_0M$$

Where, $U_0$ = velocity of solute (cm/s), $C_0$ = initial concentration ($mol/cm^3$) and M = molecular weight (g/mol)

From operating conditions, $U_0$ = 0.025 m/s, $C_0$ = 8.3 $\mu g/m^3$ or $4.138 \times 10^{-5}$ $mol/m^3$ and M of Ag/TiO2 = 155.7352 g/mol

$$F_A = (0.025 \text{ m/s})(4.138\times10^{-5} \text{ mol/m}^3)(155.7352 \text{g/mol})$$
$$= 5.76\times10^{-4} \text{ g/m}^2\text{.h}$$

When, $t_{sat}$ = 1776 day and $C/C_0 = 0.012$

$$\text{Area above the breakthrough curve graph} = \int_0^{1776} \left(1 - C/C_0\right) dt$$
$$= 1754.688 \text{ h}$$

And, Mass of adsorbent per unit cross sectional area of bed = Bed height (cm) × Density (g/cm$^3$)

$$\text{Density} = \text{Mass of packed bed/Bed volume}$$
$$= 5 \text{ g}/12.964 \text{ cm}^3$$
$$= 0.368 \text{ g/cm}^3$$

where, Bed volume = 16.5 cm, mass of packed bed = 5 g and Bed volume = 12.964 cm$^3$ (Operating conditions)

Thus, Mass of adsorbent per unit cross sectional area of bed = 16.5 cm × 0.369 g/cm$^3$

$$= 6.369 \text{ g/cm}^2$$

Therefore, $q_{sat}$ = $(5.76\times10^{-4} \text{ g/m}^2\text{.h}) \times (1754.688 \text{ h}) \times (6.369 \text{ g/cm}^2)$

$$= 1.587 \text{ mg Hg/g Ag/TiO}_2$$

<u>Break point condition</u>; $C/C_0 = 0.012$ and $t_b$ = 696 day

$$\text{Area above the breakthrough curve graph} = \int_0^{696} \left(1 - C/C_0\right) dt$$

$= 687.648$ h

Therefore, $q_b = (5.76\times10^{-4}\ g/m^2.h) \times (687.648\ h) \times (6.369\ g/cm^2)$

$= 0.622$ mg Hg/g $Ag/TiO_2$

$$\text{Bed capacity} = \frac{0.622 \text{ mg Hg/g } Ag/TiO_2}{1.587 \text{ mg Hg/g } Ag/TiO_2}$$

$$= 0.392$$

# APPENDIX D

# Adsorbents characterization

## D.1 XRD Pattern

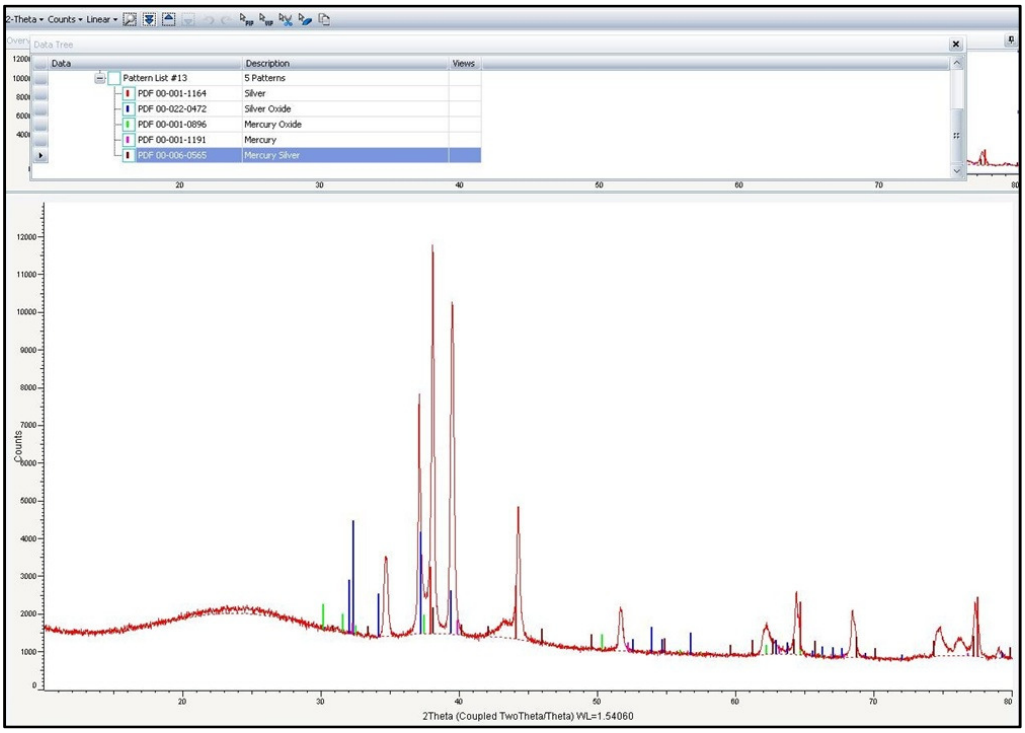


**Figure D.1** XRD pattern of GAC

| No. | Title | Value |
|---|---|---|
| 1 | Formula | Ag |
| | Name | Silver |
| | Pattern Number | 00–001–1164 |
| 2 | Formula | Hg O |
| | Name | Mercury Oxide |
| | Pattern Number | 00–001–0896 |
| 3 | Formula | Hg |
| | Name | Mercury |
| | Pattern Number | 00–001–1191 |
| 4 | Formula | $Ag_2Hg_3$ |
| | Name | Mercury Silver |
| | Pattern Number | 00–006–0565 |

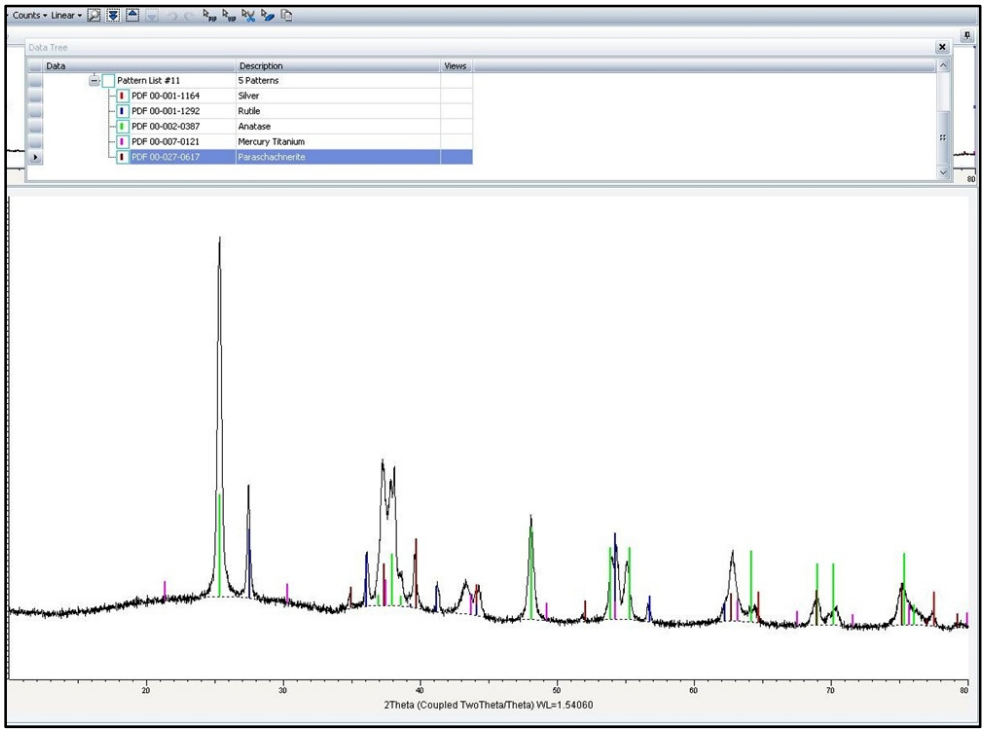


**Figure D.2** XRD pattern of $TiO_2$

| No. | Title | Value |
|---|---|---|
| 1 | Formula | Ag |
| | Name | Silver |
| | Pattern Number | 00–001–1164 |
| 2 | Formula | Hg |
| | Name | Mercury |
| | Pattern Number | 00–001–1191 |
| 3 | Formula | $Ag_3Hg_2$ |
| | Name | Silver Mercury |
| | Mineral Name | Paraschachnerite |
| | Pattern Number | 00–027–0617 |

# BIOGRAPHY

Born in 1988 in a Bangkok in Thailand, Juthathip Sinthao has grown up as an only child of Visanu and Rungrapee Sinthao. She finished her high school at Thanyarat School, Lamphakkut district, Pathumthani. She then continued her higher education at the Faculty of Engineering in Srinakharinwirot University where she took up Chemical Engineering. In May 2010, she pursued further education by taking up Master's degree in Environmental Science at the International Post–graduate Program in Environmental Management, which is a joint program with the National Center of Excellence for Environmental and Hazardous Waste Management (NCE–EHWM). Ms. Juthathip Sinthao has done jobs such as assistant researcher at Srinakharinwirot University, Clean Technology Project 2554, and Carbon Footprint Label of Dried Shrimp 100 g and UHT soymilk plus 250 ml.

**Publications:**

J. Sinthao, S. Chairakorn 2012. ***Removal of Gaseous Mercury in Natural Gas by Silver Supported Material***. In Proceeding of the 2nd TIChE International Conference for Material Science and Engineering at the Greenery Resort, Khao Yai Nakornratchasima, Thailand on October 25–26, 2012.